

SHOREFACE AND BEACH DYNAMICS  
OF THE COASTAL REGION FROM  
CAPE HENRY TO FALSE CAPE, VIRGINIA

by

L. D. WRIGHT, G. S. KIM, C. S. HARDAWAY,

S. M. KIMBALL, and M. O. GREEN

VIRGINIA INSTITUTE OF MARINE SCIENCE  
SCHOOL OF MARINE SCIENCE  
COLLEGE OF WILLIAM AND MARY  
GLOUCESTER POINT, VA 23062

Technical Report Obtained Under Contract With

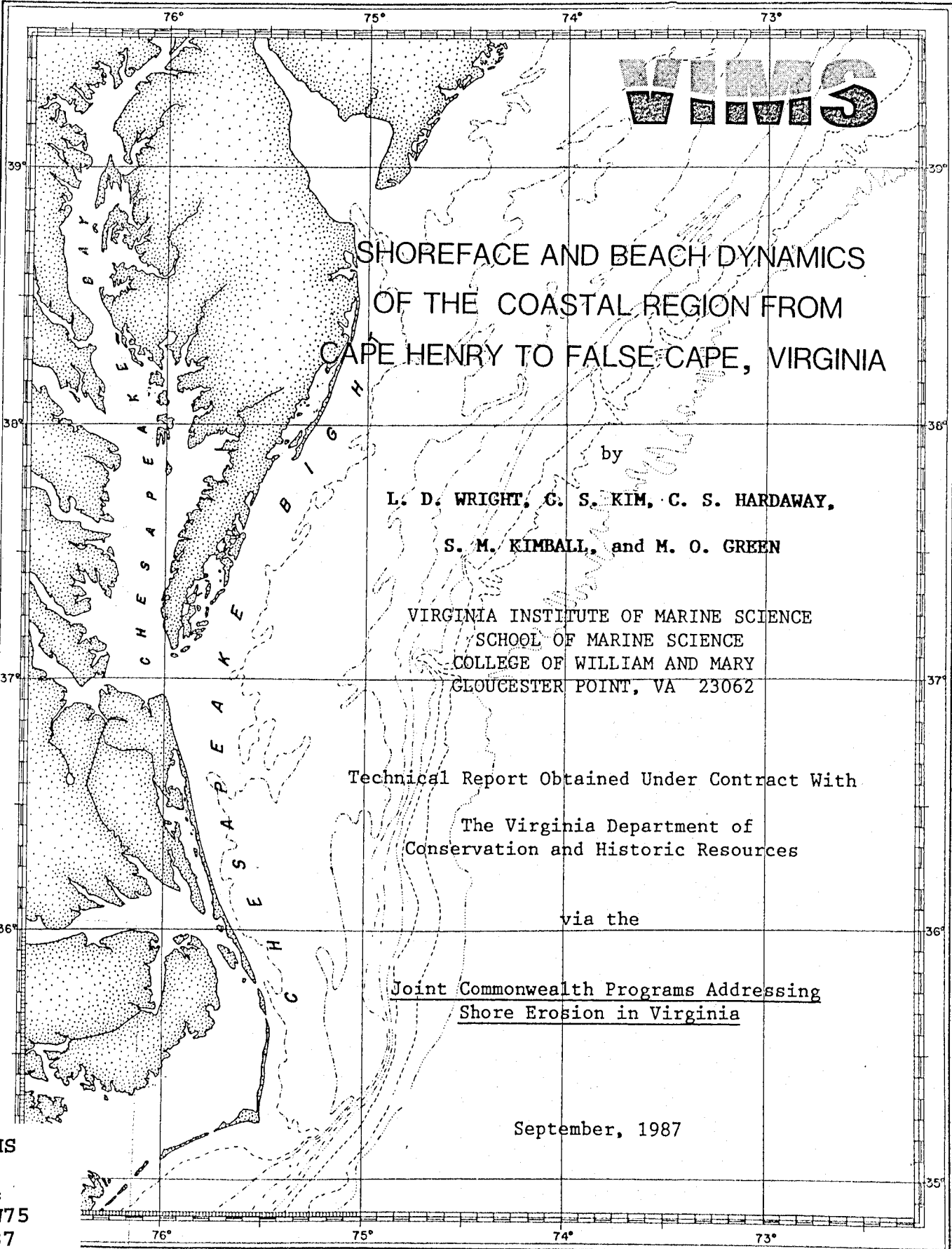
The Virginia Department of  
Conservation and Historic Resources

via the

Joint Commonwealth Programs Addressing  
Shore Erosion in Virginia

September, 1987

VIMS  
GC  
214  
V8W75  
1987



VIMS  
GC  
214  
V8 W75  
1987

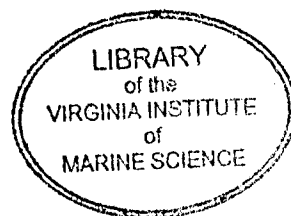
**SHOREFACE AND BEACH DYNAMICS OF THE COASTAL REGION FROM  
CAPE HENRY TO FALSE CAPE, VIRGINIA**

by

L. D. Wright, C. S. Kim, C. S. Hardaway,

S. M. Kimball, and M. O. Green

Virginia Institute of Marine Science  
School of Marine Science  
College of William and Mary  
Gloucester Point, VA 23062



Technical Report Obtained Under Contract With

The Virginia Department of  
Conservation and Historic Resources

via the

Joint Commonwealth Programs Addressing  
Shore Erosion in Virginia

September, 1987

## PREFACE

A Memorandum of Understanding between the Virginia Department of Conservation and Historic Resources (DCHR) and the Virginia Institute of Marine Science (VIMS) came into effect on July 1, 1986. By this Memorandum of Understanding, it was agreed that DCHR and VIMS would collaborate with regard to joint Commonwealth programs addressing shore erosion in the Commonwealth of Virginia with VIMS providing applied research under contract to DCHR. The contract monitor for this collaborative effort is Jack Frye, DCHR's Shoreline Programs manager.

A major objective specified in the Scope of Work in the FY 1986/87 contract from DCHR to VIMS was as follows: "(e) VIMS will apply computer models to predict shallow water wave modifications by depth and current refraction and frictional dissipation as well as inshore sediment transport. In FY 1986/1987 these analyses will be conducted first for the coastal reach extending from Cape Henry to False Cape, VA and embracing Virginia Beach." This report addresses that objective. Subsequent reports in this series will deal with other coastal regions of the Commonwealth. The Virginia barrier islands are the subjects of ongoing analyses being carried out under the FY 1987/88 contract.

This report is essentially technical in nature; however, it has been written with planners and decision makers as well as scientists and engineers in mind. In order to permit coastal scientists and coastal engineers to evaluate the methodologies and assumptions by which our conclusions were reached, we have included in Sections IV-A and V-A full expositions of the physical principles and equations underlying our analyses. Many readers may wish to skip these more technical sections. The remaining sections, including the Conclusions, should be comprehensible without knowledge of Sections IV-A and V-A. Use and location of place names in this report follows the 7.5 minute topographic maps published by the U.S. Geological Survey. Following this convention our diagrams refer to the reach north of Rudee Inlet as "Virginia Beach". All sectors are, of course, within the City of Virginia Beach.

This study was supported by a contract from the Virginia Department of Conservation and Historic Resources through the Shoreline Programs which is under the auspices of the Division of Soil and Water Conservation and by the Virginia Institute of Marine Science through the Shoreface Dynamics research objective. The manuscript was typed and edited by C.D. Gaskins and L.T. Marshall. Figures were drafted by K. Stubblefield and M.J. Shackelford. Bathymetric data were digitized by L. Calliari.

## TABLE OF CONTENTS

	Page
<b>EXECUTIVE SUMMARY</b> .....	1
<b>I INTRODUCTION</b> .....	4
<u>A. Statement of the Problem</u> .....	4
<u>B. Limits of the Study Area</u> .....	6
<u>C. Approach and Methodology</u> .....	6
<b>II SHOREFACE CHARACTERISTICS, SEDIMENTS, AND DYNAMIC FORCINGS</b> ....	12
<u>A. Continental Shelf and Shoreface Geology</u> .....	12
<u>B. Beach Sediments</u> .....	18
<u>C. Wave and Tide Regimes</u> .....	22
<u>D. Wind-Driven and Tidal Currents Over the Shoreface</u> .....	24
<b>III BEACH CHARACTERISTICS AND BEHAVIOR</b> .....	26
<u>A. Beach/Surfzone Profiles and Their Variability</u> .....	26
<u>B. Spatial Variability of Changes in Beach Volume and         Shoreline Position</u> .....	28
<u>C. Existing Anthropogenic Controls and Their Impact</u> .....	30
<b>IV WAVE MODIFICATIONS OVER THE SHOREFACE</b> .....	34
<u>A. Background</u> .....	34
1. Some basic wave equations .....	34
2. Shoaling, refraction, and diffraction .....	43
3. Wave energy dissipation by bed friction and by wave- current interaction .....	48
4. Breakers and surf .....	52
<u>B. Modelling Results</u> .....	55
1. Temporal and spatial variability of wave modifications over the shoreface .....	55
2. The role of bottom friction .....	60
3. Breakers and surf .....	69

TABLE OF CONTENTS (continued)

	Page
V LITTORAL DRIFT AND LITTORAL DRIFT GRADIENTS AS CONTRIBUTORS TO NET BEACH EROSION OR ACCRETION .....	75
<u>A. Background</u> .....	75
1. Classical formulae and their limitations .....	75
2. Basic principles governing longshore currents and sand transport .....	78
3. Alternative littoral drift formulae used in these analyses .....	83
<u>B. Modelling Results</u> .....	84
1. Estimates of longshore currents .....	84
2. Estimates of littoral drift .....	88
3. Alongshore gradients in littoral drift .....	93
VI BEACH STABILITY AND CROSS-SHORE SEDIMENT FLUX .....	101
<u>A. Background</u> .....	101
<u>B. Model Predictions of Beach Stability</u> .....	103
<u>C. Sea Level Rise and Chronic Beach Instability</u> .....	105
VII IMPLICATIONS FOR EROSION CONTROL AND BEACH NOURISHMENT .....	106
VIII CONCLUSIONS AND PROGNOSIS .....	108
IX REFERENCES .....	110

## EXECUTIVE SUMMARY

The coastal region from Cape Henry, Virginia to False Cape, Virginia is characterized by dynamic changes in beach volume and shoreline position. In a few localized areas, beaches are accreting and undergoing seaward advance. For the most part, however, erosion and shoreline retreat prevail. As a consequence, the highly developed resort strip of Virginia Beach requires annual sand nourishment amounting to 229,543 cubic meters (300,000 cubic yards). A roughly equivalent amount of sand is lost annually from the residential Sandbridge reach; however, that reach is not the beneficiary of sand replenishment and is thus highly threatened.

The processes which drive the beach and nearshore changes vary considerably in space and time. The spatial variability is the result of modulations of waves and wave induced processes by the complex topography of the shoreface and inner shelf fronting the beaches. In this study we employed a state-of-the-art computer model to evaluate the nature of these modifications and their impact on coastal processes. The model estimates wave modifications by shoaling, refraction, diffraction, and loss of wave energy by frictional interaction with the bottom. This newer model does not suffer from those shortcomings which limited earlier models. However, this component of the hydrodynamic model does not deal explicitly with wave refraction through wave-current interaction. Those effects may be locally important in the Cape Henry reach and are being considered in an additional model component for bay and inlet conditions that is under development. Additional subroutines in this model component estimate the longshore transport of sand within the surfzone. The model was run for 58 different

sets of commonly occurring deepwater wave conditions, including the case of hurricane-generated waves.

Results show that storm waves breaking off the Sandbridge reach are significantly larger than those which break farther to the north, including those which break off the resort strip of Virginia Beach. The reason for this is that Virginia Beach is fronted by a wide, shallow shoreface shoal area which causes appreciable frictional attenuation of larger waves. In contrast, the upper shoreface profile fronting Sandbridge is relatively steep and thus produces less reduction in wave energy prior to wave breaking.

Longshore variations in breaker height also contribute a driving force for longshore currents. Longshore currents and the alongshore transport of sand is predicted to be instantaneously and locally quite intense, particularly during storms. However, when integrated over a year, gradients in net longshore sand transport are only able to explain, adequately, erosion from a node of littoral drift divergence south of Sandbridge and the accretion of Croatan Beach south of Rudee Inlet. It is inferred that the erosion of most other sectors probably involves seaward sand loss primarily. Using a relatively crude index of beach stability with respect to onshore-offshore transport, most sectors are predicted to be unstable for over 17% of the time.

The results indicate that, with possibly one exception, groins or groin fields would be an ineffective means of shore protection and would probably increase erosional tendencies. Sand nourishment is the best shore protection means but relatively large quantities are required. In order for emplaced sand to remain stable on the intertidal beaches for at least 75% of

the time, the median grain size of the fill material should be 0.25 mm or larger. Finer material, if available in sufficiently large quantities, could be used to widen and flatten the surfzone and thereby decrease beach sensitivity.

## I INTRODUCTION

### A. Statement of the Problem

The economically and recreationally important coastal reaches extending from Cape Henry southward to False Cape near the Virginia-North Carolina state line are very unstable. Some sections of this coast, particularly the Sandbridge reach, are experiencing rapid, property-threatening recession; other sectors such as Croatan Beach are undergoing accretion. The beach fronting the intensely developed resort strip of Virginia Beach requires 229,543 cubic meters (300,000 yd<sup>3</sup>) of artificial sand nourishment annually. There have been numerous studies of the beach changes which have occurred on Virginia Beach and Sandbridge Beach including analyses of some of the causes of these changes. Goldsmith et al. (1977) prepared a comprehensive review of the earlier studies. More recent studies include those by Dolan et al. (1985), Everts (no date), Boyd (1985), Dean (1985), Waterway Survey and Engineering Ltd. (1986), and The Traverse Group, Inc. (1980). It is not our intention to duplicate previous efforts.

The purpose of this report is to address the following questions:

(1) What roles do the morphologically complex shoreface region fronting the beaches play in modulating the waves and wave-induced processes which drive beach and surf-zone dynamics? (2) How important are longshore variations in breaker height and what coastal sectors are subject to the most intense wave attack? (3) What fractions of the net annual loss or gain of sand from or to different coastal segments are explicable in terms of gradients in the net annual longshore sediment flux? (4) How stable are the different sectors of the coast with respect to possible offshore (shore-normal) sand

losses? (5) What are the implications of our analyses as to the appropriateness of future shore protection options including sand nourishment? Most of these questions have, of course, been addressed before; however, we have employed some recently developed techniques and concepts which have not hitherto been applied to this coastal region.

Extensive computer modelling of the modifications to incident waves by refraction and shoaling over the shoreface of the middle Atlantic Bight was carried out in the early 1970's by Goldsmith et al. (1974). However, those analyses suffered from an ailment common to most computer refraction analyses of the era: simple refraction theory fails in regions where complex bathymetry causes strong wave convergence. The procedure employed in this study overcomes this limitation by including diffraction effects in the analyses. Furthermore, the modelling efforts of Goldsmith et al. (1974) were completed prior to the most important recent advances in our understanding of wave and wave-current boundary layers, and thus considered the dissipation of wave energy by bottom friction and wave-current interactions in only a nominal way. In the present study, particular attention is given to the role of frictional dissipation, acting in concert with refraction, shoaling, and diffraction since the variable configuration and slope of the shoreface must cause significant variability in the amount of total wave energy dissipation. In addition, our modelling of wave-induced longshore sand transport takes into account pressure gradient forces produced by longshore variations in breaker height; thereby our approach departs from most conventional approaches which rely on the "CERC Formula" and consider only breaker angle.

Evaluations, albeit crude ones, of the relative importance of alongshore versus offshore sediment loss are essential to determine the most appropriate means of protecting any given reach. In the majority of cases, sand replenishment is, of course, likely to be the "most appropriate" response to erosion problems. However, the frequency distribution of breaker heights and steepnesses must be known in order to select fill material of the correct size to permit the material to remain stable on a particular beach.

#### B. Limits of the Study Area

This study was focused on the shoreface region shown in Figures I-1 & I-2. Specifically, we are concerned with the area bounded to the north by Cape Henry, Virginia at the entrance to Chesapeake Bay, to the south by the Virginia-North Carolina state line, to the east by the 20 m depth contour, and to the west by the present day intertidal beach. This region is part of the Middle Atlantic Bight.

#### C. Approach and Methodology

We have utilized field, literature search, and computer modelling methodologies in addressing our objectives although many of the conclusions reported here are derived from the computer modelling efforts. Descriptions of shoreface geological and morphological characteristics are based on published literature, recent bathymetric surveys compiled in 1986 by the Commonwealth of Virginia, Department of Mines, Minerals, and Energy, Division of Mineral Resources in cooperation with the U.S. Minerals Management Service (DMR, 1986), and our own surveys. The Virginia Institute of Marine Science field surveys of the shoreface have consisted of subbottom profiling using a Datasonics Model SBP-5000 subbottom profiling system which

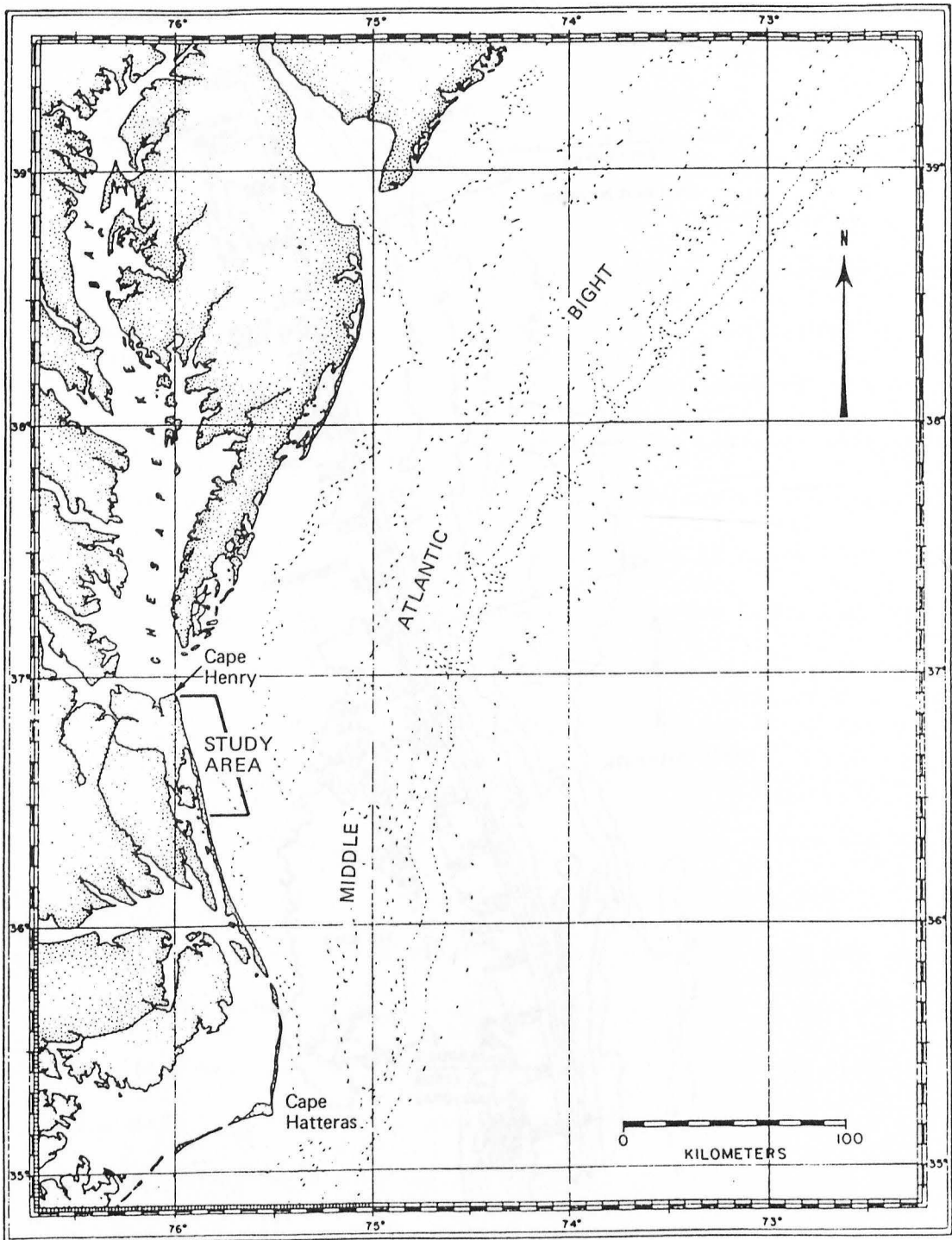


Figure I-1. Location map of the study region.

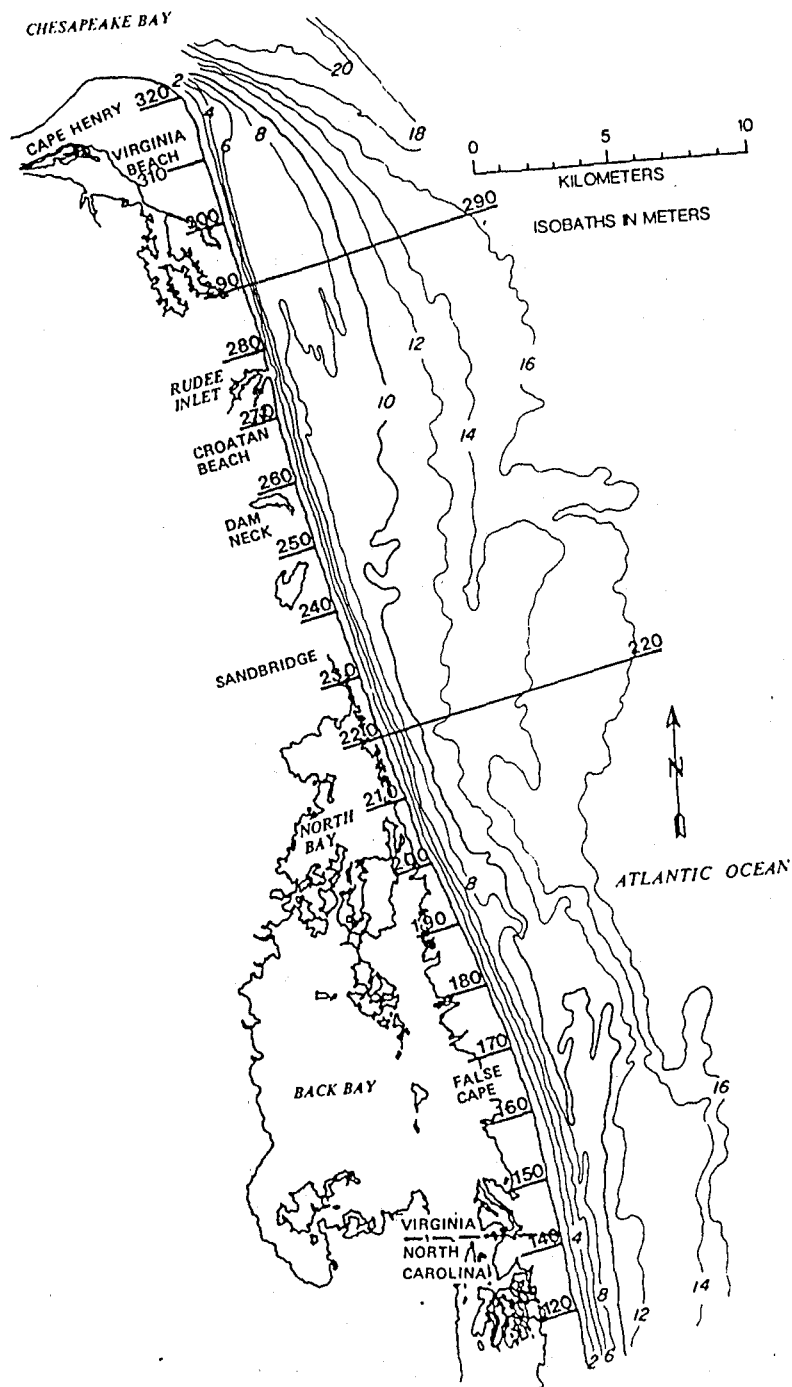


Figure I-2. Coastal configuration and bathymetry of the study region and location of sectors and profiles referred to in the following analyses.

operates at 3.5 kHz and side-scan sonar mapping using an EG & G SMS 960 Sea Floor Mapping System which operates at 100 kHz and produces scale-rectified imagery fully corrected for slant range angle and vessel speed.

Wave data recorded several times daily by the U.S. Army Corps of Engineers Field Research Facility (FRF) at Duck, North Carolina 70 kilometers to the south of the study area are probably representative of the study area and are considerably more reliable than are hindcast wave statistics. Our descriptions of the wave climate are based largely on these data; deepwater wave conditions used as inputs to our computer model were selected on the basis of the FRF data. For descriptions of extreme events not recorded by the FRF, results of model predictions of storm waves (Resio and Hayden, 1973) were used. Information concerning the tidal and wind driven currents over the shoreface was derived from a fairly large body of literature and from VIMS field observations. Near-bottom flows due to combined waves and currents over the shoreface at the Dam Neck disposal site were recorded from 5 February to 18 February, 1986 using one of the VIMS instrumented benthic boundary layer tripods. During the Dam Neck deployment, the tripod supported a Sea Data Model 635-9RS wave and current meter which incorporates a Paroscientific pressure sensor, a Marsh McBirney 2-axis electromagnetic current meter (3.8 cm sphere) and an in situ burst-programmable data logger. A Datasonics Model ASA 920 digital sonar altimeter with a resolution of 5 mm was attached to the tripod to record bed responses. The burst interval was 1 hour, the sampling duration was 34 minutes at each burst, and the sampling interval ( $\Delta t$ ) within a burst was 1 second. Additional VIMS observations of shoreface benthic flows were made from a moored vessel (R/V Seahawk) in September, 1983.

For computer modelling of shoreface modification of incident waves, we acquired, from the U.S. Army Waterways Experiment Station (WES) in Vicksburg, Mississippi, a computer model "RCPWAVE" recently developed by Ebersole et al. (1986) of the Coastal Engineering Research Center. The program was modified slightly to run on the VIMS Prime 9955 Computer. This model is a linear wave propagation model designed for engineering applications. The model computes the changes in wave characteristics that result naturally from refraction, shoaling and diffraction over complex shoreface topography. Unlike earlier models, "RCPWAVE" deals with the problem of convergent wave rays by estimating the diffusion of energy from regions of convergence to regions of divergence via the process of diffraction. The model also deals with dissipation within the surf zone by a more realistic state-of-the-art approach developed by Dally et al. (1984). The model was verified by Ebersole et al. (1986) who compared model predictions with laboratory and field data. To this fundamental linear-theory-based model we have added routines which employ recently developed understandings of wave boundary layers to estimate wave energy dissipation due to bottom friction. Our revision also estimates wave-induced longshore surf zone currents and littoral drift by means of three different theoretical models, two of which incorporate the effects of longshore gradients in breaker height. The backgrounds to the several analyses are discussed in the relevant sections of this report.

The model was run for 58 separate sets of incident wave conditions (deepwater wave height, period, and direction) which were selected on the basis of the FRF (Duck, N.C.) field data. Bathymetric data used as input were from the DMR (1986) compilation. Depth versus x, y coordinate

information was digitized and stored in a gridded array; horizontal grid dimensions were  $\Delta x = 100$  m by  $\Delta y = 250$  m. Breaker conditions, longshore currents, and littoral drift were calculated for 160 separate beach cells, each having a shore parallel length of 250 m.

## II SHOREFACE CHARACTERISTICS, SEDIMENTS, AND DYNAMIC FORCINGS

### A. Continental Shelf and Shoreface Geology

The study area delineated in Figure I-2 is situated within the Virginia Coastal Plain Province. The morphologic complexity and pronounced spatial variability of bed slopes of the shoreface and inner shelf as illustrated in Figures II-1 and II-2 play a major role in determining the nearshore processes. This morphology is, in turn, directly attributable to the local geological history. Six stratigraphic units have been identified that form the substrate in this region (Williams, in review). These units, ranging from late Miocene to late Pleistocene in age, are overlain by a veneer of modern Holocene sediments transported into the area from the Chesapeake Bay and from shoreface sources.

In the Middle Atlantic Bight, the inner continental shelf is the inundated lower coastal plain surface. The present configuration is the result of multiple episodes of transgression and regression driven by glacial and post-glacial variability in global sea level. This complex shelf morphology is defined as a "palimpsest" surface; that is, a region where the original features have been partially modified, but not wholly destroyed, by subsequent shelf processes (Swift et al., 1972). In addition to morphologic features formed by long-term and large-scale processes, there exists a secondary set of features created by modern flow and transport regimes through and around the mouth of the Chesapeake Bay.

During the last major lowstand of sea level (>15,000 yrs bp) much of what one now sees as the inner continental shelf was subaerial. Fluvial processes were the predominant factors in morphologic development. The

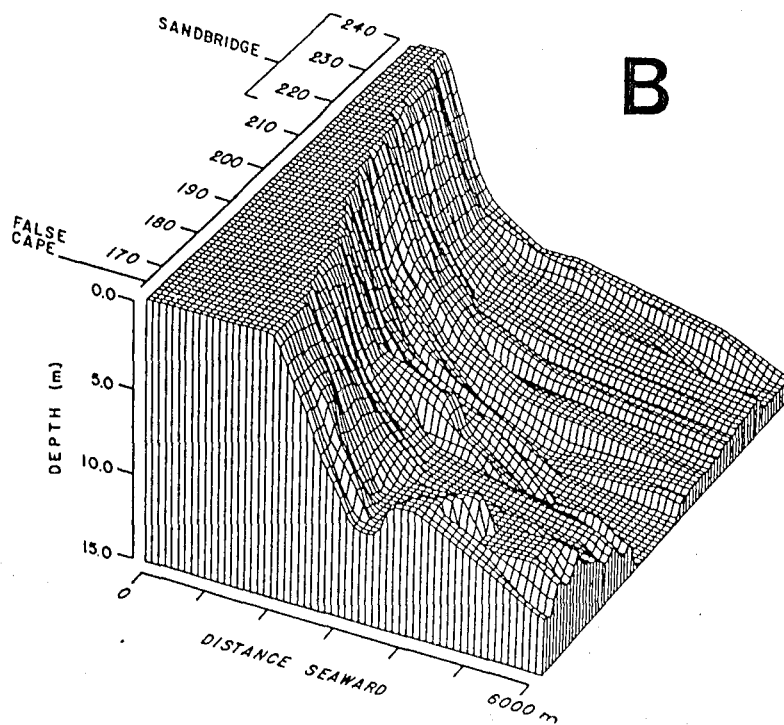
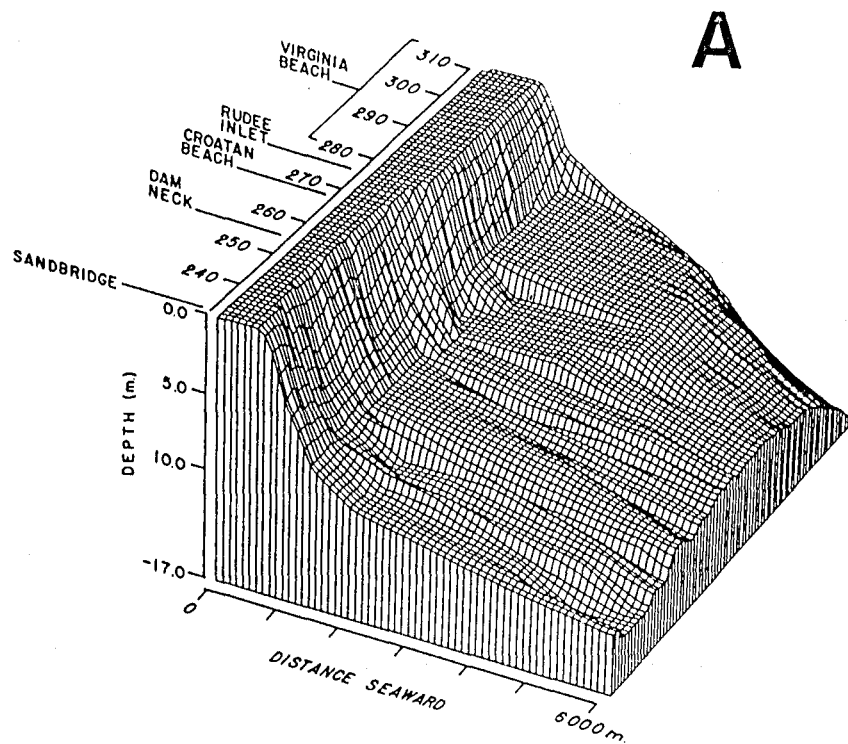


Figure II-1. Shoreface morphology: (a) northern sectors; and (B) southern sectors.

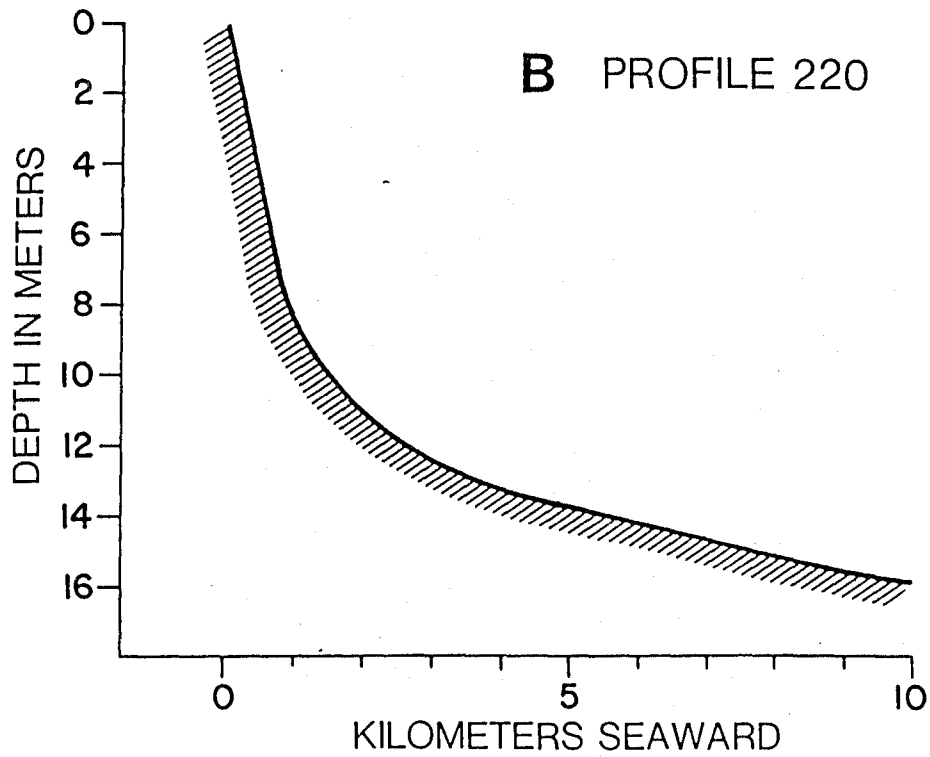
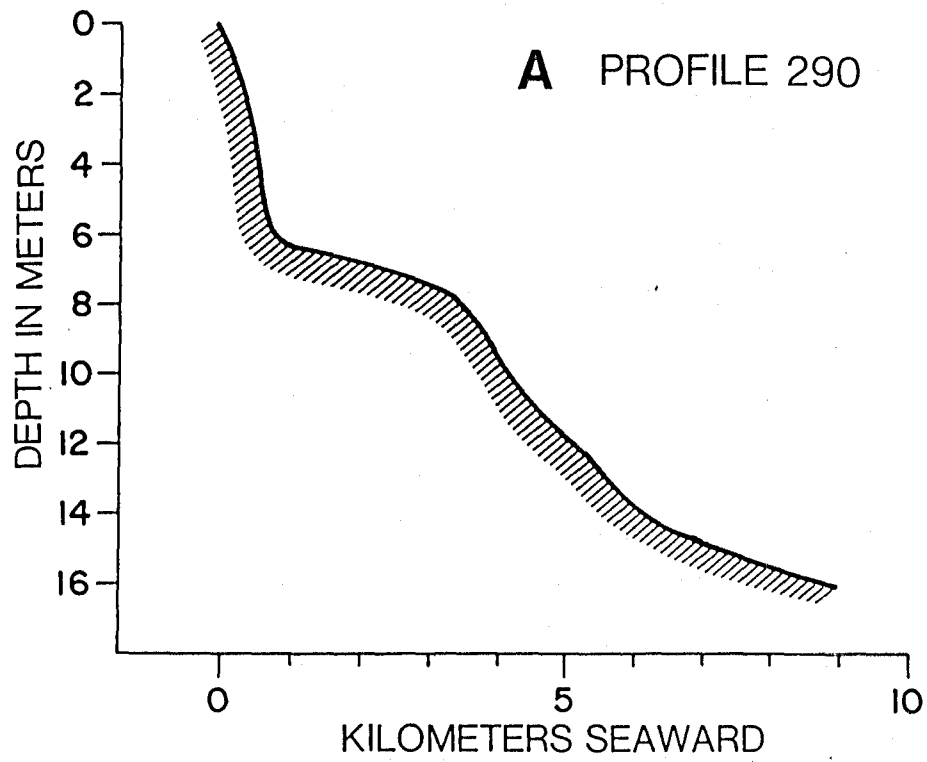


Figure II-2. Shoreface profile configurations: (A) profile 290; and (B) profile 220. Profile locations are shown in Figure I-2.

ancestral Susquehanna River, located along the axis of the present day Chesapeake Bay, and its tributaries, including the James River system, were responsible for creating channels and resultant sedimentary deposits many miles to the east of the modern shoreline. These deposits reflect the upland areas that the rivers drained. Consequently, relict deposits of coarse sand and gravel from glacial outwash survive.

Between the last glacial episode (c. 15,000 yrs bp) and 6,000-4,000 yrs bp, there was a rapid rise in sea level as the glaciers melted (Belknap and Kraft, 1977). Rates of sea level rise during that period approached 10-12 mm/yr (Nummedal, pers. comm.). Since that time, the rate of rise has slowed to a global rate of 1.2 mm/yr and a local, relative rate varying from 2.7 to 4.4 mm/yr (Froemer, 1980; Nummedal, pers. comm.). During the period of rapid transgression, many of the subaerial topographic features were modified by marine processes, creating the present configuration of filled channels, shoals, remnant barriers and relict shorelines (Stubblefield and Duane, in press). The complexity of the inner shelf deposits can be seen in the acoustic sub-bottom reflection records depicted in Figure II-3.

Several of these shelf features are recognizable on bathymetric charts (Figures I-2 and II-1) and have distinct effects on wave modification patterns in the study area. Duane et al. (1972) described shoal retreat massifs as large constructional sand features that are remnants of retreat paths of littoral drift convergences at estuary mouths or cusped forelands during transgressive periods (Stubblefield and Duane, in press). One such feature has been mapped at the southern boundary of the study reach (Stubblefield and Duane, in press). Williams (in review) describes the broad Virginia Beach Platform at the northern boundary of the study area

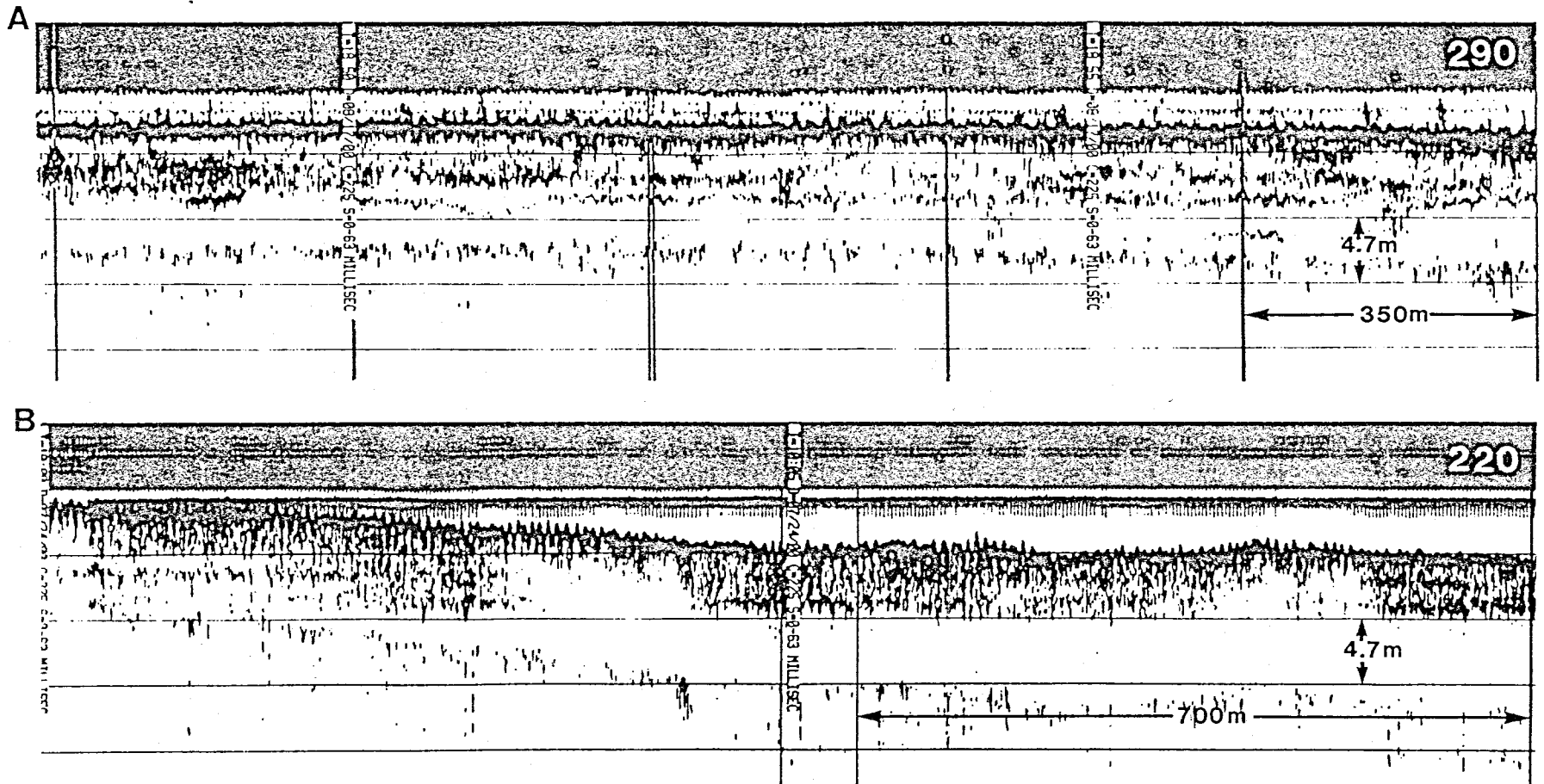


Figure II-3. 3.5 kHz subbottom profiles: (A) profile 290; (B) profile 220.

(Figures II-1 and II-2A) as a portion of the Virginia Beach Massif. In addition to the Virginia Beach Platform, east of the Atlantic Inbound Channel, there exists a broad, shallow shoal between the Atlantic Inbound channel and the shoreface and extending south as far as Rudee Inlet, known as Cape Henry Shoal. This feature is a modern ebb-tidal shoal resulting from depositional patterns engendered by flow from the Chesapeake Bay. The presence of these two broad shoals results in a broad, dissipative platform (Figure II-2A, Transects 280-310) that provides a wave-damping mechanism along northern Virginia Beach.

Field (1979) described a series of sub-parallel sand ridges in the Middle Atlantic Bight off the Maryland and Virginia coasts. These shoal fields are common in this reach of the inner continental shelf and are remarkably regular. The shoals vary in length from 6 to 60 km, are spaced between 1 and 6 km, and have amplitudes ranging as high as 10 m (Duane et al., 1972; Field, 1979). All sources note that the nearshore shoal fields are aligned on a NE strike at a reasonably constant 20 to 30 degrees from the trend of the present coastline. In some cases, the offshore shoal merges with the nearshore bar system and becomes shoreface connected. Such a case exists in the region of False Cape, Virginia, and accounts for the relatively wide shoreface platform in that area (Figure II-1B, transects 165-170). The amplitudes of the ridges in the False Cape area can exceed 7 m less than 1 km from the shoreline; sidescan data across the ridge field show small amplitude sand waves indicating an active sediment transport regime (VIMS, unpublished data). These data indicate that the ridge field exerts a dissipative influence over the wave climate in the shorezone.

If one assumes, as do Duane et al. (1972), that the linear shoal fields are the result of ridges associated with a previous retreating estuary system, then one would expect to see cross-cutting sequences of fluvial systems in the intershoal areas. Payne (1970) discusses the Virginia Beach Valley, trending NW between the False Cape ridge field and a linear shoal field located in 20 m of water east of the Back Bay Beach area, in the context of pre-existing river channels, perhaps associated with the ancestral Susquehanna system. Recent shallow acoustic sub-bottom profiling substantiates the existence of a major channel system, with channel depths in excess of 30 m and several kilometers in width (VIMS, unpublished data). Several episodes of channel infilling can be documented, with evidence of differential compaction of the channel sediments. The continental shelf slope in this area (Transects 220-260, Figure II-2B) is steeper than elsewhere in the study area, and the 10 m contour is closer to the shoreline. The indentation of the shoreface allows waves of greater amplitude to reach the nearshore than at other segments of the reach.

#### B. Beach Sediments

Goldsmith et al. (1977) characterize the beaches in the study area as being one of two general morphologic types: wide, active beaches, either erosional or accretional, and narrow, inactive beaches. Based on a series of 629 surveys, Goldsmith et al. conclude that the wider beaches have lower slope gradients than the narrow beaches and are thus, more dissipative in nature and better able to recover after storms. The narrower beaches, although more stable in low energy conditions, developed more pervasive and longer lasting changes following storm conditions.

Goldsmith et al. (1977) and others underscore the importance of the six or more Pleistocene glacial cycles in creating not only the controlling morphologic features, but also the character of sediment sources in the area. Swift (in The Traverse Group, Inc., 1980) describes the textural variation of beach materials in the Virginia Beach area and attributes those differences to inherited traits from heterogeneous Pleistocene sediments in the substrate. In addition, modern sediments distributed by tidal flow in and around the Chesapeake Bay entrance contribute an important component to the northern Virginia Beach sedimentology.

The Traverse Group, Inc. (1980), utilized sediment data collected between 1951 and 1977 by the U.S. Army Corps of Engineers to summarize conditions at five profile and sampling locations along the resort strip at Virginia Beach. These data are summarized in Table II-1. It should be remembered that there is not only a wide spatial separation between data collection sites, but there is no uniformity in collection times. Therefore, some of the trend information extracted from these data may reflect the effects of seasonal variations of the beachface.

Conclusions reached by The Traverse Group, Inc. (1980) include:

1. In general, sediments are unimodal and normally distributed.
2. Average D50 values do not vary much between profiles.
3. Average D50 values within profiles have become less variable through time.
4. Temporal variability is greater than spatial variability.
5. Sediments have become generally finer and better sorted through time. This may be related to repeated beach renourishment.

Table II-1. Median Grain Size Diameters ( $D_{50}$ ) of Surface Sand Samples Collected on Beach Profiles Above MLW Elevation, 1951 to 1977<sup>1</sup> (from The Traverse Group, Inc., 1980).

SITE 1: 1800' So. of south end of boardwalk near Rudee Inlet

Sample Location	Date Sample Taken											Average 1977
	Mar 51	June 66	Aug 66	Nov 67	June 68	Oct 69	Sept 70	Aug 72	Jan 75	Feb 77	Mar 77	
BACKSHORE	0.29 <sub>mm</sub>	-----	0.28 <sub>mm</sub>	0.27 <sub>mm</sub>	0.31 <sub>mm</sub>	0.29 <sub>mm</sub>	0.32 <sub>mm</sub>	0.30	.29	0.30 <sub>mm</sub>	0.28	.29
HIGH WATER	0.35	-----	0.35	0.27	0.26	0.29	0.21	0.38	.27	0.21	0.25	.23
MEAN WATER	0.35	0.35	0.53	0.31	0.22	0.25	0.18	0.24	.29	0.26	0.25	.26
LOW WATER	0.43	-----	0.80 <sup>2</sup>	0.34	0.38	0.26	0.24	0.24	.34	0.19	0.18	.19

SITE 2: Prolongation of 7th St. at south end of boardwalk

BACKSHORE	0.32	-----	0.24	0.30	0.30	0.31	0.23	.35	-----	0.28	0.27	.28
HIGH WATER	0.24	-----	0.33	0.29	0.26	0.25	0.24	.40	.31	0.19	0.29	.24
MEAN WATER	0.80 <sup>2</sup>	0.24	0.26	0.30	0.31	0.19	0.21	-----	.31	0.16	0.19	.18
LOW WATER	0.73 <sup>2</sup>	-----	0.27	0.31	0.18	0.33	0.20	.25	.28	0.17	0.18	.18

SITE 3: Prolongation of southside of 22nd Street

BACKSHORE	0.27	-----	0.26	0.23	0.28	0.29	0.28	.18	-----	0.28	0.29	.28
HIGH WATER	0.31	-----	0.31	0.28	0.29	0.34	0.32	.32	-----	.19	0.32	.26
MEAN WATER	0.22	0.20	0.23	0.31	0.36	0.37	0.27	.22	.30	.19	0.21	.20
LOW WATER	0.38	-----	0.29	0.38	0.28	0.91 <sup>2</sup>	0.16	.18	.36	.16	0.18	.23

SITE 4: Prolongation of southside of 35th Street

BACKSHORE	0.30	-----	0.23	0.24	0.33	0.30	0.30	.32	-----	0.30	0.29	.30
HIGH WATER	0.34	-----	0.27	0.29	0.25	0.34	0.35	.33	.27	0.20	0.27	.24
MEAN WATER	0.34	0.18	0.34	0.30	0.34	0.38	0.27	-----	.30	0.18	0.23	.21
LOW WATER	0.34	-----	0.38	0.37	0.26	1.20 <sup>2</sup>	0.16	.42	.40	0.21	0.19	.20

SITE 5: Prolongation of northside of 49th Street

BACKSHORE	0.35	-----	0.24	0.29	0.28	0.31	0.30	.28	.29	0.31	0.28	.30
HIGH WATER	0.44	-----	0.29	0.26	0.24	0.32	0.29	.27	.32	0.23	0.27	.25
MEAN WATER	0.45	-----	0.35	0.30	0.35	0.29	0.22	-----	.32	0.18	0.24	.21
LOW WATER	0.41	-----	0.28	0.27	0.44	0.21	0.16	.24	.34	0.18	0.18	.18

<sup>1</sup>Table courtesy of Norfolk District, U. S. Army Corps of Engineers

<sup>2</sup>Denotes noticeably coarser samples. Profile averages recalculated using values of  $\bar{x}_{(LW,1951)} = 0.39$ ;  $\bar{x}_{(MW,1951)} = 0.34$ ;  $\bar{x}_{(LW,1966)} = 0.30$ ;  $\bar{x}_{(LW,1969)} = 0.27$  are reported in Table 2.2

The U.S. Army Corps of Engineers, as part of its engineering study for the disposal of dredged material from the Atlantic Inbound Channel, sampled sediments along 20 profiles sited between Back Bay (Transect 170, Figure I-2) and Fort Story (Transect 370, Figure I-2). Samples were collected during August, 1985, at five points (foredune, berm, foreshore, swash, low tide terrace) along each of the profile transects. The following conclusions were reached, applicable to the reach between Rudee Inlet and Fort Story:

1. D50 values for material in the foreshore increases threefold (0.25 mm to 0.75 mm) from south to north. Sorting is better along the resort strip than farther north. This is attributed to the effects of sand replenishment along the resort strip.
2. Sediment seaward of the foreshore also increases in size in the northward direction. However, at the 3 m depth contour, there is no significant longshore variation in grain size.
3. The finest material on the subaerial beach has an average D50 of 0.20 mm. At the 3 m depth contour, D50 varies between 0.18 mm and 0.20 mm, indicating that the target average D50 for beach nourishment material should be greater than 0.20 mm.

Textural information for the reach south of Rudee Inlet to Back Bay is indicative of the following conditions:

1. D50 values for foreshore samples are consistently larger than other subaerial samples, in contrast to within-profile variation north of the inlet. This difference is attributed to the natural condition of the southern beaches.

2. D50 values for foreshore samples increases threefold northward. This trend is corroborated by data collected in February, 1987, following a storm recovery period (VIMS, unpublished data, Table II-2), despite the observed seasonal variation in absolute D50.
3. D50 of samples at the 3 m depth are uniformly coarser (D50 = 0.23) than those collected north of Rudee Inlet. Samples are generally less well sorted south of Rudee Inlet than northward.
4. The finest sand shoreward of the foreshore has an average D50 of 0.25 mm, compared to 0.20 mm north of Rudee Inlet. Seaward of the foreshore sample, D50 ranges between 0.21 mm and 0.26 mm. On the winter beach, minimum D50 seaward of the foreshore is 0.26 mm and varies to a maximum of 0.32 mm (Table II-2).

#### C. Wave and Tide Regimes

Wave hindcast statistics compiled by Saville (1954) showed that by far the largest and most frequent waves impinging on the Chesapeake Bay entrance (and hence on Virginia Beach) enter the shallow water region incident from the east-northeast and northeast. More recent analyses (Resio and Hayden, 1973; Beauchamp, 1974) substantiate this, as do direct observational data compiled at the U.S. Army Corps of Engineers Field Research Facility (FRF) at Duck, North Carolina (Birkemeier et al., 1981). The northeasterly waves are generated, principally, by mid-latitude northeasterly storms ("northeasters") of fall and winter. The lowest waves occur in summer. The average significant wave height of the waves which reach the FRF wave rider at a depth of 17 m is only 0.88 m; the corresponding mean period is 8.9 sec. However, much higher waves accompany storms and deep water wave heights exceed 4 m frequently during the period October-February. Analyses

Table II-2. Variability of Sand Size on Sandbridge Beach  
(VIMS data, from samples collected February, 1987)

Subenvironment	Sector 217		Sector 222		Sector 225		Sector 230		Sector 236		Sector 240		Sector 243	
	D <sub>50</sub> (mm)	$\bar{D}$ (mm)	D <sub>50</sub> (mm)	$\bar{D}$ (mm)	D <sub>50</sub> (mm)	$\bar{D}$ (mm)	D <sub>50</sub> (mm)	$\bar{D}$ (mm)	D <sub>50</sub> (mm)	$\bar{D}$ (mm)	D <sub>50</sub> (mm)	$\bar{D}$ (mm)	D <sub>50</sub> (mm)	$\bar{D}$ (mm)
Foredune	0.28	0.28	0.31	0.31	0.32	0.32	0.29	0.29	0.28	0.28	0.29	0.29	0.29	0.29
Berm	0.21	0.21	0.28	0.27	0.26	0.26	0.35	0.33	0.23	0.23	0.23	0.23	0.23	0.23
Σ Foreshore	0.28	0.27	0.27	0.27	0.27	0.27	0.24	0.24	0.27	0.26	0.26	0.26	0.26	0.25
Swash	0.27	0.27	0.26	0.25	0.21	0.21	0.24	0.24	0.22	0.22	0.28	0.27	0.23	0.22
Step	0.41	0.39	0.39	0.39	0.38	0.37	0.32	0.32	0.34	0.33	0.26	0.25	0.35	0.34
1.5 m Depth	0.26	0.26	0.31	0.31	0.26	0.27	0.29	0.29	0.23	0.23	0.32	0.31	0.29	0.29

D<sub>50</sub> = median grain size (millimeters).

$\bar{D}$  = mean grain size (millimeters).

conducted by Thompson (1977) indicate that the waves at Virginia Beach are lower than those off Nags Head which is very near to the Field Research Facility.

The astronomical tides affecting the reach are semidiurnal, dominated by the  $M_2$  component. At Virginia Beach the mean tidal range is 1.04 m (3.4 ft) and the mean spring range is 1.25 m (4.1 ft).

Storm surge is a contributor to abnormal water levels and coastal flooding although the most extreme water levels can be expected when high storm surges coincide with high spring tides. Dolan et al. (1985) estimate that surge heights at Sandbridge should exceed 0.6 m (2.1 ft) four times per year and should exceed 1.07 m (3.5 ft) once per decade. Resio and Hayden (1973) found that although winter northeasters generate larger waves than hurricanes, it is the less frequent hurricanes which produce the largest storm surges.

#### D. Wind-Driven and Tidal Currents Over the Shoreface

On an annual time scale, a net southwesterly drift of bottom water at about  $6 \text{ cm sec}^{-1}$  prevails over the shelf of the mid-Atlantic Bight (Bumpus, 1965; Boicourt and Hacker, 1976; Butman et al., 1979). However, storm transports are more important and Vincent et al. (1981) refer to the shelf of the mid-Atlantic Bight as storm-dominated. Beardsley and Boicourt (1981), in a review of continental-shelf circulation for the Middle Atlantic Bight, discuss the temporal and spatial structure of the surface-wind stress and pressure fields with emphasis on the synoptic-scale motions characterized by periods in excess of 5 days and length scales of more than 500 km. The latter motions are closely associated with winter storms (extratropical cyclones) capable of driving strong, transient current fields

that cross the inner shelf in phase with the forcing. Ludwick (1977; 1978) has identified a storm wind-driven, southerly-setting coastal jet with speed up to  $48 \text{ cm sec}^{-1}$  at depths of 8-13 m off Virginia Beach. Wright et al. (1986a) reported similar jet-like flows off Duck, N.C. On a shorter time scale, reversing semi-diurnal tidal currents, dominated by the  $M_2$  component, have speeds on the order of  $10 \text{ cm sec}^{-1}$  (Redfield, 1958).

Data from the VIMS benthic boundary layer tripod, deployed off Dam Neck over the period February 5-18, 1985 at a depth of 15 m over the Dam Neck dredged material disposal site revealed an extremely energetic benthic regime (Boon et al., 1987). At elevations of less than 1 meter above the bed, wave-induced orbital velocities during a northeaster approached  $1 \text{ m s}^{-1}$ . Wind-driven net near-bottom currents setting toward the southeast attained speeds of over  $0.4 \text{ m s}^{-1}$  (Boon et al., 1987).

that cross the inner shelf in phase with the forcing. Ludwick (1977; 1978) has identified a storm wind-driven, southerly-setting coastal jet with speed up to  $48 \text{ cm sec}^{-1}$  at depths of 8-13 m off Virginia Beach. Wright et al. (1986a) reported similar jet-like flows off Duck, N.C. On a shorter time scale, reversing semi-diurnal tidal currents, dominated by the  $M_2$  component, have speeds on the order of  $10 \text{ cm sec}^{-1}$  (Redfield, 1958).

Data from the VIMS benthic boundary layer tripod, deployed off Dam Neck over the period February 5-18, 1985 at a depth of 15 m over the Dam Neck dredged material disposal site revealed an extremely energetic benthic regime (Boon et al., 1987). At elevations of less than 1 meter above the bed, wave-induced orbital velocities during a northeaster approached  $1 \text{ m s}^{-1}$ . Wind-driven net near-bottom currents setting toward the southeast attained speeds of over  $0.4 \text{ m s}^{-1}$  (Boon et al., 1987).

### III BEACH CHARACTERISTICS AND BEHAVIOR

#### A. Beach/Surfzone Profiles and Their Variability

Beach profile surveys conducted by the Engineering Department of the City of Virginia Beach are routinely analyzed at the Virginia Institute of Marine Science. Most of these surveys are confined to the subaerial and intertidal portions of the beach and are intended to provide data on temporal changes in the volume of the beach above mean low water. However, several of the profiles are surveyed to a distance of 610 m (2000 ft) offshore and these provide some valuable insights into surfzone and beach characteristics. Figure III-1 shows profiles from the northern end of Virginia Beach (sector 304), Croatan Beach adjacent to Rudee Inlet (sector 276), just south of Dam Neck (sector 246) and the southern portion of Sandbridge Beach (sector 222).

Several important features are apparent from Figure III-1. Probably the most significant of these is that comparisons of the 1981 and 1984 profiles indicate that the profiles are active to water depths greater than 7 meters (23 ft). Only at sector 304 is "closure" encountered by the time the 7 m depth contour is reached. The Sandbridge (sector 222) profiles in particular show significant sand losses out to the limit of the surveys. These tendencies suggest that the beach volume changes must embrace at least the upper part of the shoreface.

The profiles also provide some very limited insights into the morphodynamic characteristics of the beach and surf zone. Bar-trough surfzone topography generally characterizes profiles of sector 304, 276, and 246 whereas the topography of the Sandbridge surfzone is more similar to the

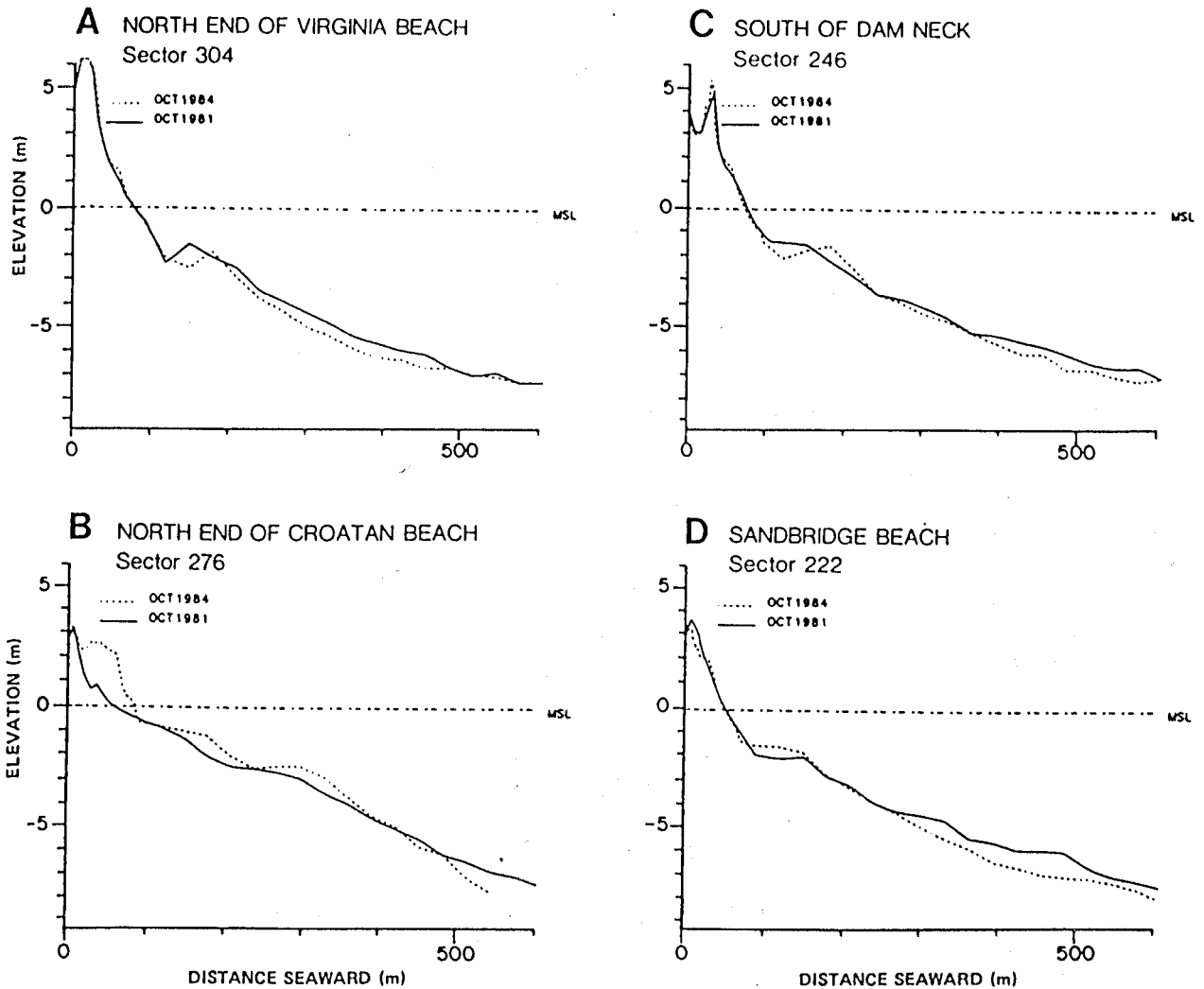


Figure III-1. Characteristic beach profiles, surveyed in 1981 and 1984, at: (A) the northern end of Virginia Beach (sector 304); (B) Croatan Beach adjacent to Rudee Inlet (sector 276); (C) just south of Dam Neck (sector 246); and (D) the southern portion of Sandbridge Beach (sector 222).

low-tide terrace state discussed by Wright and Short (1984). The most dissipative and, hence, most stable (Wright and Short, 1984; Wright et al., 1985) profile is the accreting profile at the north end of Croatan Beach (sector 276).

#### B. Spatial Variability of Changes in Beach Volume and Shoreline Position

Data concerning beach volume changes and changes in shoreline position are derived from numerous sources. The surveys conducted by the City of Virginia Beach are probably the most reliable source. In addition, Everts et al. (1983) used the position of mean high water to determine shoreline changes over the period 1849 to 1980; Dolan et al. (1985) conducted a detailed analysis of aerial photography encompassing the period 1937 to 1984. Figure III-2 summarizes the alongshore variability of subaerial beach volume change and shoreline position change. The estimates are based on the VIMS analyses of City of Virginia Beach survey data showing changes between October, 1980 and January, 1984. Data for the beach fronting the Virginia Beach boardwalk are not included; however, this reach is known to require an annual nourishment of 229,543 m<sup>3</sup> (300,000 yd<sup>3</sup>).

Sandbridge and the sectors just to the south of Sandbridge have been receding at fairly rapid rates. This is evident from Figure III-2 and has been reported by several others. For the Sandbridge reach as a whole the loss of subaerial beach volume above mean low water (by our estimates) has amounted to 148,000 m<sup>3</sup> yr<sup>-1</sup> (193,000 yd<sup>3</sup> yr<sup>-1</sup>). The total volume loss, including the subtidal portions, has been estimated to be between 199,000 m<sup>3</sup> yr<sup>-1</sup> (260,000 yd<sup>3</sup> yr<sup>-1</sup>; Boyd, 1985) and 229,543 m<sup>3</sup> yr<sup>-1</sup> (300,000 yd<sup>3</sup> yr<sup>-1</sup>; Waterway Survey and Engineering, 1986).

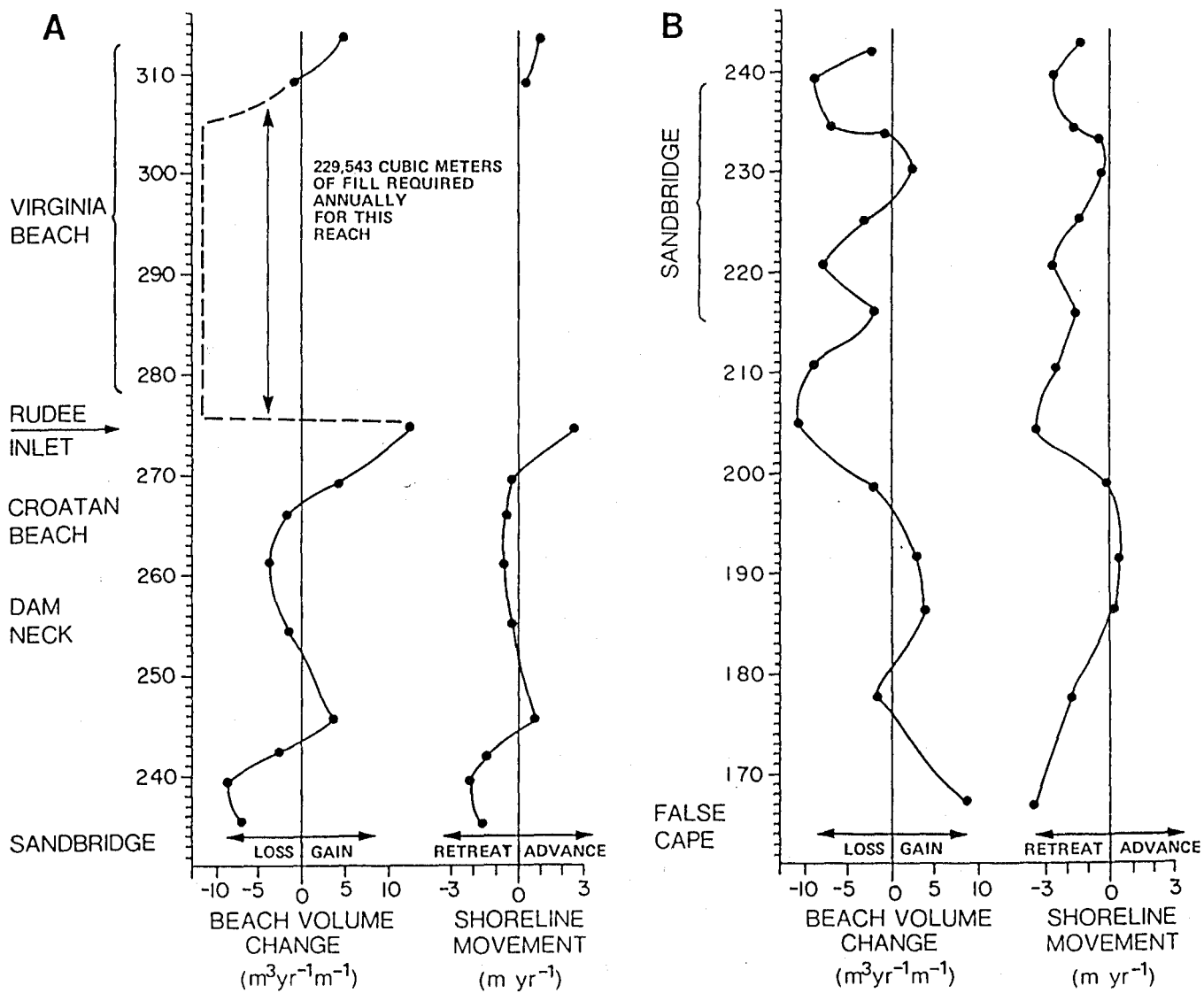


Figure III-2. Alongshore variations in temporal changes in subaerial beach volume ( $m^3 yr^{-1} m^{-1}$ ) and shoreline position. Based on VIMS analyses of surveys conducted by the City of Virginia Beach.

In contrast to the situation at Sandbridge, the southern region of Dam Neck and most of Croatan Beach are experiencing accretion. To some extent, at least, these beaches are probably beneficiaries of sand transported northward from Sandbridge. Accretion of Croatan Beach has been greatly facilitated by the southern jetty of Rudee Inlet.

### C. Existing Anthropogenic Controls and Their Impact

The loss of shorefront property over recent history has necessitated human intervention in coastal processes along the commercial section (Rudee Inlet to 49th Street) as well as along the Sandbridge residential reach. The jetties flanking Rudee Inlet were constructed to maintain navigability but have also impacted beach processes.

The history of shore protection measures at Virginia Beach is summarized in a recent report on hurricane protection by the U.S. Army Corps of Engineers (1984, pp. 27-29) from which the following has been excerpted:

"The entire stretch of beach from Rudee Inlet to 89th Street is protected to some degree. The area from Rudee Inlet to 57th Street is protected by a sand berm and a bulkhead, whereas the section from 57th Street to 89th Street is protected by a sand berm and an irregular sand dune. There is also an existing Federally authorized beach erosion project that extends from Rudee Inlet to 49th Street. The authorized project calls for a beach berm 100 feet wide at elevation 5.4 feet above NGVD. A history of the development of the bulkhead from Rudee Inlet to 57th Street is presented in the following paragraphs.

One of the earliest seawalls of record at Virginia Beach was built about 1900 and extended from 11th to 17th Streets. It consisted of round piles placed several feet apart on center, with some type of sheeting. Due to lack of maintenance, weather, and age, the wall was abandoned prior to 1925.

A concrete seawall was built between 31st and 33rd Streets about 1916. This wall is reported to have been of the gravity type, and was strengthened by tiebacks subsequent to its construction. It was destroyed by the storm of 2-3 March 1927.

A timber bulkhead and boardwalk was constructed between 14th and 16th Streets in 1925. These structures were demolished, and the fill washed out behind the bulkhead by the storm of March 1927.

A concrete, gravity-type seawall was constructed between 9th and 11th Streets about 1925. This wall was 3-foot-wide at the base on a 5-foot-wide footing, tapering to a 1-foot width at the top, and about 10 feet high. The wall tipped forward and settled when the soil wall was washed out in the storm of March 1927.

A timber bulkhead was constructed about 1929 between 42nd and 45th Streets at the locality known as Cavalier Shores, just north of the Cavalier Hotel. It was completely destroyed in the storm of 23 August 1933 as a result of water overtopping the wall.

All of the structures listed above were designed as bulkheads or retaining walls to protect property in the rear. While in existence, they halted the erosion of the backshore, but probably accelerated the erosion of the beach immediately in front, particularly when waves impinged directly against the walls and bulkheads. During storms, they deprived the beach of material that would ordinarily have been eroded from the unprotected backshore.

Today, the most intensively developed portion of the Virginia Beach oceanfront, extending from 7th Street to 35th Street, is protected by a seawall which was originally constructed in 1927 by the town of Virginia Beach. The wall consists of 22" x 17" reinforced concrete bearing piles, on 14-foot centers, 25 feet long, with a top elevation of plus 11.5 feet NGVD and panels set between the piles. These panels consist of three or four pre-cast reinforced concrete slabs fitted into grooves in the bearing piles.

In 1934, the town of Virginia Beach completed construction of a timber bulkhead between Cavalier Drive and 44th Street. In 1938, the town completed construction of a similar timber bulkhead between 35th Street and 40th Street. The two timber bulkheads constructed by the town of Virginia Beach in 1934 and 1938 consist of 12" round piles, 30 feet long, spaced 4' - 6" center to center, staggered on both sides of two 8" x 8" wales. Between the wales are three 2" x 10" Wakefield type sheet pilings about 14 feet long. All timber in the bulkheads has been heavily treated with creosote.

In 1934, The Cavalier Hotel Corporation erected a cantilever, concrete-capped, steel sheet pile bulkhead in front of their property extending from 40th Street to Cavalier Drive. The town of Virginia Beach rehabilitated the sections of wall from 7th to 17th Streets in 1953.

No major modifications were made to the wall until much of it was destroyed in 1962. In 1962 after the storm, 4,800 feet of the boardwalk and wall required major repair. The repairs were made by the Corps of Engineers under the provisions of the Federal Disaster Act of

1950, Public Law 81-875. The repair included replacing damaged and missing curtain wall slabs, replacing damaged and missing boardwalk deck panel, and constructing a concrete cap. In addition, some 5,500 feet of timber bulkheading had to be replaced and 1,260 feet needed major repair. Also, residents north of 49th Street constructed different types of bulkheads to protect their property. Currently, the existing bulkhead extends north to 57th Street. Since 1962, no major modification has been made to the existing bulkhead except for the area from 2nd Street to 7th Street where a new timber bulkhead was constructed in 1983."

At the present time, annual beach nourishment from Rudee Inlet to 49th Street is necessary to provide an adequate recreational beach area. Nourishment also importantly offers a degree of protection to the bulkhead from Rudee Inlet to 57th Street. During the winter, northeast storms deflate the beach and expose the bulkhead. Once exposed the bulkhead acts as a vertical barrier to subsequent storm activity and effectively increases the water depth at the wall. When a vertical wall is present, stable beach features may appear less frequently than on a beach with no such barrier (Green, 1986).

The Rudee Inlet jetties have a significant effect on sediment transport. The weir feature and sand trap retain material for a sand bypassing operation. This provides about  $92,000 \text{ m}^3$  ( $120,000 \text{ yd}^3$ ) to the Virginia Beach commercial strip annually. The jetties are positive features in terms of beach maintenance both north and south of the Inlet.

The residential area of Sandbridge has been in existence for several decades. Up until recently there has been little need for hardening the shoreline due to an adequate protective beach and few cottages. Although shoreline erosion has proceeded at a historical rate of well over 1 meter per year, there was previously enough dune volume between cottages and high water for adequate protection. By the late 1970s and early 1980s shorefront

cottages were becoming larger and more expensive and the dunes were getting narrower and less protective. Bulldozing of the beach area was and still is widely practiced after storm events. Intermittent bulkheads began appearing in greater numbers as cottages and septic fields became exposed after winter storms. In 1986 some Sandbridge residents were given special permission to construct a high continuous wooden bulkhead. At present about 7% of Sandbridge Beach is protected by bulkheads. Recently, however, permission to construct bulkheads has been granted for the entire Sandbridge reach.

During the winter of 1986-1987, VIMS personnel made frequent trips to Sandbridge, especially after the many northeast storms. A series of photos show the progressive decrease in beach width following each storm event. Flanking and loss of backfill was frequent. However, the structure has remained intact. In February of 1987, the Air National Guard was called upon to bulldoze beach sand up into dunes along the entire length of Sandbridge. It took approximately one month to construct the dune. A small northeaster on March 10, 1987 removed the bulldozed dunes. Without the dunes, however, there would have been more damage to cottages.

## IV WAVE MODIFICATIONS OVER THE SHOREFACE

### A. Background

Well-established theoretical precepts underlie the wave transformation analyses which were performed in this study. For the benefit of readers who may be unfamiliar with principles of wave mechanics, some of the governing concepts and equations need explicit statement prior to the presentation of results.

#### 1. Some basic wave equations

Some of the important wave parameters are introduced as follows:

Wave amplitude,  $a$ , is the maximum displacement of water surface above or below the mean water level. The wave height,  $H$ , is the vertical distance from a wave trough ( $-a$ ) to a wave crest ( $+a$ ); for small amplitude waves  $H = 2a$ . At any given time or at any given location, the instantaneous surface elevation is expressed by  $\eta$ ; the time history of  $\eta$  defines the wave surface ( $\eta$  maximum =  $+a$ ,  $\eta$  minimum =  $-a$ ). The time interval (i.e., seconds) separating successive crests ( $\eta$  maxima) or troughs ( $\eta$  minima) at any fixed point in space is the wave period,  $T$ . The distance separating successive crests or troughs at any instant in time is the wave length,  $L$ . For the specific case of deep water waves, deep water wavelength is designated by  $L_\infty$ . In terms of  $T$  and  $L$  it is meaningful, for sinusoidal oscillations, to define the radial frequency,  $\omega = 2\pi/T$ , (which has units of radians per sec) and the wave number,  $k = 2\pi/L$ , (which has units of radians per meter). The wave phase speed,  $C = L/T$ , is the rate at which the individual wave forms propagate, whereas, the group velocity,  $C_g$ , is the rate of energy transmission or conceptually the rate at which a wave train

travels (in deepwater designed at  $C_{\infty}$  and  $C_{g\infty}$  respectively). Oscillation of the water surface is accompanied by orbital (or quasi orbital) motion of water particles which oscillate with horizontal and vertical orbital velocities  $u$ ,  $v$ , and  $w$  which respectively parallel the  $x$ ,  $y$ , and  $z$  coordinates. The velocity potential,  $\phi$ , which can be used to describe the motion when flow is irrotational is defined by

$$u = \frac{\partial \phi}{\partial x}, \quad v = \frac{\partial \phi}{\partial y}, \quad \text{and} \quad w = \frac{\partial \phi}{\partial z}.$$

Wave motions, like other fluid motions, must satisfy the basic conditions of continuity, conservation of momentum, and a few boundary conditions.

Because irrotationality may be assumed, except in the bottom boundary layer which is typically thin, small amplitude waves may be described in terms of the velocity potential,  $\phi$ . The continuity condition is defined by Laplace's equation

$$\frac{\partial^2 \phi}{\partial x^2} + \frac{\partial^2 \phi}{\partial y^2} + \frac{\partial^2 \phi}{\partial z^2} = 0 \quad (1)$$

and the momentum principle by Bernoulli's generalized equation

$$\rho \frac{\partial \phi}{\partial t} + \frac{\rho}{2} \left[ \left( \frac{\partial \phi}{\partial x} \right)^2 + \left( \frac{\partial \phi}{\partial y} \right)^2 + \left( \frac{\partial \phi}{\partial z} \right)^2 \right] + p + \rho g z = f(t) \quad (2)$$

For the varying free surface, defined by the surface position,  $\eta$ , where pressure,  $p$ , is assumed zero, equation 2 is replaced by the free surface dynamic boundary condition

$$\frac{\partial \phi}{\partial t} + \frac{1}{2} \left[ \left( \frac{\partial \phi}{\partial x} \right)^2 + \left( \frac{\partial \phi}{\partial y} \right)^2 + \left( \frac{\partial \phi}{\partial z} \right)^2 \right] + g\eta = 0 \quad (3)$$

Wave motions are also constrained by some additional boundary conditions.

These are (e.g. Mooers, 1976; Madsen, 1976):

- i. At the sea bed ( $z = -h$ ; where  $h$  is water depth),  $w = 0$ ,  
 $\frac{\partial \phi}{\partial z} = 0$ ; i.e., the fluid cannot enter or issue from the boundary.
- ii. At the sea bed, tangential velocity vanishes  
 $u, v = 0, \frac{\partial \phi}{\partial x}, \frac{\partial \phi}{\partial y} = 0$ , i.e., friction requires that at fixed boundaries there can be no flow.
- iii. At the sea surface vertical velocity vanishes  
 $w = 0, \frac{\partial \phi}{\partial z} = 0$ , i.e., flow does not pass through the surface.
- iv. Where the free surface of the sea varies with time and space relative to the still water level ( $z = 0$ ) by an amount  $\eta = \eta(x, t)$ , the kinematic boundary condition must apply

$$\frac{\partial \eta}{\partial t} + \frac{\partial \phi}{\partial x} \frac{\partial \eta}{\partial x} = \frac{\partial \phi}{\partial z} \quad (4)$$

i.e., oscillations in surface elevation  $\eta$  must be accompanied by oscillations in vertical flow ( $w$ ) immediately beneath the surface.

For linear wave theory, the equation for the dynamic boundary condition (eq. 3) is linearized when it is possible to assume that the convective inertia term,  $\frac{1}{2}(u^2 + w^2)$ , in the Bernoulli equation makes a very small contribution to total pressure relative to the contribution of  $\frac{\partial \phi}{\partial t}$ , and that when averaged over a complete wave cycle,

$$\frac{\overline{\frac{1}{2}(u^2 + w^2)}}{\left| \overline{\frac{\partial \phi}{\partial t}} \right|} \ll 1 \quad (\text{e.g. Kinsman, 1965}). \quad \text{This permits the term}$$

$$\frac{1}{2} \left| \left( \frac{\partial \phi}{\partial x} \right)^2 + \left( \frac{\partial \phi}{\partial y} \right)^2 + \left( \frac{\partial \phi}{\partial z} \right)^2 \right| \quad \text{to be dropped from equation 3 so that the}$$

relationship between the free surface profile defined by  $\eta$  and the velocity potential takes on the simplified form

$$\eta = -\frac{1}{g} \frac{\partial \phi}{\partial t} \quad (5)$$

at the surface. Substitution in the kinematic boundary condition equation (eq. 4) then gives the condition

$$\frac{\partial^2 \phi}{\partial t^2} + g \frac{\partial \phi}{\partial z} = 0 \quad (6)$$

at the surface. This linearizing assumption does not, of course, apply to non-linear waves such as Stokes waves; however, higher order non-linear wave effects have not been considered in this study (Kinsman, 1965 offers a detailed discussion of the linearization process).

For a progressive sinusoidal wave of amplitude  $a$ , radial frequency  $\omega = 2\pi/T$ , and wave number  $k = 2\pi/L$ , the surface displacement  $\eta$  as a function of time,  $t$ , and space,  $x$  is given by

$$\eta = -\frac{1}{g} \frac{\partial \phi}{\partial t} = a \cos (kx - \omega t) \quad (7)$$

The velocity potential as a function of time,  $t$ , and location in the  $x, z$  plane (at or below the surface) has the general form

$$\phi = a \frac{g}{\omega} \frac{\cosh k(z+h)}{\cosh kh} \sin (kx - \omega t) \quad (8)$$

which for short or deepwater waves reduces to

$$\phi = a \frac{g}{\omega} e^{kz} \sin (kx - \omega t) \quad (9)$$

and for long (shallow water) waves to

$$\phi = a \frac{g}{\omega} \sin (kx - \omega t) \quad (10)$$

(i.e. for long waves the velocity potential is uniform with depth).

For short and intermediate (i.e., dispersive) waves, the dispersion relationship is

$$\omega^2 = kg \tanh kh . \quad (11)$$

This relationship expresses the dependence of  $k$  (and hence,  $L$ ) on  $\omega$  (hence,  $T$ ) and depth,  $h$ . From equation 11 we can find the length,  $L$

$$L = g \frac{T^2}{2\pi} \tanh kh . \quad (12)$$

As depth decreases,  $\tanh kh$  decreases; therefore,  $L$  decreases with both decreasing period,  $T$ , and decreasing depth,  $h$ . Since  $T$  remains constant with depth, in waters of intermediate depth  $L$  varies only with depth  $h$ . For short waves  $\tanh kh \rightarrow 1$  so

$$L_{\infty} = g \frac{T^2}{2\pi} \quad (13)$$

Similarly, the phase speed,  $C$  is

$$C \equiv \frac{\omega}{k} = \frac{L}{T} = \frac{g}{\omega} \tanh kh \quad (14)$$

or for short waves

$$C_{\infty} = \frac{g}{\omega} = g \frac{T}{2\pi} \quad (15)$$

In shallow water ( $\frac{h}{L} < 0.05$ ) the long wave speed is dependent only on depth in accordance with

$$C = (gh)^{\frac{1}{2}} \quad (16)$$

Equations 11 through 16 indicate that at intermediate and shallow depths, both  $L$  and  $C$  decrease with depth. As will be discussed later, this has important consequences on the boundary modifications of waves through the processes of shoaling and refraction.

The pressure field,  $p_w$ , due to the wave motion is in phase with the surface profile:  $p_w$  maxima accompany  $\eta$  maxima. For progressive waves

$$p_w = \rho g a \frac{\cosh k(z+h)}{\cosh kh} \cos(kx - \omega t) \quad (17)$$

which reduces, for short waves, to

$$p_w = \rho g a e^{kz} \cos (kx - \omega t) . \quad (18)$$

For long waves  $p_w$  is dependent simply on  $\eta$  so

$$p_w = \rho g \eta \quad (19)$$

By linear wave theory, water particles under waves move in closed orbits or bidirectional paths, experiencing no net translation over a complete wave cycle (i.e., there is no net mass transport). At intermediate depths, at least, the resulting orbital velocities near the bed play major roles in initiating sediment transport. The velocities are equal to the ratio of the total length of particle excursion relative to wave period (i.e., relative to the time available to complete the excursion). Orbital velocities consist of both horizontal,  $u$ , and vertical,  $w$ , components; the latter vanishes near the bed. The general form for the horizontal velocity component,  $u$ , as a function of  $x$ ,  $z$ , and  $t$  for progressive waves is

$$u = a\omega \frac{\cosh k(z + h)}{\sinh kh} \cos (kx - \omega t) \quad (20)$$

The vertical component is

$$w = a\omega \frac{\sinh k(z + h)}{\sinh kh} \sin (kx - \omega t) \quad (21)$$

At the bed  $w = 0$  and the maximum free-stream horizontal velocity,  $u_b$  is

$$u_b = \frac{a\omega}{\sinh kh} = \frac{\pi H}{T \sinh kh} \quad (22)$$

The energy,  $E$ , of a wave per unit horizontal area consists of potential energy,  $E_p$ , due to the displacement of water surface, and kinetic energy,  $E_k$ , due to the orbital velocities  $u$  and  $w$ . Wave energy is proportional to

the square of wave amplitude (or height) and is obtained by integrating the Bernoulli equation over wave length and with depth in accordance with

$$E = \underbrace{\frac{1}{L} \int_0^L \int_0^{\eta} \rho g z dz dx}_{\text{Potential energy, } E_p} + \underbrace{\frac{1}{L} \int_0^L \int_0^{-h} \frac{1}{2} \rho (u^2 + w^2) dz dx}_{\text{Kinetic energy, } E_k} \quad (23)$$

For progressive waves of constant amplitude, this reduces to

$$E = \frac{1}{2} \rho g a^2 = \frac{1}{8} \rho g H^2 \quad (24)$$

and

$$E_p = E_k = \frac{1}{4} \rho g a^2 = \frac{1}{16} \rho g H^2 \quad (25)$$

The quantity  $E$  is also referred to as the specific energy or energy density; the total energy per wave length is  $E \times L$ .

An equally important quantity is the rate of transmission of energy in the direction of wave travel or energy flux,  $E_f$  (also referred to as wave power; it has units of power, e.g., watts). The energy flux is a vector quantity equal to the product of the energy density,  $E$ , (eq. 24) and the wave group velocity,  $C_g$ , i.e.

$$E_f = E C_g \quad (26)$$

Whereas the phase speed,  $C$ , of a wave is the rate of propagation of the wave form, the group velocity,  $C_g$ , is the rate of forward propagation of the energy contained in a train (or group) of waves (for a discussion of group velocity see Lighthill, 1978, pp. 254-260). The group velocity is given by

$$C_g = C n = \frac{\partial \omega}{\partial k} \quad (27)$$

where

$$n = \frac{1}{2} \left( 1 + \frac{2kh}{\sinh 2kh} \right) \quad (28)$$

Equation 27 reduces respectively for deepwater (short) and shallow water (long) waves to

$$C_g = C/2 \quad (29)$$

and

$$C_g = C = \sqrt{gh} \quad (30)$$

In waters of intermediate depth,  $C_g$  initially increases slightly with decreasing depth, then continues to decrease significantly as the waves shoal.

Equation 26 expresses the energy flux per unit width of wave crest (e.g., watts/meter). The total energy flux across an advancing wave front of width  $b$  is  $E C_g b$ . When energy is not dissipated, it must be assumed that energy flux is conserved as waves propagate from one region to another, or into shallow water. This means, of course, that any decrease in either  $C_g$  or  $b$  must be accompanied by an increase in  $E$  and, hence, in  $H$ .

In addition to the transmission of energy (energy flux), wave motion also results in an associated flux of momentum or wave "thrust" in the direction of propagation which is fundamental in causing variations in mean water level (i.e. setup or setdown), wave-current interactions, and nearshore circulation in the form of rips and longshore currents. When the horizontal momentum flux in the presence of waves is integrated over depth, the total flux is found to consist of two parts: (1) a part involving the hydrostatic pressure field ( $\rho g z$ ) and thus not directly dependent on wave motion; and (2) a part involving the "excess" momentum flux due to the waves alone which Longuet-Higgins and Stewart (1962; 1964) refer to as radiation stress. The radiation stress concept follows, somewhat, the analogue of the radiation pressure produced by a photon stream (e.g.,

LeBlond and Mysak, 1978, p. 114; the theory, originally developed by Longuet-Higgins and Stewart, 1962; 1964, is also discussed by LeBlond and Mysak, 1978; Phillips, 1977; and Le Mehaute, 1976). Radiation stress,  $S$ , is a tensor having components  $S_{xx}$ ,  $S_{yy}$ ,  $S_{xy}$  designating respectively the x flux of x momentum, the y flux of y momentum and the x flux of y momentum. The x component is in the direction of wave travel whereas the y component parallels wave crests. For waves advancing into shallow water these components may also be regarded as shore normal and shore parallel respectively. The terms  $S_{xx}$  and  $S_{yy}$  are in other words the forward and sideways transports of momentum.

In the direction of wave travel the  $S_{xx}$  radiation stress is

$$S_{xx} = \frac{1}{T} \int_0^T \int_{-h}^{\eta} (p_w + \rho u^2) dt dz \quad (31)$$

In a general form the  $S_{xx}$  and  $S_{yy}$  radiation stress components are given by

$$S_{xx} = E \left( \frac{2C_g}{C} - \frac{1}{2} \right) = E \left( \frac{2kh}{\sinh 2kh} + \frac{1}{2} \right) \quad (32)$$

and

$$S_{yy} = E \left( \frac{C_g}{C} - \frac{1}{2} \right) = E \left( \frac{kh}{\sinh 2kh} \right) \quad (33)$$

where  $E$  is energy density (eq. 24). For short waves  $C_g/C = \frac{1}{2}$  so equations

32 and 33 reduce to

$$S_{xx} = \frac{1}{2} E \quad (34)$$

and

$$S_{yy} = 0 \quad (35)$$

For long waves  $C_g = C$  and

$$S_{xx} = \frac{3}{2} E = \frac{3}{4} \rho g a^2 = \frac{3}{16} \rho g H^2 \quad (36)$$

and

$$S_{yy} = \frac{1}{2} E = \frac{1}{4} \rho g a^2 = \frac{1}{16} \rho g H^2 \quad (37)$$

The  $S_{xy}$  component of radiation stress which is particularly important as providing the driving thrust for longshore currents in the surf zone is

$$S_{xy} = \frac{1}{T} \int_0^T \int_{-h}^{\eta} \rho uv dz \quad (38)$$

which some may recognize as somewhat analogous to the familiar Reynold's stress. The x and y components, u and v, of the orbital velocity,  $U_0$ , depend on the incidence angle,  $\alpha$ , the wave rays make relative to the bottom contours or the shore, or in other words,  $u = U_0 \cos \alpha$  and  $v = U_0 \sin \alpha$ . In terms of energy density E and incidence angle  $\alpha$  the  $S_{xy}$  component is given by

$$S_{xy} = E n \cos \alpha \sin \alpha \quad (39)$$

## 2. Shoaling, refraction, and diffraction

Wind-generated gravity waves, incident from deepwater toward a coastline, are modified as they propagate across the nearshore zone into water of decreasing depth. For the moment, we consider the modifications which take place from the greatest depth at which wave motion is affected by the bed up to, and not including, the point at which the waves break. Breakers and surf-zone processes are discussed shortly. The modifications begin when the waves become "intermediate" with respect to the ratio  $h/L$  of water depth to wave length. The outer limit of wave-bottom interaction is strictly defined at  $h/L = \frac{1}{2}$ ; however, for most practical purposes the significant modifications occur for depths at which  $h/L < \frac{1}{4}$ . The extent of the modification increases with decreasing  $h/L$ . The simplest of these

modifications involve changes in  $L$ ,  $C$ ,  $C_g$ . Primary nearshore wave modifications include: (1) shoaling; (2) refraction; (3) diffraction; and (4) frictional dissipation. These processes are particularly important in producing increases or decreases in wave height, and hence in radiation stress and orbital velocity. Considering wave height variations due to those processes, wave height,  $H$  at any given position and depth, relative to deepwater wave height,  $H_\infty$  is

$$H/H_\infty = K_s K_r K_d K_f \quad (40)$$

where  $K_s$ ,  $K_r$ ,  $K_d$ , and  $K_f$  are respectively the shoaling, refraction, diffraction, and friction coefficients. In the case of shoaling, refraction and diffraction, the total energy flux is conserved but is redistributed so as to change  $H$ . In the case of bottom friction, wave height is reduced because of absolute dissipation of energy; this process is considered in the next subsection.

As waves move into shallow water, the group velocity,  $C_g$ , changes in accordance with equation 27: initially it increases slightly, then it decreases rapidly. However, energy flux (eq. 26) is conserved. Hence, changes in  $C_g$  must be accompanied by opposite changes in  $E$  or, in other words, in  $H^2$ . The shoaling process involves changes in wave height to compensate for an opposite change in group velocity which results in response to changing water depth. The shoaling coefficient  $K_s$  is given by

$$K_s = \left( \frac{C_\infty}{2nC} \right)^{1/2} = H/H_\infty \quad (41)$$

where  $n$  is given by equation 28. As waves shoal (in the absence of currents) the ratio  $H/H_\infty$  initially decreases slightly to a value of about 0.91 at intermediate depths in the vicinity of  $h/L_\infty = .157$  ( $h/L = .19$ ).

Shoreward of this position,  $H/H_{\infty}$  increases rapidly and may reach values of 1.5-2.0 in the case of long, low swell before the waves break. For this reason, long-period swell can produce high breakers even when deep water height is relatively low. Because these changes are due to opposite changes in  $C_g$ , there is no change in energy flux.

When waves approach the shore at an angle oblique to the alignment of the bottom depth contours, the changes in  $C$  which accompany depth changes in intermediate and shallow water produce corresponding changes in the angle of wave incidence,  $\alpha$ . This process of wave refraction is a fundamental mechanism whereby the aspect and plan configuration of the nearshore zone modify the direction of wave incidence and cause redistribution of energy density and radiation stress. Wave refraction involves changes in the direction of wave rays which are the paths along which wave energy is radiated (i.e., lines parallel to the direction of wave propagation). In the case of long-crested swell, the rays are perpendicular to wave crests. The effect of wave refraction is to cause wave rays to become more normal to depth contours (crests to become more parallel to contours) as depth decreases or to become more oblique as depth increases.

The relationship between angle of incidence,  $\alpha$ , and wave phase speed,  $C$ , is expressed by Snell's Law:  $\sin\alpha/C = \text{constant}$ . From this principle the change in angle of incidence between any two consecutive points (designated 1 and 2) is simply

$$\sin \alpha_2 = \frac{C_2}{C_1} \sin \alpha_1 \quad \text{or relative to deepwater conditions} \quad (42)$$

$$\sin \alpha = \frac{C}{C_{\infty}} \sin \alpha_{\infty} \quad (43)$$

where  $C$  is obtained from Equation 11.

As with wave shoaling, the refraction process per se does not involve any net loss (or gain) of energy flux. However, a major consequence of wave refraction is that the total energy flux, which is conserved overall, is often concentrated or deconcentrated as the wave rays bend on approaching the shore. This produces, respectively, an increase or decrease in energy density and, hence, in wave height. If  $b_{\infty}$  represents the horizontal spacing between two adjacent wave rays in deep water and  $b$  represents the spacing between the same two rays at some point in shallow water after refraction, then conservation of energy flux requires that

$$E_f b = E_{f_{\infty}} b_{\infty} = \text{constant} \quad (44)$$

where  $E_f$  and  $E_{f_{\infty}}$  are respectively the energy fluxes per unit width of crest in shallow and deep water. Energy flux is thus concentrated when rays converge and deconcentrated when they diverge in accordance with

$$\frac{E_f}{E_{f_{\infty}}} = \frac{b_{\infty}}{b} \quad (45)$$

Since  $C_g$  is dependent only on depth and is independent of  $b$ , the only variable free to respond is  $E$  which varies only with  $H^2$ . The variation in wave height due to refraction is then simply

$$\frac{H}{H_{\infty}} = \left( \frac{b_{\infty}}{b} \right)^{\frac{1}{2}} = K_r \quad (46)$$

i.e., the quantity  $\left( \frac{b_{\infty}}{b} \right)^{\frac{1}{2}}$  is the refraction coefficient,  $K_r$  and, for the case of a straight beach with parallel depth contours

$$K_r = \left( \frac{b_{\infty}}{b} \right)^{\frac{1}{2}} = \left( \frac{\cos \alpha_{\infty}}{\cos \alpha} \right)^{\frac{1}{2}} \quad (47)$$

In the presence of complex topography (e.g., alternating promontories and embayments), refraction causes convergence of rays and  $K_r > 1$  off headlands

and over shoals and divergence and  $K_r < 1$  in embayments. This can produce appreciable alongshore variation in breaker height. Wave refraction is also produced by wave-current interactions. Current refraction of waves is not included in the analyses presented here; however, these effects are incorporated into a model currently being developed at VIMS.

Quite obviously, the increase in wave height with increasing  $K_r$  as expressed by equation 46 must have a limit. Otherwise  $H$  would approach infinity as  $b/b_\infty \rightarrow 0$ . Simple models predict wave rays to cross and, at the point of intersection,  $b = 0$ ; however, in nature this takes place without  $H$  becoming ludicrously large. In reality, the process of wave diffraction operates in regions of pronounced ray convergence to transmit energy along the direction perpendicular to the ray (i.e. along the wave "crest") from areas of highly concentrated energy (high waves) to areas of less concentrated energy (lower waves). A similar process is responsible for diffraction of wave energy around breakwaters, headlands and promontories. Unlike refraction, diffraction is related to the transfer of energy along the wave crest from regions of high  $H$  to regions of low  $H$  and is not caused primarily by depth changes. Computation of diffraction effects is more complicated and involves more than a simple analytical expression.

In practice, diffraction effects are computed numerically and concurrently with the effects of refraction and shoaling. The "RCPWAVE" model (Ebersole et al., 1986) treats, simultaneously, the complete wave transformation process (refraction, shoaling, diffraction) for linear waves propagating over bottom topography assumed to have mild slopes. The "mild slope" equation (Smith and Sprinks, 1975) is

$$\frac{\partial}{\partial x} \left( C C_g \frac{\partial \phi}{\partial x} \right) + \frac{\partial}{\partial y} \left( C C_g \frac{\partial \phi}{\partial y} \right) + \omega^2 \frac{C}{C} \phi = 0 \quad (48)$$

Ebersole et al. (1986) point out that this approach is good for application to nearshore regions of limited spatial extent but is impractical for estimating far-field transformations over long distances. Our use of the model has focused on a relatively small nearshore region. In carrying out the computations for modifications outside the surf zone, reflection of wave energy is assumed negligible and the diffraction effects in the direction of wave advance are considered negligible in comparison to diffraction effects normal to rays (Ebersole et al., 1986). Computational efficiency is increased by these simplifying assumptions which permit the forward scattering of the wave to be expressed by

$$\frac{\partial \phi}{\partial x} = \left[ ik - \frac{1}{2k CC_g} \frac{\partial}{\partial x} (k CC_g) \right] \phi + \frac{1}{2k CC_g} \frac{\partial}{\partial y} \left( CC_g \frac{\partial \phi}{\partial y} \right) \quad (49)$$

where  $i = \sqrt{-1}$  and  $x$  is defined as the principal direction of propagation (Ebersole et al., 1986).

### 3. Wave energy dissipation by bed friction and by wave-current interaction

The nearshore processes considered up to now have not involved any change in total energy flux. However, as waves move shoreward over a shoaling bed, frictional interactions between the bottom and the wave orbital currents cause an absolute expenditure of energy resulting in attenuation of wave height. The total amount of energy lost by frictional dissipation at the bed increases with increasing wave height, decreasing nearshore gradient and increasing bottom roughness. Where the continental margin and shoreface profile are narrow and steep, frictional dissipation of energy is small, relative to the effects of shoaling and refraction. However, over very flat, wide shoreface profiles such as that fronting

Virginia Beach, waves must travel long distances in relatively shallow water and many dissipate much of their energy before reaching the break point. Frictional dissipation of wave energy may be further enhanced when strong tidal or wind generated benthic currents supply additional Reynolds stresses to the combined wave-current boundary layer. We have added to "RCPWAVE" procedures for estimating wave height reduction due to friction.

The maximum bed shear stress,  $\tau_w$ , under waves is

$$\tau_w = \frac{1}{2} \rho f_w u_b^2 \quad (50)$$

and the time averaged (over a wave cycle) shear stress  $\langle \tau_w \rangle$  is

$$\langle \tau_w \rangle = \frac{2}{3\pi} \rho f_w u_b^2 \quad (51)$$

where  $f_w$  is a dimensionless friction factor (Jonsson, 1966),  $\rho$  is water density and  $u_b$  is given by equation 22. The corresponding rate of energy dissipation,  $D$ , is

$$D = - \frac{dE_f}{dx} = \langle \tau_w \rangle u_b = \frac{2}{3\pi} \rho f_w u_b^3 \quad (52)$$

The rate of dissipation increases with the cube of the wave height.

The total amount of energy dissipated by bottom friction between the seaward-most position  $x_\infty$  at which wave motion first interacts with the bed and any given inshore position,  $x$ , is equivalent to the total work done by the waves over the same region and involves a cumulative loss of energy. The total reduction,  $\delta E_f$ , in energy flux is estimated by integrating over the interval  $x_\infty - x$  (following the path of wave rays) the dissipation following

$$\delta E_f(x) = \int_{x_\infty}^x D dx \quad (53)$$

The local friction coefficient  $K_f(x)$  (eq. 40) at  $x$  is thus

$$K_f(x) = [1 - (\delta E_f(x)/E_{f_\infty})]^{1/2} \quad (54)$$

where  $E_{f_\infty}$  is the original (unattenuated) energy flux.

The critical quantity in analyses of frictional dissipation is the friction factor,  $f_w$ , which is analogous to the drag coefficients used for steady flows. In early studies (e.g. Bretschneider and Reid, 1954)  $f_w$  was assumed to be a small ( $\sim 0.01$ ) constant. Much recent laboratory and field data have shown that  $f_w$  is not constant and is not necessarily small. In fact, if the bed is very rough and/or if large quantities of sand are in motion,  $f_w$  can be quite large. Our present understanding of the significance of  $f_w$  and its variability is inherited primarily from Jonsson (1966), Kamphuis (1975), Swart (1974), and Grant and Madsen (1982). In particular, we now consider  $f_w$  to vary with the relative total bed roughness  $k'_b/a_b$  where  $k'_b$  is the apparent roughness height and  $a_b = u_b/\omega$  is the orbital semi-excursion at the top of the wave boundary layer (i.e. near the bed). For large roughnesses,  $k'_b$ ,  $f_w$  can have values up to 0.24, 0.30, or larger (Grant and Madsen, 1982; Swart, 1974; Nielsen, 1983). The empirical expression obtained by Swart (1974) applies when  $(k'_b/a_b) < 0.63$  and is the most convenient:

$$f_w = e^{[5.213(k'_b/a_b)^{0.194} - 5.977]} \quad (55)$$

The apparent or effective bed roughness,  $k'_b$ , is significantly increased when sediment is in motion and when ripples are present. The amplitude of the moveable bed roughness depends on the magnitude of the actual wave-induced skin friction Shield's parameter  $\tilde{\Psi}$  relative to the critical Shield's

parameter  $\Psi_c$  necessary for the initiation of sediment transport. The contribution of wave-generated bed ripples depends on the ripple height,  $\eta$  and length,  $\lambda$ . Considering the combined effects of moveable bed roughness and a rippled bed on the apparent roughness,  $k'_b$ , Grant and Madsen (1982) give

$$\frac{k'_b}{a_b} = 160 \left( \frac{\rho_s}{\rho} + C_m \right) \frac{D_s}{a_b} \Psi_c [(\tilde{\Psi}/\Psi_c)^{1/2} - 0.7]^2 + 28 \frac{\eta^2}{a_b \lambda} \quad (56)$$

where  $\rho_s$  and  $\rho$  are sediment and water densities, and  $C_m$  is a mass coefficient ( $= \frac{1}{2}$  for spheres). Nielsen et al. (1982), on the other hand, give the simpler relationship

$$k'_b = 190 (\tilde{\Psi} - 0.05)^{1/2} D_s + 8 \eta^2 / \lambda \quad (57)$$

based on several data sets. In Nielsen's expression, the critical Shield's parameter  $\Psi_c$  is assumed to be 0.05. Obviously, this assumption cannot be made when the bottom is muddy or when organisms are influencing the sediment properties;  $\Psi_c$  will vary with the substrate type and conditions. When the excess shear stress becomes large, the ripples or biogenic roughness elements can be expected to vanish and moveable bed roughness will dominate.

Over the majority of shoreface beds, current boundary layers interact with wave boundary layers. It was recognized over fifteen years ago by Lundgren (1972) that wave-induced oscillations near the bottom of a current boundary layer add to the friction of the latter by providing additional eddy viscosity. Grant and Madsen (1979) developed a model that considers the combined shear stresses and eddy viscosities due to both waves and currents. Christofferson and Jonsson (1985) addressed the question of how current boundary layers add to the frictional effects "felt" by the waves.

Although the role of currents in enhancing wave friction is implicit in the Grant and Madsen (1979) model, the importance of this effect has been emphasized mainly by Christofferson and Jonsson (1985) who showed that the current causes an increase in the wave friction factor,  $f_w$ . The effect increases with increasing current velocity and decreasing angle between the current and wave incidence, i.e. when wave incidence is orthogonal to the current, the enhancement of  $f_w$  is least but is not negligible. The numerical model developed by M. O. Green and used in this study incorporates the Christofferson and Jonsson (1985) equations for current enhancement of wave friction as well as the effects of moveable bed and rippled bed roughness. Green (pers. comm.) applied the model to a set of near-bed current and wave data from the Middle Atlantic Bight shoreface (Duck, North Carolina). Although the measured near-bottom mean currents ( $z = 1$  m) exceeded  $35 \text{ cm s}^{-1}$ , the increased wave friction due to the current was only 15% of the total friction at a depth of 18 m and 5% at a depth of 8.5 m. For this reason and because of limited data on spatial variations in bottom currents off Virginia Beach, this effect has been neglected in our study.

#### 4. Breakers and surf

Linear assumptions do not apply to the processes of wave breaking and turbulent dissipation within the surf zone. For predicting wave transformations inside the surf zone, "RCPWAVE" employs empirical methods. To estimate the rate of energy flux decay across the surf zone, this model makes use of procedures developed by Dally et al. (1984).

Breaking of waves occurs when the ratio of breaker height,  $H_b$  to depth,  $h_b$ , attains some critical maximum which in older studies was assumed to be constant with a typical value of 0.78. However, empirical

studies have shown that the critical ratio is not constant but depends on bottom slope,  $\beta$ , and wave period  $T$ . The empirical equation of Weggel (1972) which is used in "RCPWAVE" for predicting the breaking condition is

$$H_b = \frac{b^*h_b}{1 + \left(\frac{b^*a^*}{g T^2}\right)} \quad (58)$$

where  $a^* = 43.75 [1 - e^{(-19 \tan\beta)}]$  and  
 $b^* = 1.56/[1 + e^{(-19.5 \tan\beta)}]$

Within the surf zone, after breaking has occurred, the local height,  $H_b(x)$  of the waves (or bores) remains limited by local depth,  $h(x)$ , and for the simple case of a saturated surf zone of constant bed slope  $\beta$

$$H_b(x) / h(x) = \gamma = \text{constant} \quad (59)$$

Field observations show that  $\gamma$  values in natural dissipative surf zones are typically much lower than the values ( $\gamma = 0.8 - 1.2$ ) observed in the laboratory for monochromatic waves. Wright et al. (1982) found, for example, that in a fully dissipative high energy surf zone with spilling breakers,  $\gamma$  was as low as 0.42. In "RCPWAVE"  $\gamma$  is assumed to be 0.4.

When the surf zone morphology is complex, for example when bar-trough topography is present, the surf zone may not be at all saturated (e.g. Wright et al., 1986b). In such cases,  $H_b(x)$  may be small enough or  $h(x)$  may be large enough for the ratio  $H_b(x)/h(x)$  to be less than the limiting value of  $\gamma$  and the surf zone will not be saturated. Unlike many models, "RCPWAVE" does not assume surf saturation. The rate of dissipation,  $D_s$ , of energy flux in the surf zone is expressed by

$$D_s = \frac{dE_f}{dx} = -\frac{K}{h} (E_f - E_{fs}) \quad (60)$$

where  $\kappa$  is a coefficient expressing the rate of energy dissipation due to the combined effects of all dissipative processes (turbulence, friction, etc.) and is set equal to 0.2 in "RCPWAVE", and  $E_{f_s}$  is the "stable" local energy flux which would be permitted if the surf zone were saturated, i.e.

$$E_{f_s} = \frac{1}{8} \rho g \gamma^2 h^2 C_g$$

By dropping the constants  $\frac{1}{8} \rho g$ , equation 60 can be rewritten

$$\frac{d(H^2 C_g)}{dx} = -\frac{\kappa}{h} \left[ H^2 C_g - (\gamma^2 h^2 C_g)_s \right] \quad (61)$$

where the subscript  $s$  designates the "stable" limiting condition.

Both inside and outside of the surf zone, gradients in  $H$  cause corresponding gradients in radiation stress  $S_{xx}$  (eq. 32). Since, in shallow water,  $S_{xx}$  varies only with  $H^2$  in accordance with equation 36, the radiation stress follows the gradient in  $H^2$  or in other words

$$\frac{d S_{xx}}{dx} = \frac{3}{16} \rho g \frac{dH^2}{dx} \quad (62)$$

Momentum balance requires that changes in momentum flux  $S_{xx}$  be balanced by a pressure gradient; this is achieved inside the surf zone by dissipation being accompanied by a setup,  $\bar{\eta}$ , of mean level above the still water level. The pressure gradient due to a slope in  $\bar{\eta}$  is related to  $dS_{xx}/dx$  by

$$\rho g (h + \bar{\eta}) \frac{d\bar{\eta}}{dx} = -\frac{dS_{xx}}{dx} \quad (63)$$

(e.g. Longuet-Higgins and Stewart, 1962; Bowen et al., 1968). If the surf zone is saturated and has a constant bed slope,  $\beta$

$$\frac{d\bar{\eta}}{dx} = -\tan\beta \left[ 1 + \frac{8}{3\gamma^2} \right]^{-1} \quad (64)$$

(Bowen et al., 1968) and the maximum setup which occurs at the beach will be

$$\bar{\eta}_{\max} = \frac{3}{8} \gamma H_b \quad (65)$$

(Svendsen and Jonsson, 1976).

## B. Modelling Results

### 1. Temporal and spatial variability of wave modifications over the shoreface

The modified "RCPWAVE" model was run for 58 different sets of incident ("deepwater") wave height ( $H_{\infty}$ ), period (T), and initial incident angle ( $\theta_{\infty}$ ). In addition to three representative case types, analyses were performed on 55 different combinations of  $H_{\infty}$ , T, and  $\theta_{\infty}$  selected from wave conditions observed at the Field Research Facility at Duck, N.C. over the entire year 1982. Table IV-1 lists the 55 different incident wave conditions considered for the representative year 1982; the temporal variability of these conditions is large and, correspondingly, there is considerable temporal variability in the degree of shoreface modifications. Owing to the complex morphology of the shoreface, there is also considerable spatial variability in the degree to which the waves are modified before they reach the surf zone.

To illustrate the spatial variability in shoreface wave transformations, three cases have been selected for detailed discussion and graphic illustration: (1) the typical or "modal wave" case characterized by normally-incident waves from the east with a height of 1.0 m and a period of 9 seconds; (2) a wave from the northeast typical of those generated by moderate northeasterly storms ("northeasters") and having a height of 2.1 m and a period of 8 seconds; and (3) a "design" wave, incident from the east with a height of 6.0 m and a period of 15 seconds, similar to the "hurricane

Table IV-1

Wave conditions used in model runs from wave conditions observed at the U.S. Army Corps of Engineers Field Research Facility, Duck, North Carolina, for the year 1982

Case #	$H_{\infty}$ (m)	T (s)	$\theta_{\infty}$ (deg)	No. of Days	Case #	$H_{\infty}$ (m)	T (s)	$\theta_{\infty}$ (deg)	No. of Days
1	0.5	5	90	5	29	1.0	7	45	11
2	0.5	7	90	7	30	1.0	9	45	10
3	0.5	9	90	17	31	1.0	11	45	3
4	0.5	11	90	18	32	1.0	15	45	2
5	0.5	15	90	10	33	1.5	5	45	2
6	1.0	5	90	4	34	1.5	7	45	11
7	1.0	7	90	10	35	1.5	9	45	4
8	1.0	9	90	17	36	2.0	5	45	1
9	1.0	11	90	7	37	2.0	7	45	9
10	1.0	15	90	5	38	2.0	9	45	1
11	1.5	5	90	1	39	3.5	9	45	1
12	1.5	7	90	8	40	0.5	5	135	8
13	1.5	9	90	8	41	0.5	7	135	15
14	1.5	11	90	2	42	0.5	9	135	24
15	2.0	7	90	6	43	0.5	11	135	16
16	2.0	9	90	2	44	0.5	15	135	7
17	2.0	11	90	5	45	1.0	5	135	1
18	2.0	15	90	1	46	1.0	7	135	13
19	2.5	9	90	3	47	1.0	9	135	14
20	2.5	15	90	1	48	1.0	11	135	7
21	3.5	9	90	1	49	1.0	15	135	2
22	3.5	11	90	3	50	1.5	5	135	1
23	0.5	5	45	2	51	1.5	9	135	4
24	0.5	7	45	5	52	1.5	11	135	2
25	0.5	9	45	1	53	2.0	9	135	1
26	0.5	11	45	6	54	3.5	11	135	2
27	0.5	15	45	3	55	3.5	15	135	1
28	1.0	5	45	5					

$H_{\infty}$  = significant deepwater wave height (meters).

T = wave period (seconds).

$\theta_{\infty}$  = azimuth of wave incidence in deepwater (90°: waves from east;  
45°: waves from northeast; 135°: waves from southeast).

waves" which are occasionally generated when a severe tropical storm lies to the southeast of the region. The "hurricane wave" case is based on observations at the FRF of Hurricane Gloria in September, 1985. All three of these cases are documented in the field data collected at the Duck, North Carolina Field Research Facility. In addition, VIMS has made direct measurement of the shoreface bottom boundary layer processes which accompany the "modal" - and "northeaster" - type waves.

Figure IV-1 shows wave height variations over the shoreface as predicted for the modal wave from the east ( $H_b = 1.0$  m,  $T = 9.0$  s) without considering the effects of frictional dissipation. The corresponding wave height patterns as predicted with the effects of bottom friction included in the analysis are illustrated in Figure IV-2. Several important features are apparent in Figures IV-1 and IV-2. If the effects of friction were ignored, as illustrated in Figure IV-1, wave heights would increase in the nearshore region as a consequence of wave shoaling; breaker heights,  $H_b$ , would significantly exceed deepwater wave height  $H_\infty$ . In reality, of course, frictional effects are present and Figure IV-2 probably represents the more realistic situation. Wave height reductions due to friction exceed increases due to shoaling with the result that  $H_b < H_\infty$ . From Figure IV-2, it can be seen that the heights of frictionally dissipated, shoaled, refracted, and diffracted "modal" waves are moderately uniform over most of the shoreface region. This comparative uniformity is characteristic of fairweather waves in general. There is, however, a tendency for breaker heights to be somewhat higher in the vicinity of Sandbridge (sectors 240-220) than elsewhere.

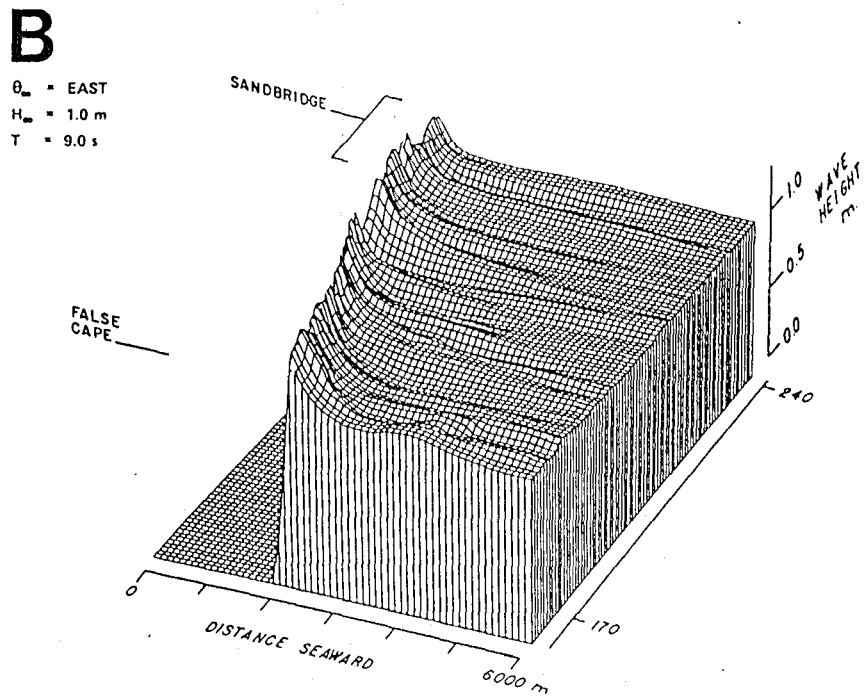
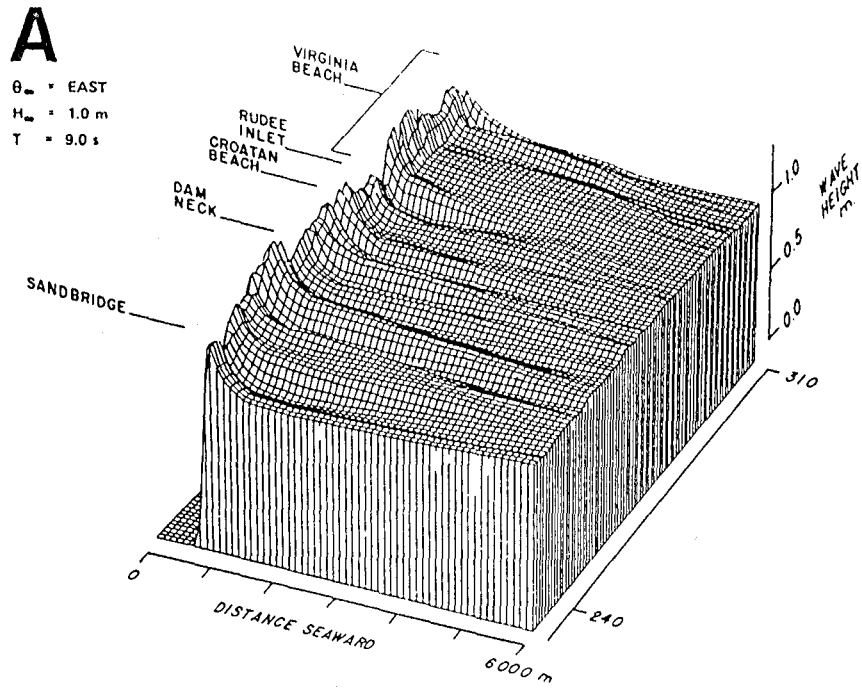


Figure IV-1. Predicted spatial variations in wave height for modal waves from the east with frictional dissipation ignored. A, northern sectors and B, southern sectors.

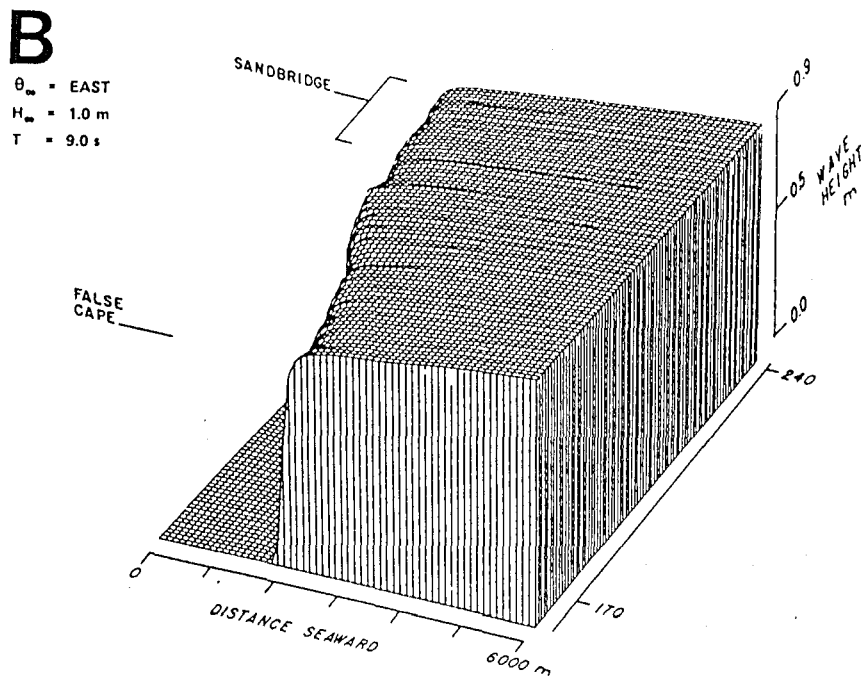
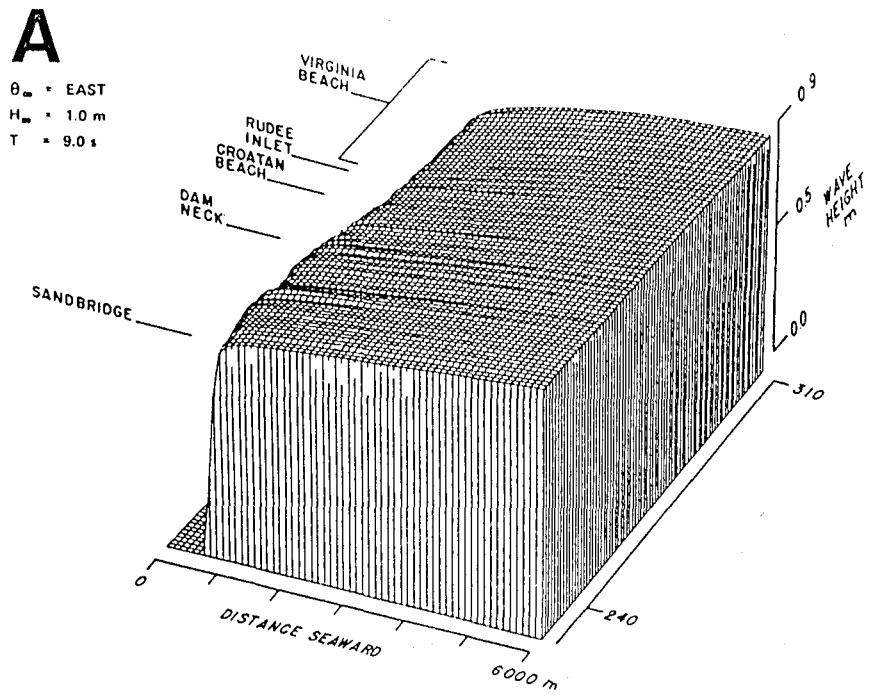


Figure IV-2. Predicted spatial variations in wave height for modal waves from the east with frictional dissipation considered.

The spatial variability of local wave and breaker heights increases dramatically as deepwater height,  $H_{\infty}$ , increases. The "without friction" and "with friction" wave height predictions for a typical northeaster-generated deepwater wave ( $\theta_{\infty}$  = northeast,  $H_{\infty}$  = 2.1 m,  $T$  = 8.0 s) are illustrated in Figures IV-3 and IV-4 respectively. The corresponding model results for the extreme "hurricane" wave, arriving from the east with an initial deepwater height,  $H_{\infty}$  of 6 meters and a period of 15 seconds are shown in Figures IV-5 and IV-6. The northeaster waves show nearshore minima over the reach from Virginia Beach to Croatan Beach (sectors 320-260) and near False Cape (sectors 160-170). A distinct region of increased nearshore wave height prevails off Sandbridge and immediately to the south of Sandbridge. The same pattern of spatial variability of nearshore wave height characterizes the hurricane wave analyses except that the relative nearshore wave height reductions and alongshore differences in breaker height are much greater for the hurricane wave case.

## 2. The role of bottom friction

From Figures IV-1, IV-3, and IV-5 it is apparent that refraction, if that process acted without accompanying friction, would produce substantial alongshore variations in wave height. As it happens, however, friction acts to reduce some of the variability caused by refraction. Since the rate of frictional dissipation is proportional to the cube of the wave height, areas with large refraction coefficients experience more frictional dissipation and hence lower friction coefficients. It is this partial opposition between refraction and frictional effects that accounts for the "smoother" wave height distributions shown in Figures IV-2, IV-4, and IV-6.

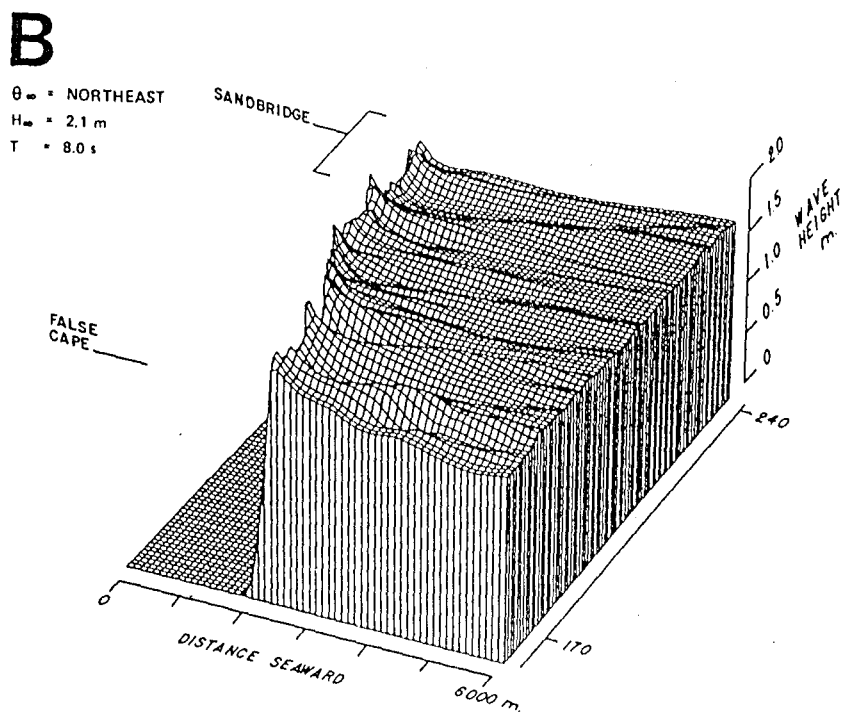
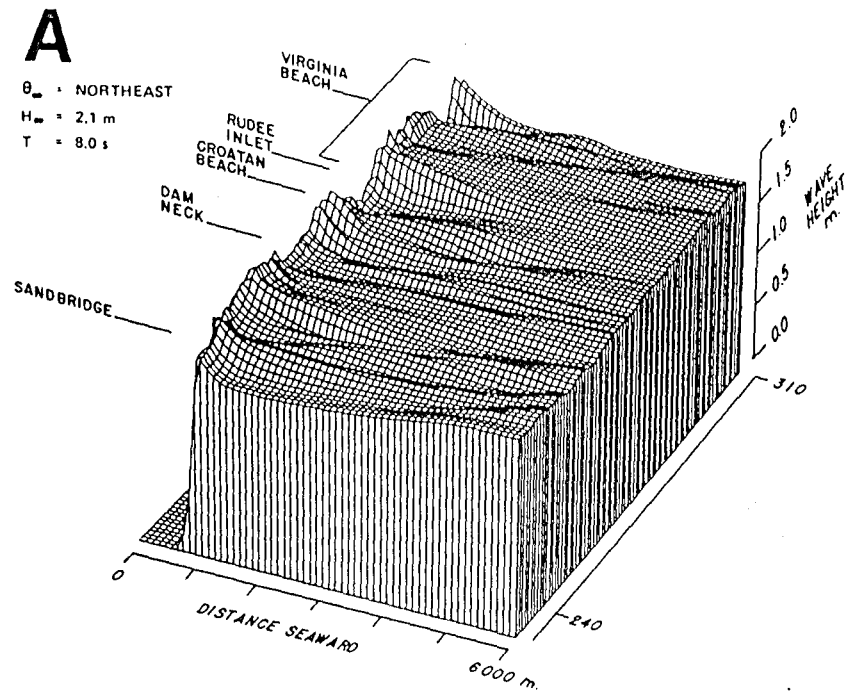
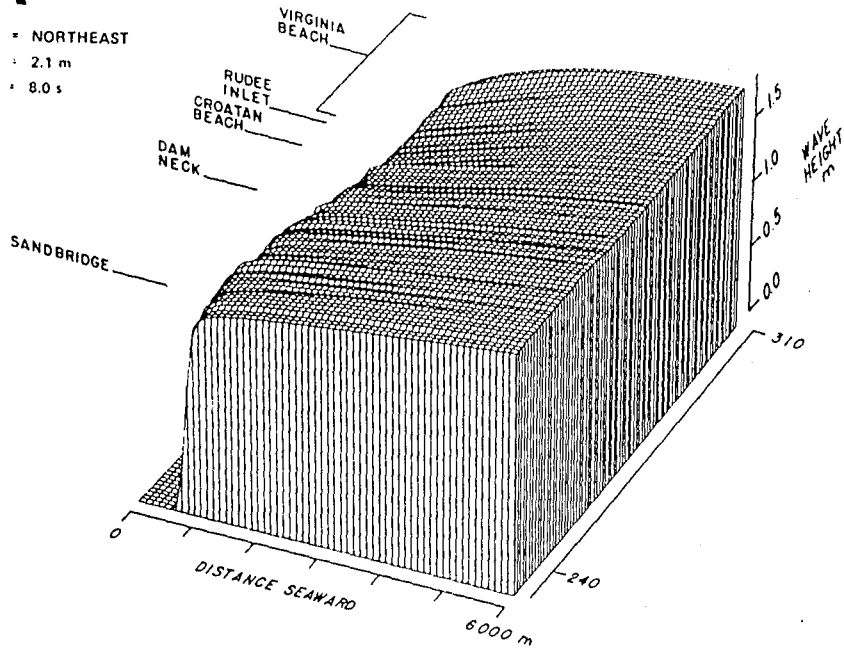


Figure IV-3. Predicted spatial variations in wave height for waves generated by a typical northeaster with frictional dissipation ignored.

**A**

$\theta_w =$  NORTHEAST  
 $H_w = 2.1$  m  
 $T = 8.0$  s



**B**

$\theta_w =$  NORTHEAST  
 $H_w = 2.1$  m  
 $T = 8.0$  s

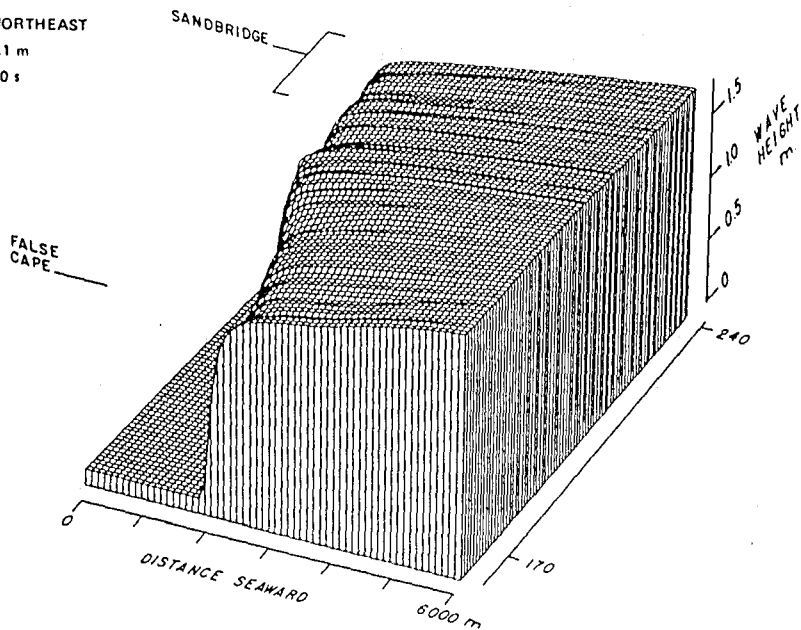


Figure IV-4. Predicted spatial variations in wave height for waves generated by a typical northeaster with frictional dissipation considered.

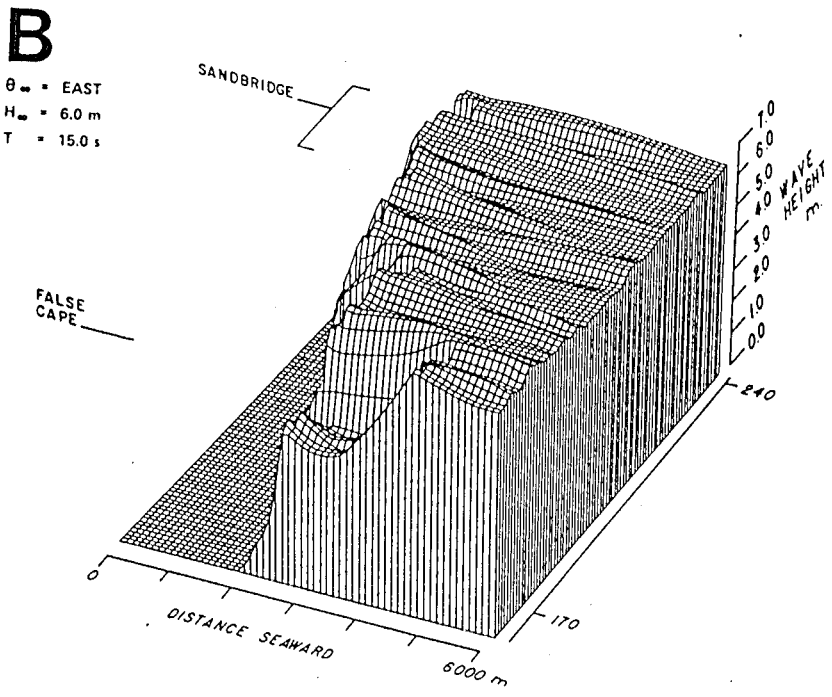
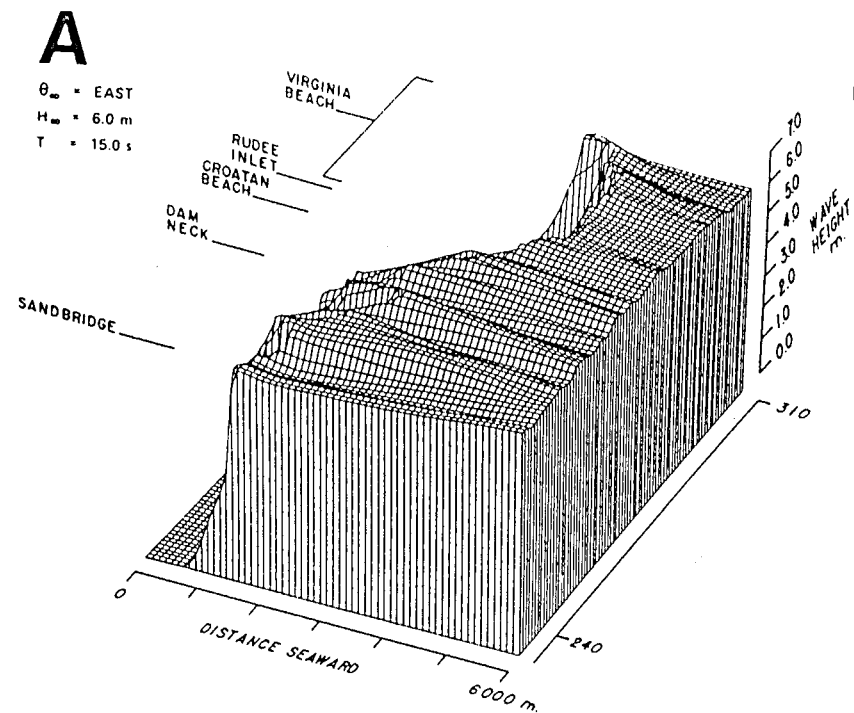
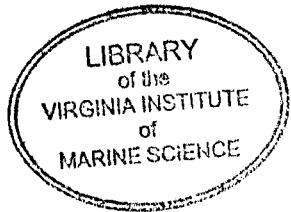


Figure IV-5. Predicted spatial variations in wave height for waves generated by a hurricane (based on deepwater waves observed during Hurricane Gloria in 1985) with frictional dissipation ignored.

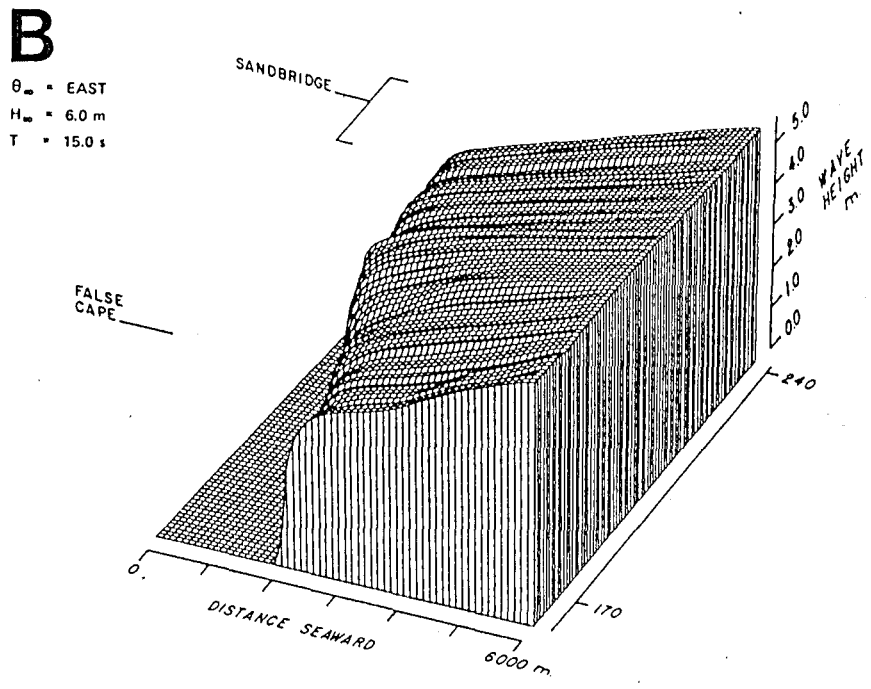
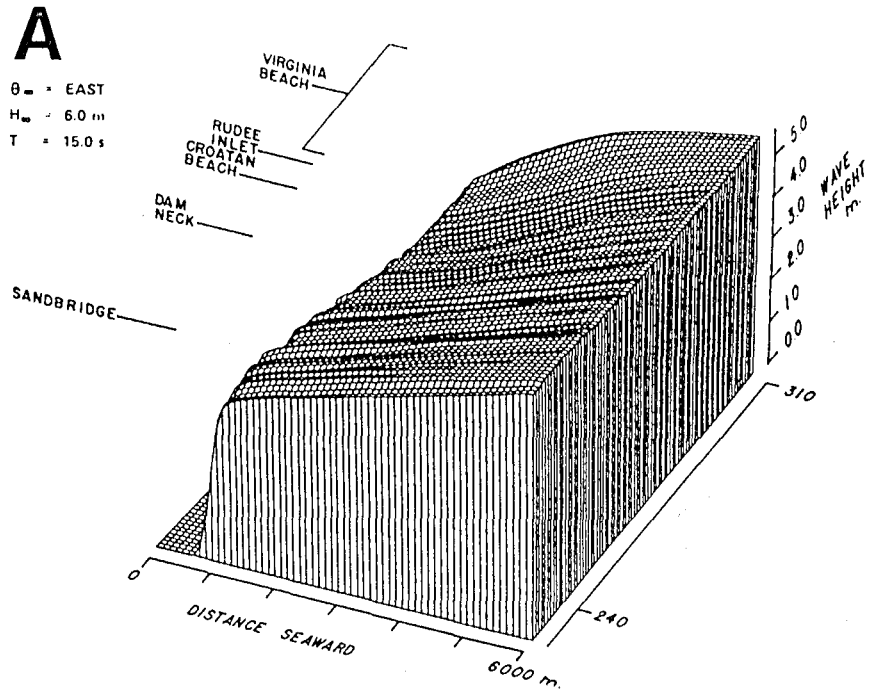


Figure IV-6. Predicted spatial variations in wave height for waves generated by a hurricane with frictional dissipation considered.

Most importantly, there is more frictional dissipation over the shallower, lower gradient regions of the shoreface than there is over the deeper, steeper regions. This is the main reason why nearshore wave heights offshore of the Virginia Beach resort strip are lower than the regional average and those off Sandbridge are higher than the regional average. To illustrate the role played by frictional dissipation, Figures IV-7 - IV-9 illustrate the shoaling transformations with friction ignored (solid curve) and friction included (dashed curve) over profile 290 off Virginia Beach and profile 220 off Sandbridge of the "modal", "northeaster", and "hurricane" wave types. The locations of the two profiles are indicated in Figure I-2 and the profile configurations are shown in Figure II-2.

Ignoring friction leads to predictions that all waves on both profile examples should undergo a shoreward increase in height outside the surf zone followed by a rapid decrease inside the surf zone. Inclusion of frictional dissipation in the model results predicts a progressive decrease in wave height for all cases; this decrease is most pronounced for the largest waves and for the shallower, lower gradient profile (290). Breakers associated with the modal wave are 65 cm lower after traversing profile 290 than would be the case if no frictional dissipation occurred. Breakers off Sandbridge are lowered by 45 cm. In this case, however, the breaker height on profile 220 is only 10 cm greater than that on profile 290 because the refraction coefficients are higher nearshore on profile 290. Breakers related to the moderate northeasterly waves are 20 cm higher off Sandbridge than off Virginia Beach (Fig. IV-8). The difference is vastly more significant where the large, destructive hurricane waves are concerned. Without frictional dissipation, the "hurricane wave" breakers would be 7 meters (23 ft) high on

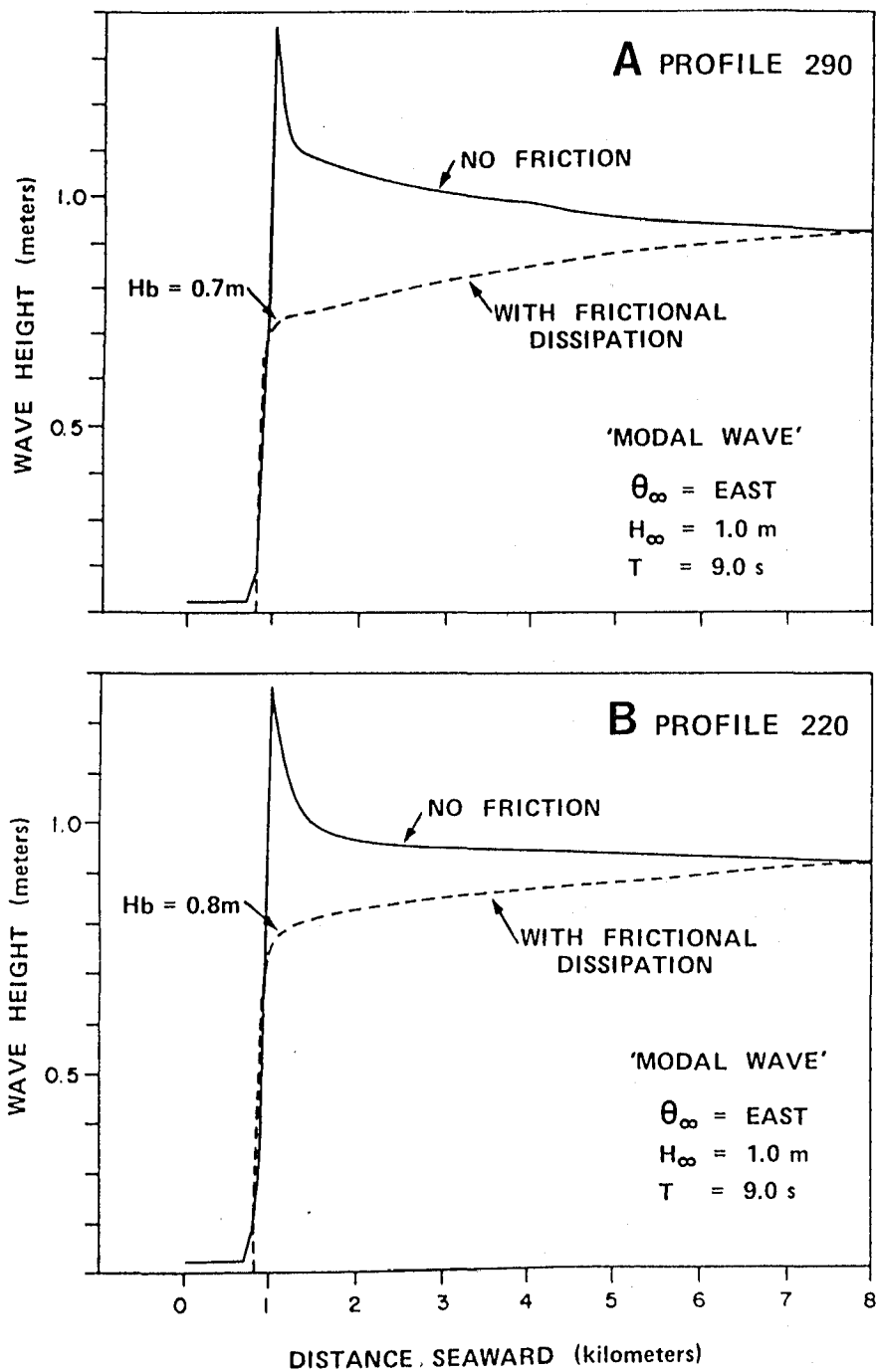


Figure IV-7. Predicted cross-shore changes in the height of the modal waves with frictional dissipation ignored (solid curve) and considered (dashed curve) for: (A) profile 290; and (B) profile 220. The profile locations are shown in Figure I-2.

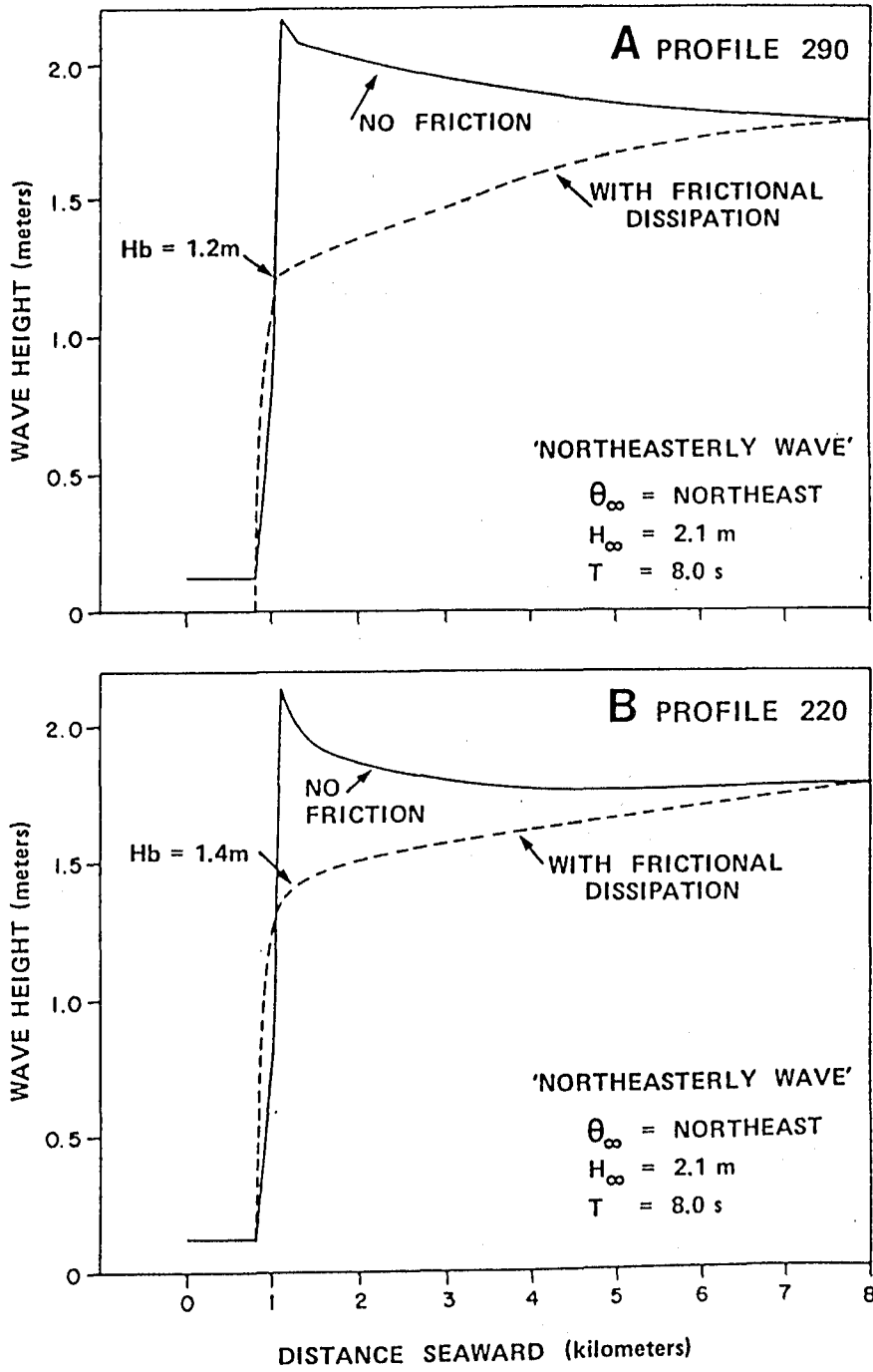


Figure IV-8. Predicted cross-shore changes in the height of "northeasterly" waves with frictional dissipation ignored (solid curve) and considered (dashed curve).

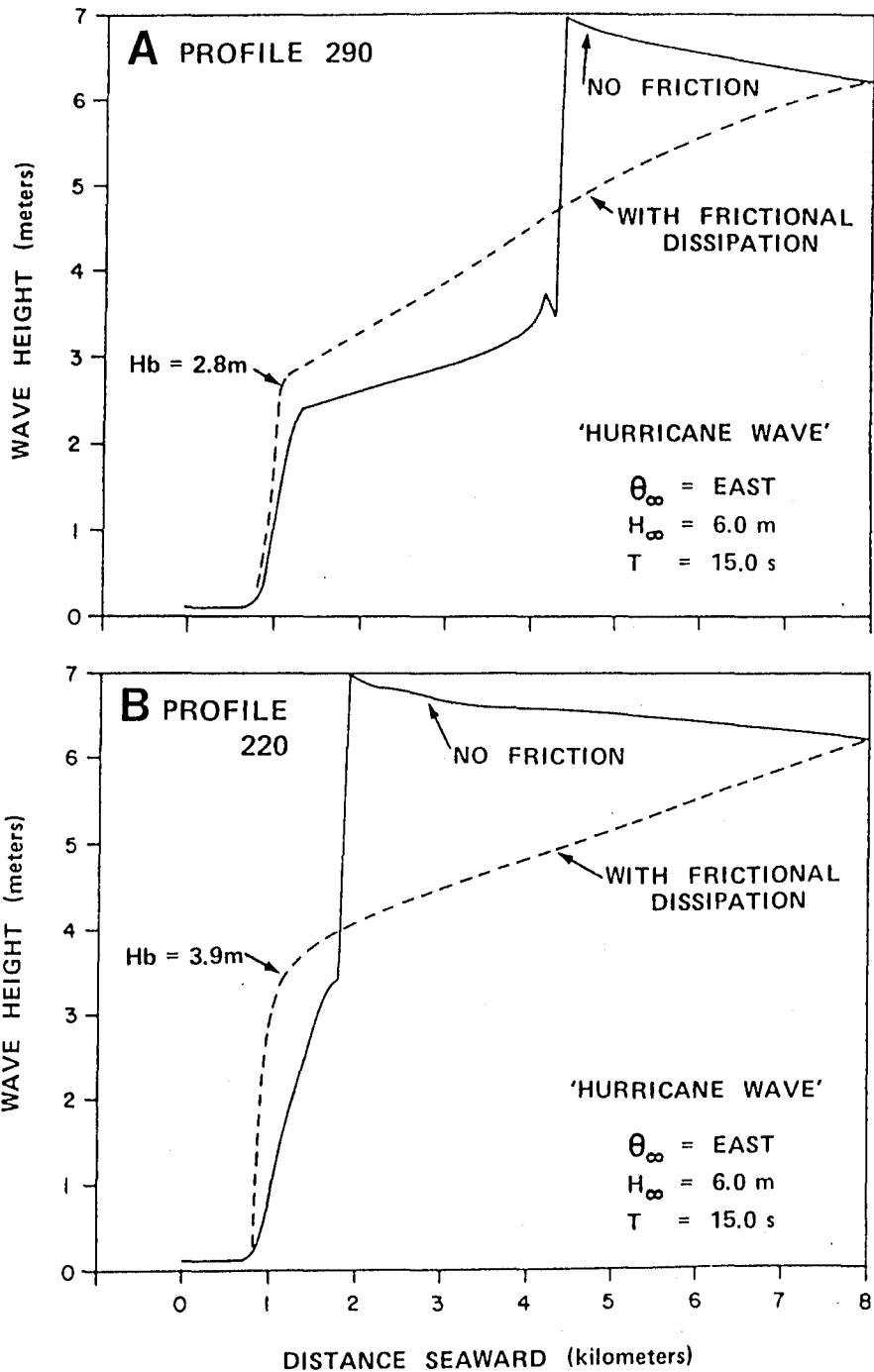


Figure IV-9. Predicted cross-shore changes in the height of "hurricane" waves with frictional dissipation ignored (solid curve) and considered (dashed curve). Note that frictional dissipation causes breakers on profile 290 to be 1.1 m lower than those on profile 220.

both profiles (Fig. IV-9). However, friction limits the breaker height on profile 290 to 2.8 meters (9.2 ft). In contrast, less intense frictional dissipation over profile 220 permits breakers as high as 3.9 m (12.8 ft) to occur off Sandbridge.

### 3. Breakers and surf

From the perspective of beach stability and behavior, it is the energy and momentum flux (radiation stress) entering the surf zone that are important. Both quantities are proportional to the square of the wave height; the height of the setup at the shore is directly proportional to the breaker height. Figures IV-10, IV-11, and IV-12 respectively summarize for the "modal", "northeaster" and "hurricane" wave cases, the corresponding alongshore variation, by sector, of maximum surf zone width,  $x_b$ , breaker height,  $H_b$ , and breaker angle  $\alpha_b$ . Estimates of  $x_b$  are crude, owing to the lack of detailed bathymetric data from the surf zone and shallow nearshore region. The values of  $x_b$  shown were determined from  $x_b = H_b / \tan \beta_n$  where  $\beta_n$  is the mean nearshore gradient seaward of the surf zone. The resulting values are thus likely to overestimate the true surf zone width in most cases. Breaker angles are zero for normally incident waves; angles are positive for waves obliquely incident from the north and negative for waves obliquely incident from the south.

The mean breaker heights for the "typical year" based on the 55 cases for 1982 are summarized for each alongshore sector in Figure IV-13. In determining the means, the values predicted for each of the 55 wave cases were weighted by the relative fraction in time that particular set of conditions prevailed in 1982 (Table IV-1). On average, breaker heights off the northern sectors (Croatan Beach, Virginia Beach, sectors 260-310) are

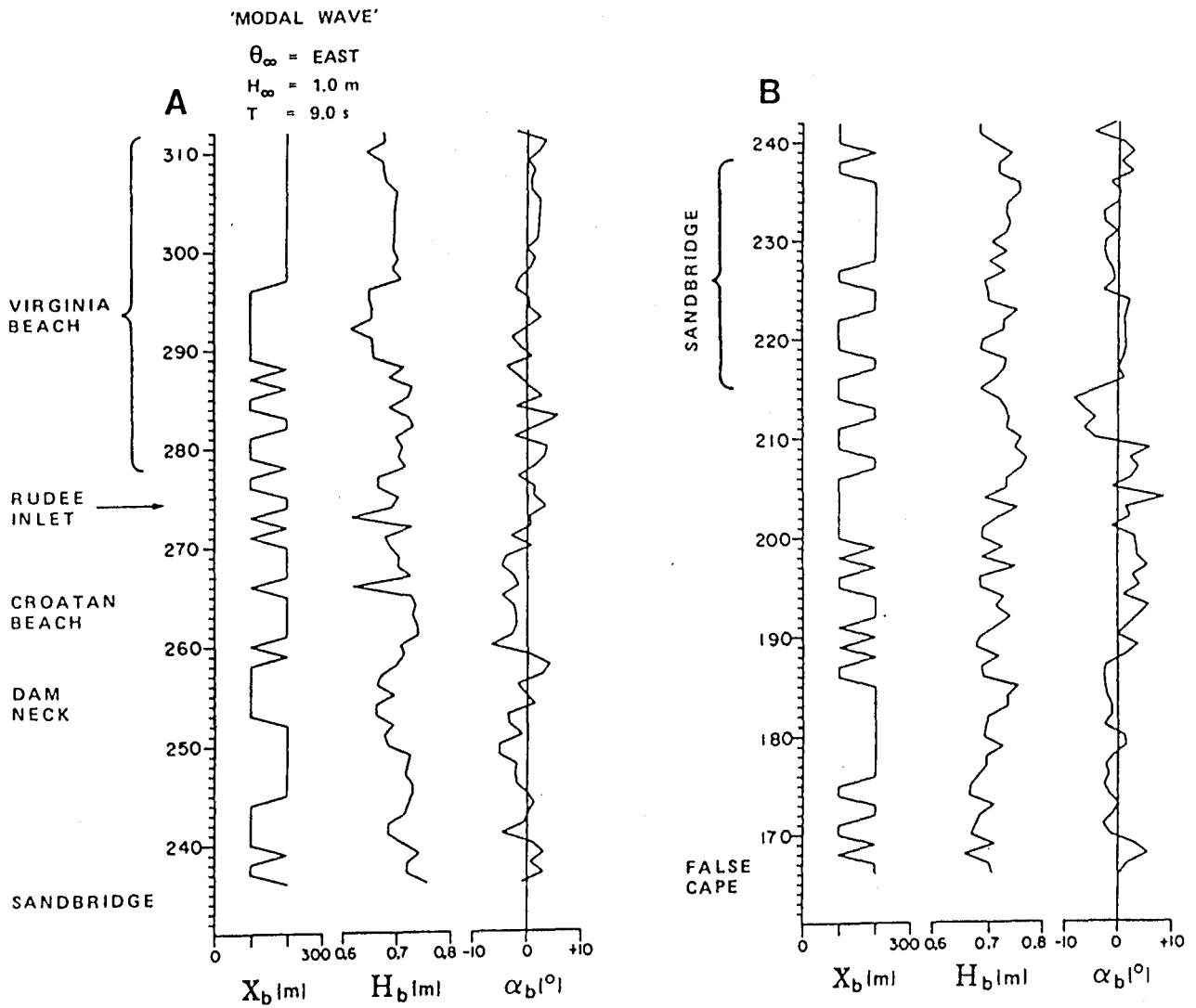


Figure IV-10. Predicted alongshore variations in surf zone width ( $x_b$ ), breaker height ( $H_b$ ), and breaker angle ( $\alpha_b$ ) for the "modal" wave case.

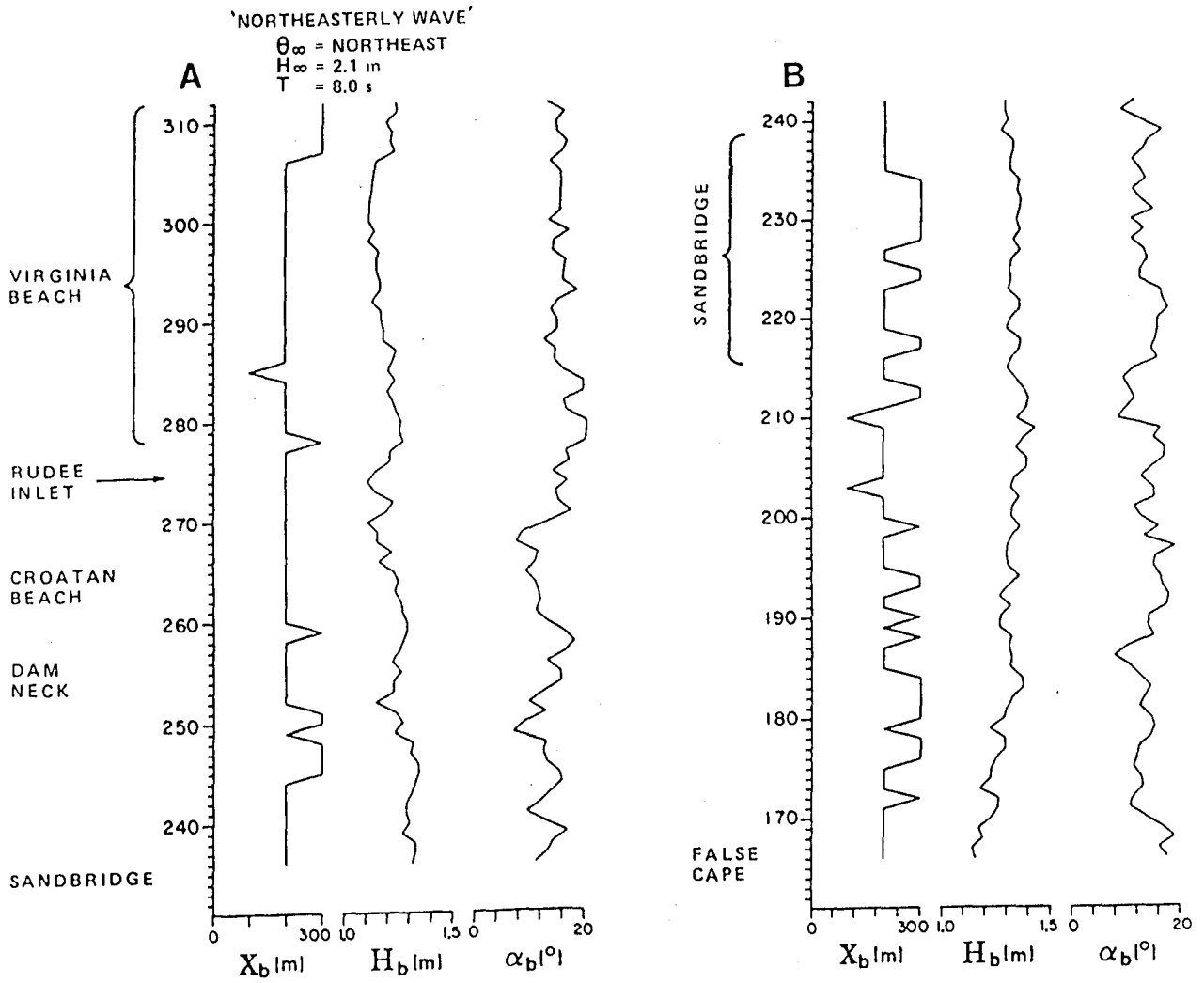


Figure IV-11. Predicted alongshore variations in surf zone width ( $x_b$ ), breaker height ( $H_b$ ), and breaker angle ( $\alpha_b$ ) for the "northeaster" wave case.

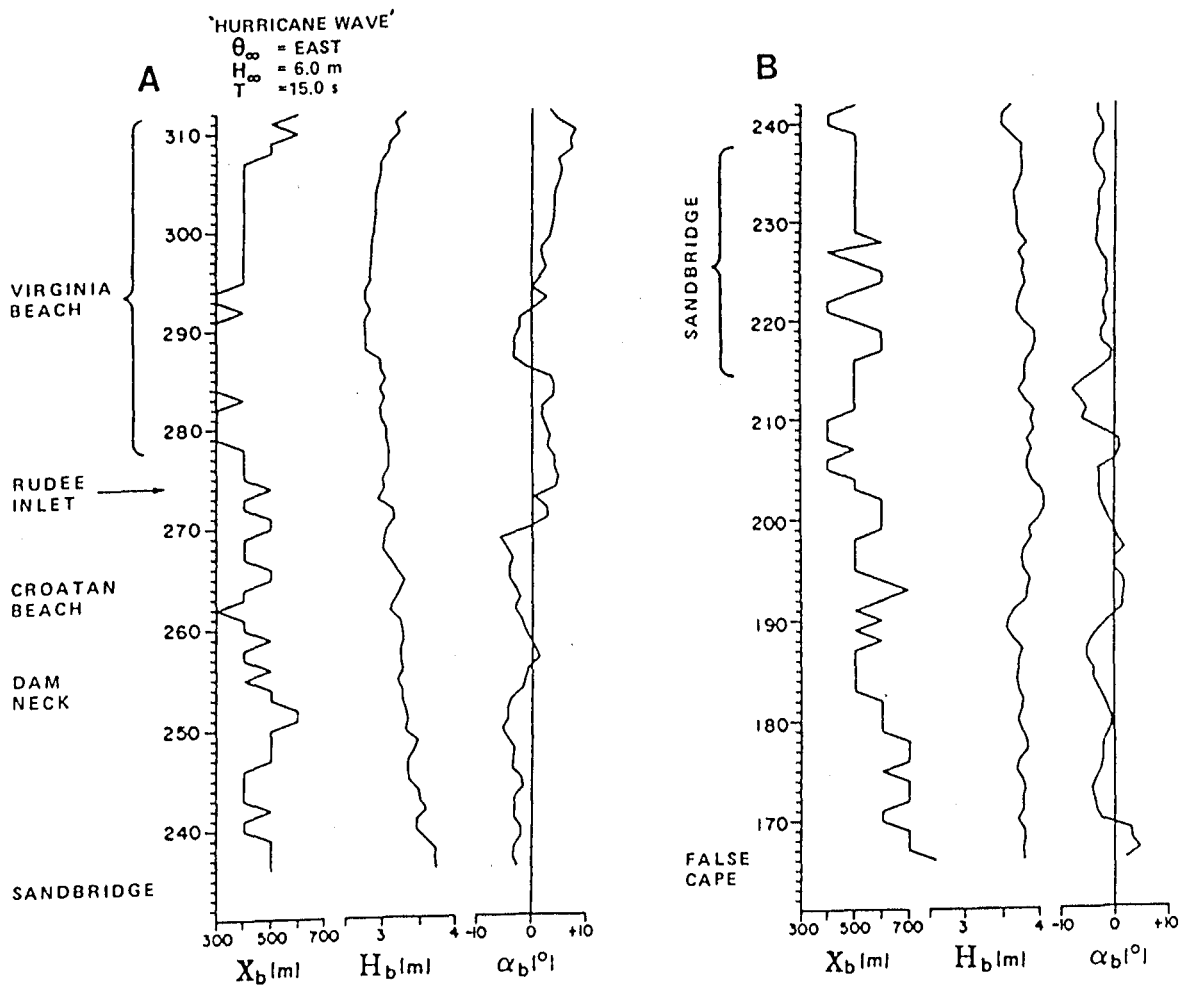


Figure IV-12. Predicted alongshore variations in surf zone width ( $x_b$ ), breaker height ( $H_b$ ), and breaker angle ( $\alpha_b$ ) for the "hurricane" wave case.

AVERAGES FOR 1982

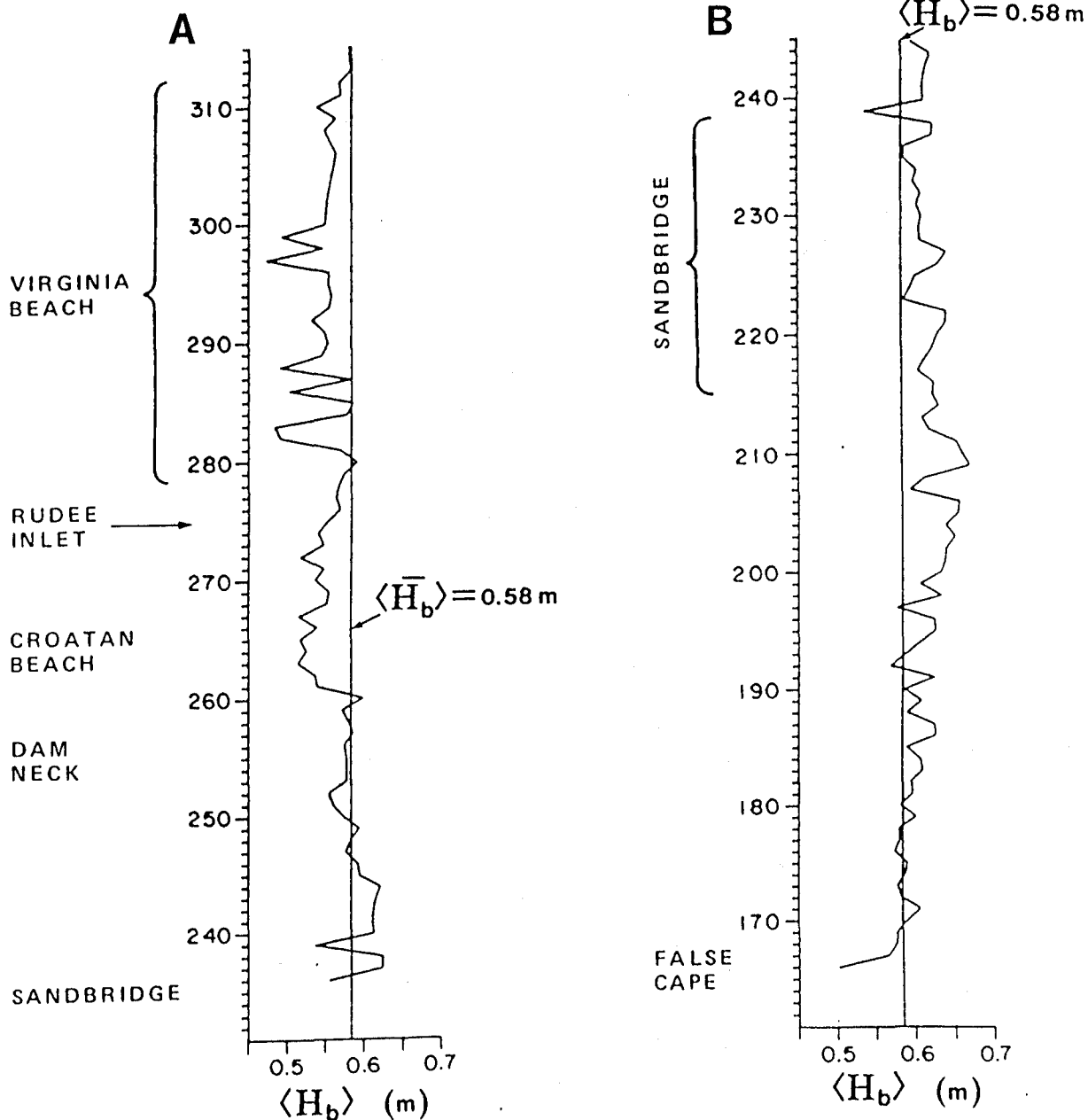


Figure IV-13. Predicted alongshore variations in time-averaged breaker height,  $\langle H_b \rangle$ , based on 55 wave cases observed in 1982. The means were determined by weighting the values obtained for each case by the percentage of time the particular waves prevailed during 1982.

lower than the regional average whereas those off the southern sectors (Sandbridge and south of Sandbridge, sectors 190-240) are higher than the regional average. From Figures IV-10 - IV-13 it is clear that there are significant alongshore gradients in breaker height. Together with breaker angle,  $\alpha_b$ , these gradients in breaker height determine the direction and intensity of longshore sand transport or littoral drift which is the subject of the following section.

## V LITTORAL DRIFT AND LITTORAL DRIFT GRADIENTS AS CONTRIBUTORS TO NET BEACH EROSION OR ACCRETION

### A. Background

The rates and directions of shore-parallel sand transport have fundamental impacts on the stability of beaches. In a general sense, longshore (or parabolic) transport can be partitioned into two parts: (1) "littoral drift" which takes place primarily within the surf zone up to the limit of wave runup; and (2) longshore transport seaward of the surf zone over the shoreface and inner shelf. Although this report deals only with the former, the latter mode is also important. In most instances, longshore sand transport is driven by one or more of four main mechanisms: (1) obliquely-incident breaking waves; (2) longshore pressure gradients in the surf zone induced by longshore variations in breaker height and setup; (3) currents induced by shore-parallel wind stress; and (4) shore parallel tidal currents. Whereas littoral drift landward of the break point is largely dominated by mechanisms 1 and 2 (or so it is assumed in classical models), mechanisms 3 and 4 are the main contributors to transport seaward of the surf zone.

#### 1. Classical formulae and their limitations

The most popular and widely used approach to estimating littoral drift has involved relating the total shore-parallel sediment mass transport rate,  $j_\ell$ , or volume transport rate  $q_\ell$ , including both beach drifting in the swash zone and suspended and bed load transport in the surf zone to a quantity called "longshore power",  $P_\ell$ . We use the quote marks because the term is conceptually inaccurate. The general form of the formula is

$$j_\ell = K P_\ell \quad \text{or} \quad q_\ell = K P_\ell \quad (66)$$

where K is an empirically determined coefficient which simply expresses the observed ratios between  $q_\ell$  and  $P_\ell$ . The "longshore power" is related to the energy flux,  $E_f(b)$  at the breakpoint and the breaker angle,  $\alpha_b$ , by

$$P_\ell = E_f(b) \sin \alpha_b \cos \alpha_b \quad (67)$$

Because K varies considerably depending on experimental circumstances and the units used, there are many different "K's". In the earlier formula (equation 66) K was not dimensionless and was dependent on whether one was working in English or metric units.

One of the earliest -and pioneering- attempts to estimate littoral drift was offered by Munch-Petersen (1938) who related the volumetric rate of transport (volume per unit time),  $q_\ell$ , to deepwater energy,  $E_o$ , and deepwater incidence angle (relative to the shore),  $\alpha_o$ . Subsequent formulae proposed by Eaton (1950), Watts (1953), Caldwell (1953), Saint-Marc and Vincent (1954), Larras (1957), Le Mehaute and Brebner (1961), Savage (1962), and Inman and Bagnold (1963) attempted to relate the volume transport rate  $q_\ell$  to  $P_\ell$ . Eaton (1950) was one of the first to commit the error of equating energy flux (the rate of energy transmission) with power (the rate of energy dissipation by performing work) since the two have the same units (e.g. ft. lbs. sec<sup>-1</sup> or joules sec<sup>-1</sup> = watts). In physical terms, they are not the same thing since energy flux does not imply any expenditure of energy whereas power does.

Using field data on the rate of pumping of sand around the tidal inlet at Lake Worth, Florida, Watts (1953) found

$$q_\ell = 11130 (P_\ell)^{0.9} \quad (68)$$

with  $q_\ell$  expressed in cubic yards per year and  $P_\ell$  expressed in ft. lbs sec<sup>-1</sup> per foot of beach. Using both field and laboratory data, Savage (1962) found

$$q_\ell = 4110 P_\ell \quad (69)$$

Bagnold (1963) and Inman and Bagnold (1963) expressed the transport rate as an immersed weight dynamic transport rate  $i_\ell$  defined by

$$i_\ell = g \left( \frac{\rho_s - \rho}{\rho} \right) j_\ell \quad (70)$$

where  $g$  is acceleration of gravity,  $\rho_s$  is the density of the sediment,  $\rho$  is water density and  $j_\ell$  is the mass transport rate of sediment ( $\text{gm cm}^{-1} \text{sec}^{-1}$ ). Since  $i_\ell$  has units of a work rate (or power, e.g.  $\text{dyn sec}^{-1}$  or watts per unit width) and hence the same units as  $P_\ell$ , then the coefficient  $K' = i_\ell/P_\ell$  becomes dimensionless. Komar and Inman (1970) used their own field data together with the field and laboratory data of others to fit a line of the form

$$i_\ell = K' P_\ell \quad (71)$$

and found  $K' = 0.77$  with  $P_\ell$  estimated from  $H_{\text{rms}}$  (the root-mean square breaker wave height). The 1984 edition of the Shore Protection Manual (CERC, 1984) gives the corresponding value of  $K' = 0.39$  with  $P_\ell$  estimated from  $H_s$  (the significant height,  $H_s = \sqrt{2} H_{\text{rms}}$ ). It must be noted that the scatter of data points around Komar and Inman's (1970) curve embraces a full order of magnitude. Komar (1983) has presented these and more recent results in terms of the volume transport rate,  $q_\ell$ , and found

$$q_\ell = 6.85 P_\ell \quad (72)$$

where  $q_\ell$  is expressed in  $\text{m}^3 \text{day}^{-1}$  and  $P_\ell$  has units of  $\text{watts m}^{-1}$  and is estimated on the basis of  $H_{\text{rms}}$ . The scatter remains large. The 1984 Shore Protection Manual (CERC, 1984, p. 4-96) points out that the accuracy of estimating  $q_\ell$  from  $P_\ell$  is  $\pm 50\%$ .

Although the "longshore power" approach (including the CERC formula) probably provides a first order estimate of littoral drift along straight,

low gradient beaches, it is too simplistic to deal with the problem of shore-parallel sediment fluxes and sediment budgets in the vicinity of shoreface irregularities and where breaker height is nonuniform alongshore as it is along Virginia Beach. There are two reasons for this:

(1) Estimation of  $\alpha_b$  is difficult even on straight beaches but when the nearshore zone is irregular, the breaker angle varies appreciably. For waves with a low angle of oblique approach, a small variation or error in  $\alpha_b$  translates into a large variation or error in  $\sin \alpha_b$  and hence in  $P_\ell$ .

(2) The "longshore power" approach does not take into account shore-parallel pressure gradients due to longshore variations in setup related to corresponding variations in either breaker height, the degree of dissipation or both. In Section IV of this report, it was shown that appreciable longshore variations in breaker height prevail along the coast from Cape Henry to False Cape.

## 2. Basic principles governing longshore currents and sand transport

The longshore transport of sand within the surf zone is not a direct response to energy flux per se but rather to the shear stresses produced by longshore currents together with the orbital velocities of the waves. As we show shortly, both the longshore thrust which drives currents and energy flux are proportioned to  $H^2$  so a reasonable correlation between littoral drift and energy flux is to be expected. Surf zone currents (longshore currents, rip currents, and simple two-dimensional vertically-segregated flows) are driven by gradients in radiation stress (equations 31-39) and associated pressure gradients. These gradients are induced by wave breaking and dissipation.

Dissipation in the surf zone causes a shoreward decrease in  $E$  and hence in the radiation stress components. The cross-shore gradient in  $S_{xy}$  (eq. 39) yields a shore-parallel thrust,  $T_y$ , which, when balanced against an opposing longshore shear stress,  $\tau_y$ , gives rise to a longshore current. Cross-shore gradients in  $S_{xx}$  are balanced by cross-shore pressure gradients due to setup. When breaker heights (or the rate of surf zone dissipation) are non-uniform alongshore the setup also varies producing longshore pressure gradient forces that are augmented by longshore gradients in  $S_{yy}$  and act either in conjunction with or in opposition to  $S_{xy}$  and  $T_y$ . Outside the surf zone, the radiation stresses produce no net currents. The current-producing forces within the surf zone come about because incident wave energy is dissipated by the processes of breaking and subsequent bore decay. Without dissipation no currents would result. For example, if incident wave energy were completely reflected back to sea, as from a seawall, there would be no dissipation and, hence, no currents. With partial reflection, as from a steep reflective beach, the currents would be reduced in strength by an amount proportional to the fraction of energy reflected. The theoretical models for surf zone circulation assume, however, that all of the incident wave energy is dissipated between the break point and the shore.

For the simple (and generally unrealistic) case where depth contours in and seaward of the surf zone are straight and parallel alongshore and breaker height,  $H_b$ , is uniform alongshore,  $d\bar{\eta}/dy = 0$  and  $dS_{yy}/dy = 0$ . In this case, the only driving force for a longshore current is related to the obliquity of wave breaking and hence to  $S_{xy}$ . Since  $S_{xy}$  also decreases shoreward in response to dissipation, momentum balance is achieved by the generation of an alongshore thrust (a force per unit area)  $T_y$  which is

$$T_y = - \frac{\partial S_{xy}}{\partial x} \quad (73)$$

The cross-shore decrease in  $S_{xy}$  involves the cross-shore decrease in  $E$  which, for the fully dissipative and saturated surf zone, depends solely on local depth  $(\bar{\eta} + h)$  and  $\gamma$  so

$$-T_y = \frac{5}{16} \rho g (\bar{\eta} + h) \gamma^2 \left[ \frac{1}{1 + 3\gamma^2/8} \right] \tan \beta \sin \alpha_b \cos \alpha_b \quad (74)$$

(Komar, 1975). This thrust is balanced against a longshore shear stress  $\tau_y$  so

$$\tau_y = -T_y \quad (75)$$

$$\tau_y = \frac{2\rho}{\pi} C_f u_b \bar{V} \quad (76)$$

where  $C_f$  is a drag coefficient (which according to Komar, 1975, typically ranges from 0.008 to 0.018),  $u_b$  is maximum orbital velocity at the break and  $\bar{V}$  is the longshore current velocity (Longuet-Higgins, 1970a, b, 1972; Komar, 1975). A constant (steady) longshore current,  $\bar{V}$ , is achieved by the balance between  $T_y$  and  $\tau_y$ . The mean longshore current velocity  $\bar{V}_{1/2}$ , halfway between the break point and the shore, is given by Komar (1975) as

$$\bar{V}_{1/2} = \frac{5\pi}{16} \left[ \frac{1}{1 + 3\gamma^2/8} \right] \frac{\tan \beta}{C_f} u_b \sin \alpha_b \cos \alpha_b \quad (77)$$

In other words, and as pointed out by Longuet-Higgins (1970a), the longshore current velocity is proportional to  $u_b$ . For long waves, the maximum orbital velocity at the break point,  $u_b$ , is

$$u_b = \left( \frac{2E_b}{\rho h_b} \right)^{1/2} = \frac{H_b}{2} \sqrt{\frac{g}{h_b}} = \frac{\gamma}{2} \sqrt{gh_b} = \frac{\gamma^{1/2}}{2} \sqrt{gH_b} \quad (78)$$

Kraus and Sasaki (1979) followed by Gourlay (1982) replaced  $C_f$  with the combined wave-current friction factor

$$f_{wc} = 2 C_f$$

and substituted  $\frac{\gamma^{1/2}}{2} \sqrt{gH_b}$  for  $u_b$  to give

$$\bar{V}_{1/2} = \frac{5\pi}{32} \left[ \frac{\gamma^{1/2}}{1 + 3\gamma^2/8} \right] \frac{\tan \beta}{f_{wc}} \sqrt{gH_b} \sin 2 \alpha_b \quad (79)$$

which is equivalent to equation 77. The corresponding form for the space-averaged longshore current velocity (averaged over the entire surf zone) is

$$\bar{V}_s = \frac{5}{24} \left[ \frac{\gamma^{1/2}}{1 + 3\gamma^2/8} \right] \frac{\tan \beta}{f_{wc}} \sqrt{gH_b} \sin 2 \alpha_b \quad (80)$$

(Gourlay, 1982). Gourlay (1982) has suggested further simplification whereby the term  $\gamma^{1/2} / (1 + 3\gamma^2/8)$  becomes a constant  $\approx 0.72$  on the assumption that  $\gamma$  only varies "over the usual range of ... 0.8 to 1.2" (Gourlay, 1982, p. 21). As noted earlier,  $\gamma$  in nature varies over a much wider range than this and can be much less than 0.8.

Despite the fact that  $\gamma$ ,  $\tan \beta$ , and  $f_{wc}$  (or  $C_f$ ) are not (or should not be) constant in the natural world, Komar and Inman (1970) and Komar (1975) concluded that

$$\bar{V}_{1/2} = 2.7 u_{\max} \sin \alpha_b \cos \alpha_b \quad (81)$$

From a later analysis which included additional data, Komar (1979) obtained an improved fit to the relation

$$\begin{aligned} V_{1/2} &= 1.17 \sqrt{gH_b} \sin \alpha_b \cos \alpha_b \\ &= 0.58 \sqrt{gH_b} \sin 2 \alpha_b \end{aligned} \quad (82)$$

Shore-parallel pressure gradients due to nonuniform setup and breaker height can drive longshore currents and seaward-flowing rip currents even when wave incidence is shore-normal and  $T_y = 0$ . Conceptually, at least, a progressive unidirectional pressure gradient can generate a simple longshore

current. Commonly, however, topographic periodicities in the surf zone or complex topography causes longshore alternations in setup producing circulation cells involving both alongshore transport and offshore transport by way of rip currents.

As explained by Bowen (1969), inside the surf zone where energy is dissipated, nonuniformity results in forces due to  $\partial S_{yy}/\partial y$  and  $\partial \bar{\eta}/\partial y$  which act in conjunction to produce a net driving force,  $F_y$ , which causes flow from regions of high breakers to regions of low breakers. This force is

$$\begin{aligned} F_y &= \rho g (\bar{\eta} + h) \frac{\partial \bar{\eta}}{\partial y} + \frac{\partial S_{yy}}{\partial y} \\ &= \rho g (\bar{\eta} + h) \frac{\partial \bar{\eta}}{\partial y} + \frac{1}{8} \rho g H \frac{\partial H}{\partial y} \end{aligned} \quad (83)$$

The force  $F_y$  can act either with or against  $T_y$ .

Komar (1975) and, more recently, Gourlay (1982) and Vemulakonda (1984) have considered the combined effects of both oblique breaker angle and nonuniform longshore breaker height on longshore currents. Both Komar and Gourlay assume fully dissipative and saturated surf zone conditions. Komar (1975) gives for the mid-surf zone current,  $V_{1/2}$ ,

$$V_{1/2} = 2.7 u_b \sin \alpha_b \cos \alpha_b - \frac{\pi \sqrt{2}}{C_f \gamma^3} \left( 1 + \frac{3\gamma^2}{8} - \frac{\gamma^2}{4} \cos^2 \alpha_b \right) u_b \frac{\partial H_b}{\partial y} \quad (84)$$

More exactly,

$$\begin{aligned} V_{1/2} &= \frac{5\pi}{16} \left[ \frac{1}{1 + 3\gamma^2/8} \right] \frac{\tan \beta}{C_f} u_b \sin \alpha_b \cos \alpha_b \\ &\quad - \frac{\pi \sqrt{2}}{C_f \gamma^3} \left( 1 + \frac{3\gamma^2}{8} - \frac{\gamma^2}{4} \cos^2 \alpha_b \right) u_b \frac{\partial H_b}{\partial y} \end{aligned} \quad (85)$$

(Komar, 1975). In this study, we estimated  $V_{1/2}$  via two methods: equation 82, which ignores longshore gradients in breaker height and equation 85 which includes longshore gradients in  $H_s$ .

### 3. Alternative littoral drift formulae used in these analyses

We used three alternative methods to estimate littoral drift at each sector. The three formulae used are all "total load" formulae, meaning that they are intended to estimate the combined transport due to both bed load and suspended load. The "CERC Formula" (equation 71) was utilized to provide one set of estimates which, of course, ignore longshore variations in  $H_b$ .

A somewhat improved estimate of immersed weight longshore sand transport,  $i_\ell$ , which, potentially at least, has the ability to relate longshore transport to longshore current speed and direction is that proposed by Inman and Bagnold (1963) and later refined by Komar and Inman (1970). It has the form

$$i_{\ell t} = K_\ell' (E C_g)_b \cos \alpha_b \frac{V_{1/2}}{u_b} \quad (86)$$

Komar and Inman (1970) determined  $K_\ell'$  to be 0.28 when  $H_{rms}$  is used or 0.14 when significant height,  $H_g$ , is used. Longshore current velocity,  $V_{1/2}$ , is estimated from equation 85.

The third set of estimates is obtained by applying Gourlay's (1982) modified version of equation 86 which includes the effects of longshore nonuniformity of breaker heights and has the form

$$i_\ell = K_\ell^* (E C_g)_b \cos \alpha_b \left[ \sin 2 \alpha_b - \frac{K_{\Delta H}}{\tan \beta} \frac{\partial H_b}{\partial y} \right] \quad (87)$$

where  $K_{\Delta H} = 23.7$  and  $K_\ell^* \sim 0.385 K_b$  where  $K_b$  depends on the Iribaren number,  $\xi$  given by

$$\xi = \frac{2\pi \tan \beta}{H_b g T^2} \quad (88)$$

When  $\xi \geq 1.7$ ,  $K_b = 1$ , but when  $\xi < 1.7$  then

$$K_b = \frac{0.45}{K_\ell^*} \xi \quad (89)$$

In all three sets of estimates, the immersed weight transport rate,  $i_\ell$ , was converted to instantaneous volume transport rate,  $q_\ell$ , via

$$q_\ell = \frac{i_\ell}{g (\rho_s - \rho) (1 - p)} \quad (90)$$

where sediment density,  $\rho_s$ , is assumed to be  $2650 \text{ kg m}^{-3}$ , water density  $\rho$  is assumed to be  $1020 \text{ kg m}^{-3}$  and the pore ratio,  $p$ , is assumed to be 0.4.

## B. Modelling Results

### 1. Estimates of longshore currents

Figures V-1 - V-3 summarize the longshore current velocities which would be expected for each coastal sector under the three sets of wave conditions: "modal", "northeaster" and "hurricane" as estimated via equations 81 and 85. Values estimated from equation 81 are labelled  $(V_{1/2})_1$ ; those estimated from equation 85 are labelled  $(V_{1/2})_2$ . Positive values indicate southerly-setting longshore currents. It can be seen from the graphs that the modal wave conditions produce relatively weak longshore currents with mean speeds of only about  $5 \text{ cm s}^{-1}$  or less; these flows have no preferred direction and change direction frequently alongshore. The longshore currents which would be generated by the normally-incident hurricane waves if breaker heights were uniform alongshore are predicted to be only moderately swifter with speeds on the order of only  $10 \text{ cm s}^{-1}$ . However, alongshore nonuniformity of breaker height results in local  $(V_{1/2})_2$  speeds on the order of  $50 \text{ cm s}^{-1}$ . Stronger, southerly setting currents are

'MODAL WAVE'

$\theta_{\infty} = \text{EAST}$

$H_{\infty} = 1 \text{ m}$

$T = 9.0 \text{ s}$

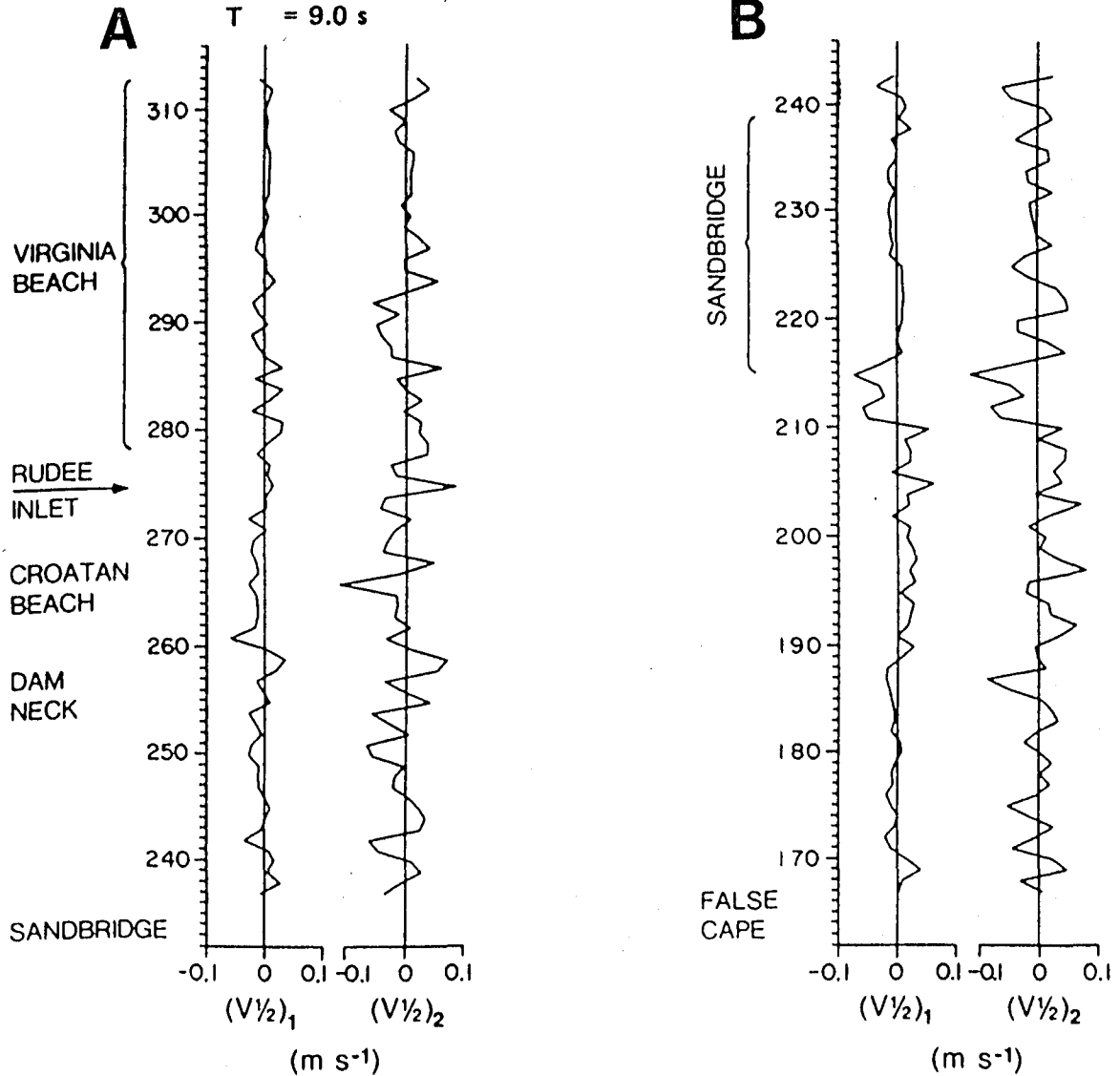


Figure V-1. Predicted alongshore variations in velocities of longshore currents generated by "modal" waves. Velocities  $(V_{1/2})$  are assumed to be in the mid surf zone. Values labelled  $(V_{1/2})_1$  ignore alongshore variations in wave height and are estimated by equation 81. Values labelled  $(V_{1/2})_2$  take the effects of alongshore variations in breaker height into account and are estimated by equation 85.

'NORTHEASTERLY WAVE'

$\theta_{\infty} = \text{NORTHEAST}$

$H_{\infty} = 2.1 \text{ m}$

$T = 8.0 \text{ s}$

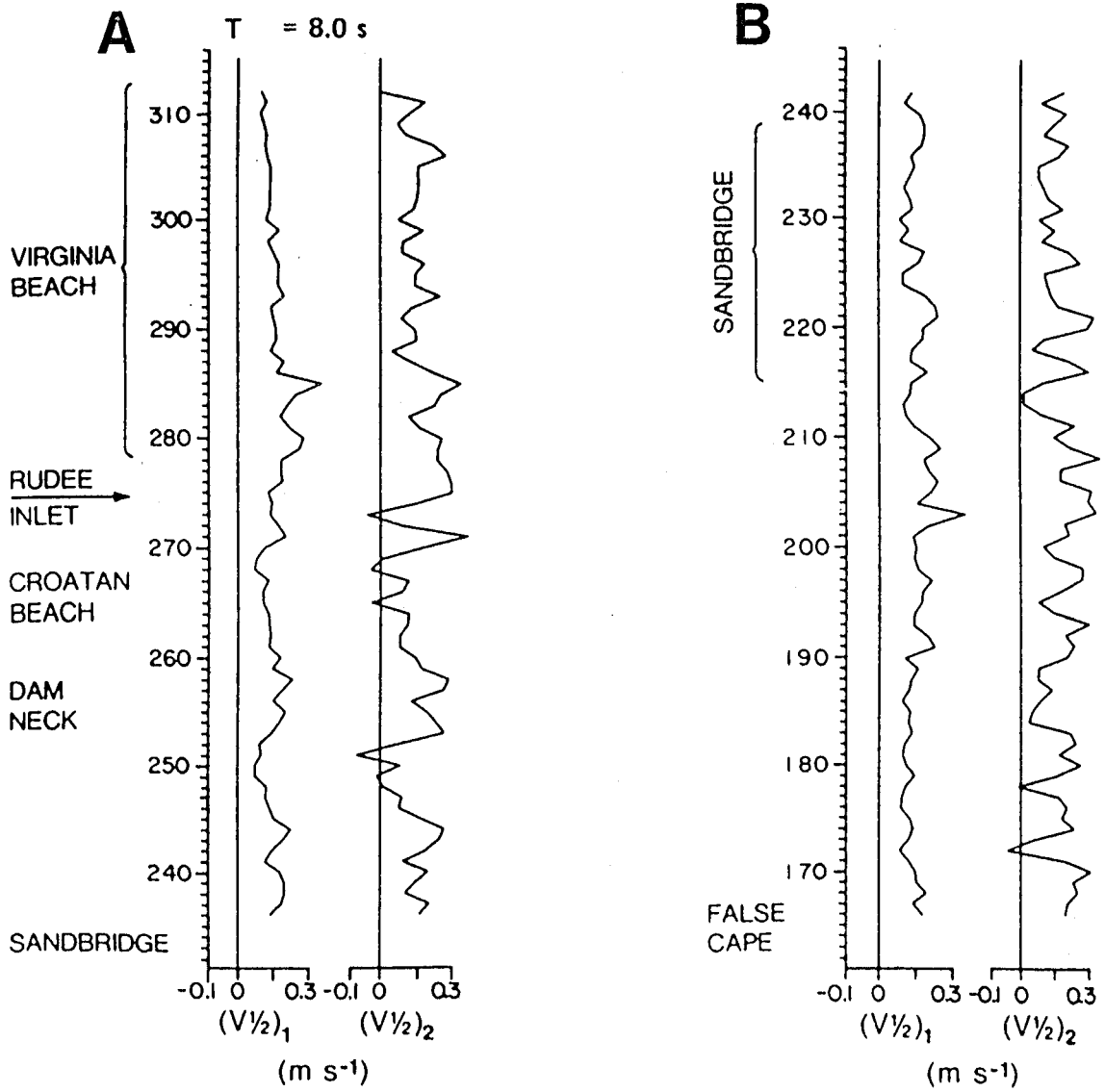


Figure V-2. Predicted alongshore variations in the velocities of longshore currents generated by northeasterly waves.

'HURRICANE WAVE'

$\theta_{\infty} = \text{EAST}$

$H_{\infty} = 6.0 \text{ m}$

$T = 15.0 \text{ s}$

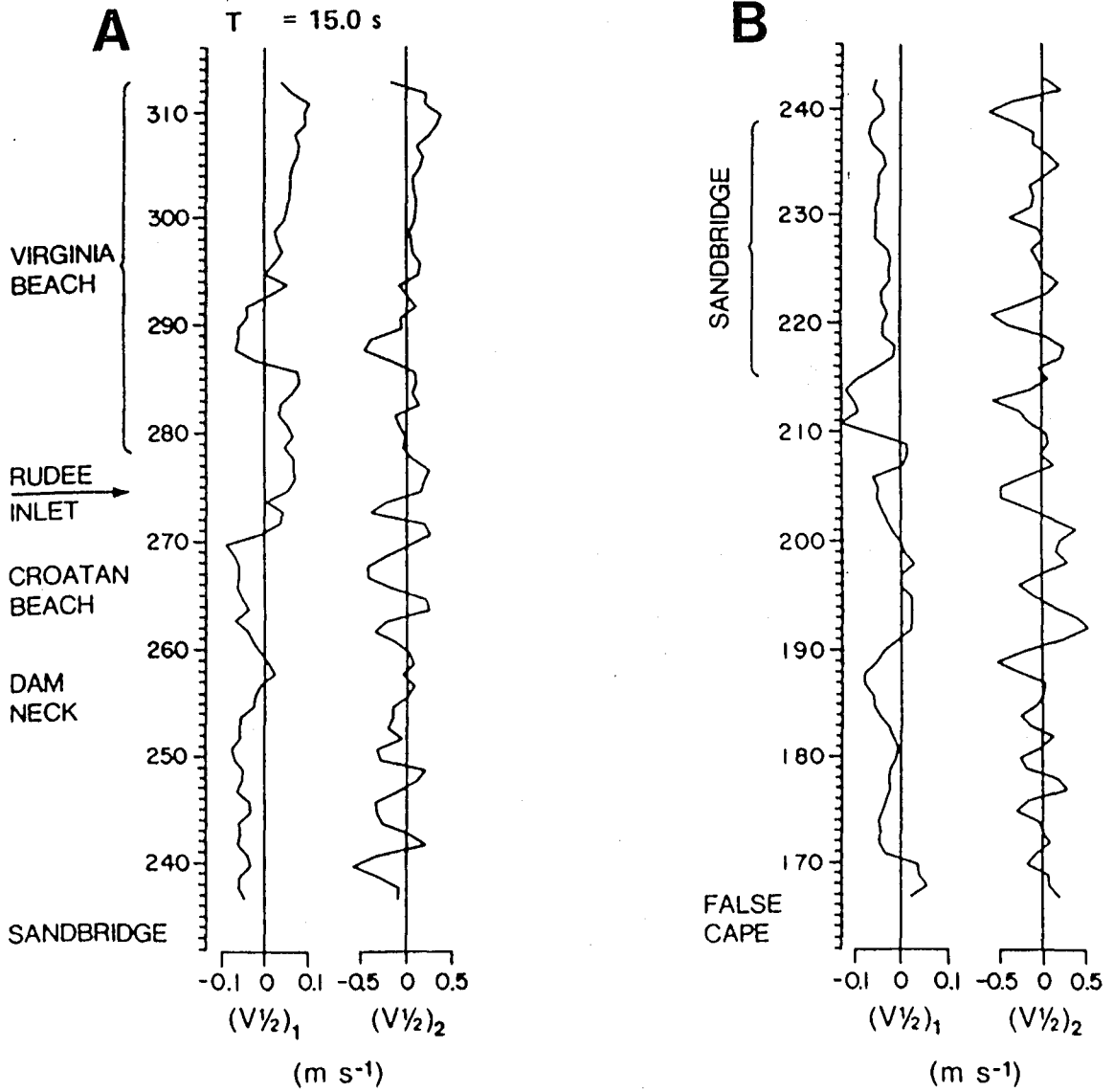


Figure V-3. Predicted alongshore variations in the velocities of longshore currents generated by hurricane waves.

associated with the typical and more frequently recurring northeaster. Those flows attain speeds of 20-30 cm s<sup>-1</sup>.

## 2. Estimates of littoral drift

Predicted littoral drift volume transport rates  $q_\ell$  (expressed in cubic meters per hour) associated with each of the three representative wave cases are summarized graphically in Figures V-4 - V-6. Estimates obtained by way of the CERC Formula (eq. 71), Komar and Inman's (1970) longshore-current approach (eq. 86) and Gourlay's (1982) approach (eq. 87) are respectively designated  $(q_\ell)_C$ ,  $(q_\ell)_K$ , and  $(q_\ell)_G$ . The net annual littoral drift rates ( $Q_\ell$ ; in m<sup>3</sup> yr<sup>-1</sup>) estimated from the 55 wave examples from the 1982 data (Table IV-1) are summarized in Figure V-7. As pointed out earlier, applications of littoral drift formulae are subject to large errors; hence, the absolute magnitudes predicted must be considered suspect, or, at best, accepted with caution. However, the relative magnitudes as they vary along the coast and under different wave conditions are probably much more meaningful as are predicted directions of transport. Of the three methods used, the CERC Formula estimates are probably the least reliable and appear excessively large. Estimates obtained via the other two methods which include the moderating effects of breaker height variations seem more reasonable.

As would be expected, "northeasters" cause pronounced littoral drift toward the south at all sectors. In general, the drift associated with hurricane-generated waves is toward the north although the direction of transport varies considerably between sectors.

The net annual transport rates  $Q_\ell$  as summarized in Figure V-7 are probably the most important. The predicted rates and directions are, for

'MODAL WAVE'

$\theta_{\infty} = \text{EAST}$

$H_{\infty} = 1.0 \text{ m}$

$T = 9.0 \text{ s}$

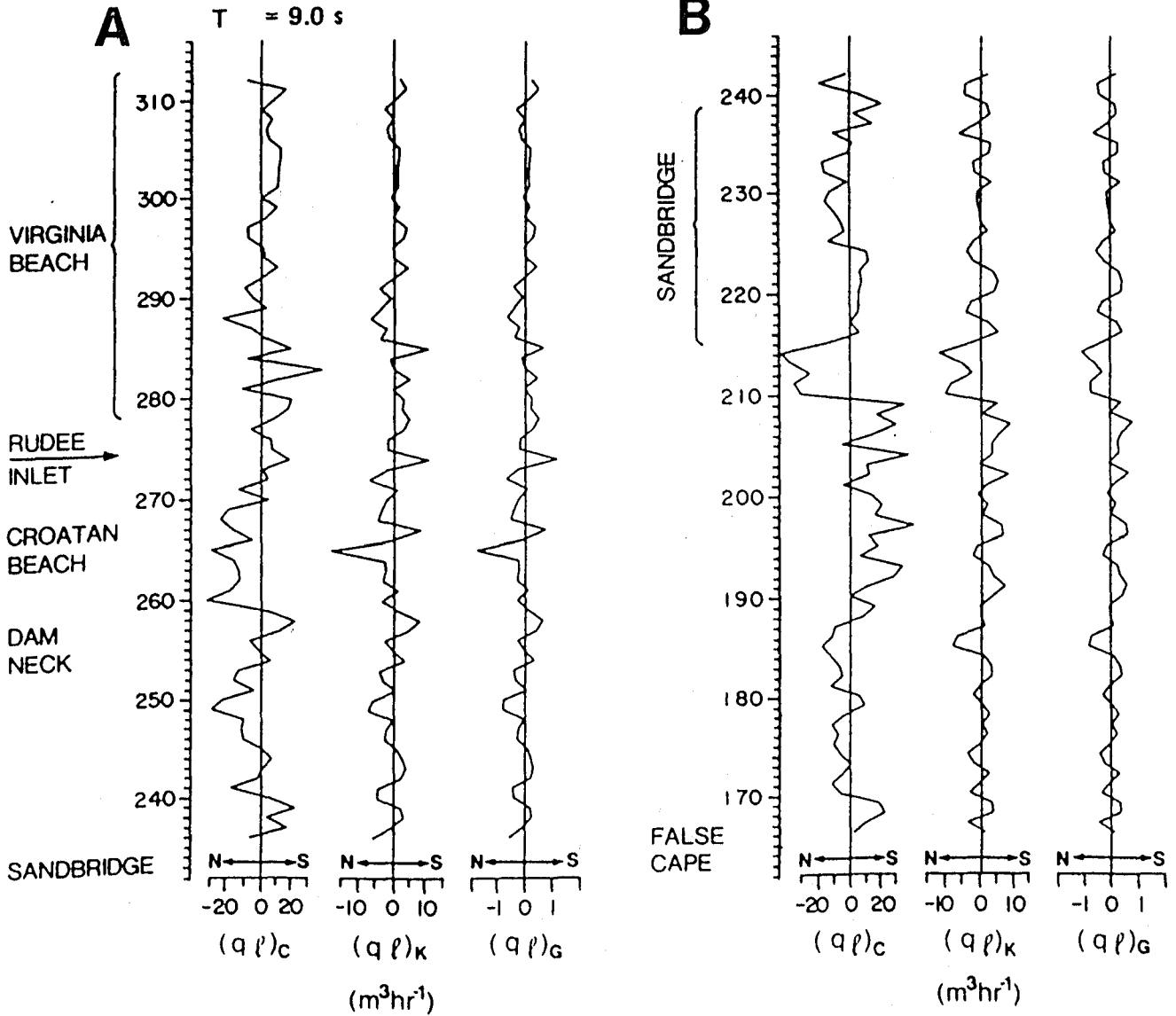


Figure V-4. Predicted alongshore variations in littoral drift volume transport rates,  $q_l$ , associated with the modal waves. The values labelled  $(q_l)_c$  were estimated by the CERC formula (eq. 71) and ignore alongshore variations in breaker height. The values labelled  $(q_l)_k$  and  $(q_l)_g$  were respectively estimated from equations 86 and 87 and include the effects of alongshore variations in breaker height.

'NORTHEASTERLY WAVE'

$\theta_{\infty} = \text{NORTHEAST}$

$H_{\infty} = 2.1 \text{ m}$

$T = 8.0 \text{ s}$

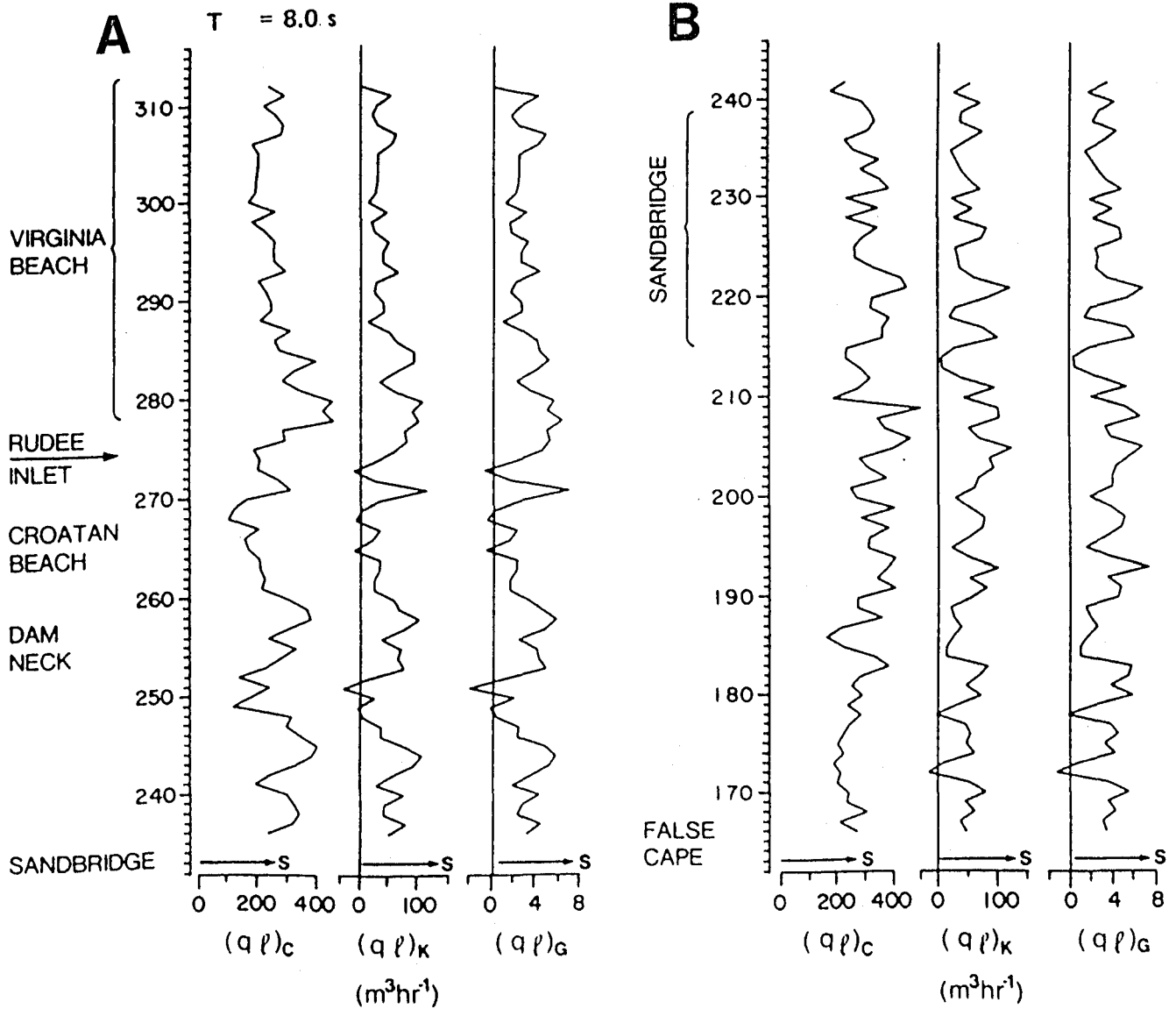


Figure V-5. Predicted alongshore variations in littoral drift volume transport rates,  $q_l$ , associated with "northeasterly" waves.

'HURRICANE WAVE'

$\theta_{\infty} = \text{EAST}$

$H_{\infty} = 6.0 \text{ m}$

$T = 15.0 \text{ s}$

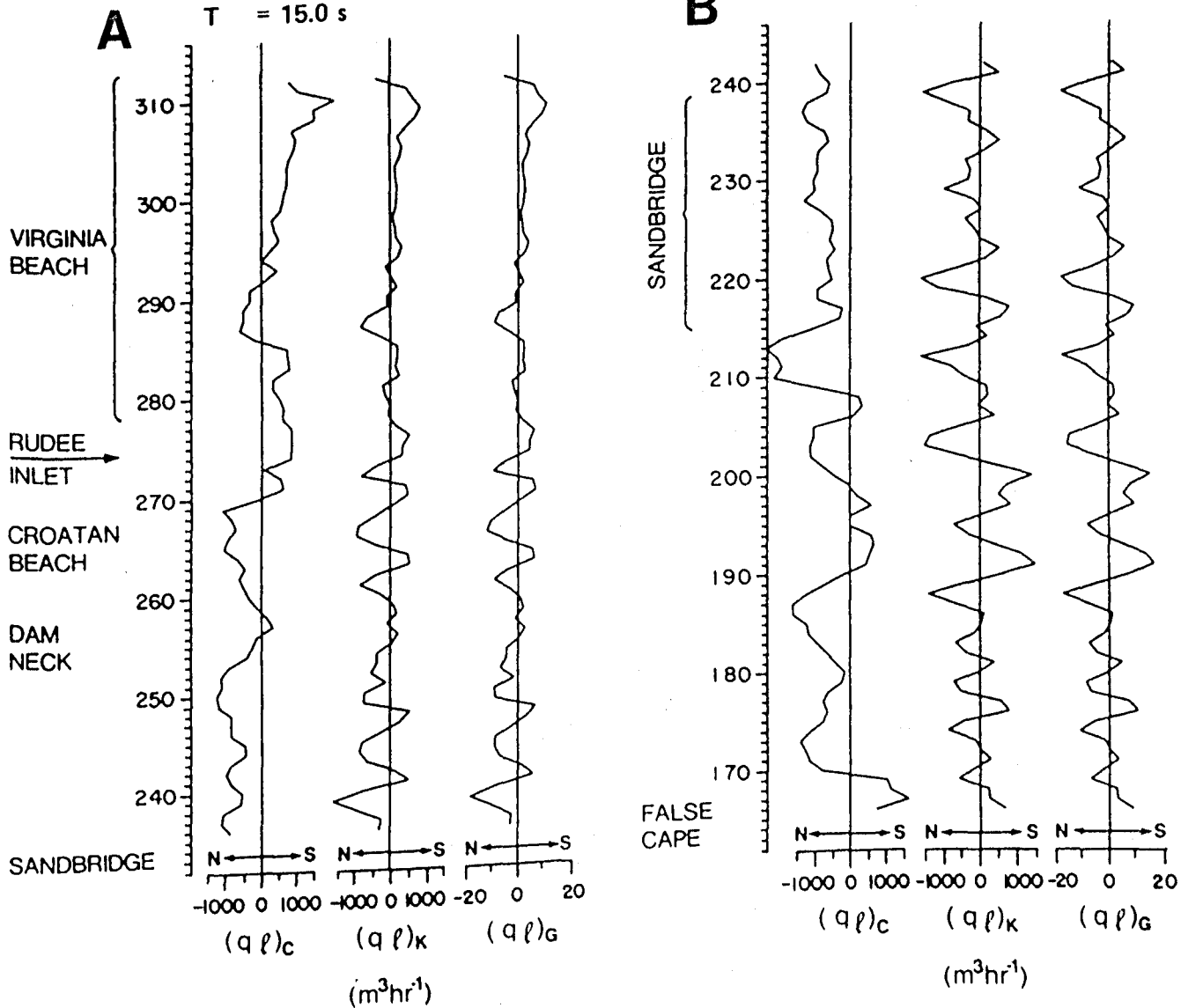


Figure V-6. Predicted alongshore variations in littoral drift volume transport rates,  $q_l$ , associated with "hurricane" waves.

NET FOR 1982

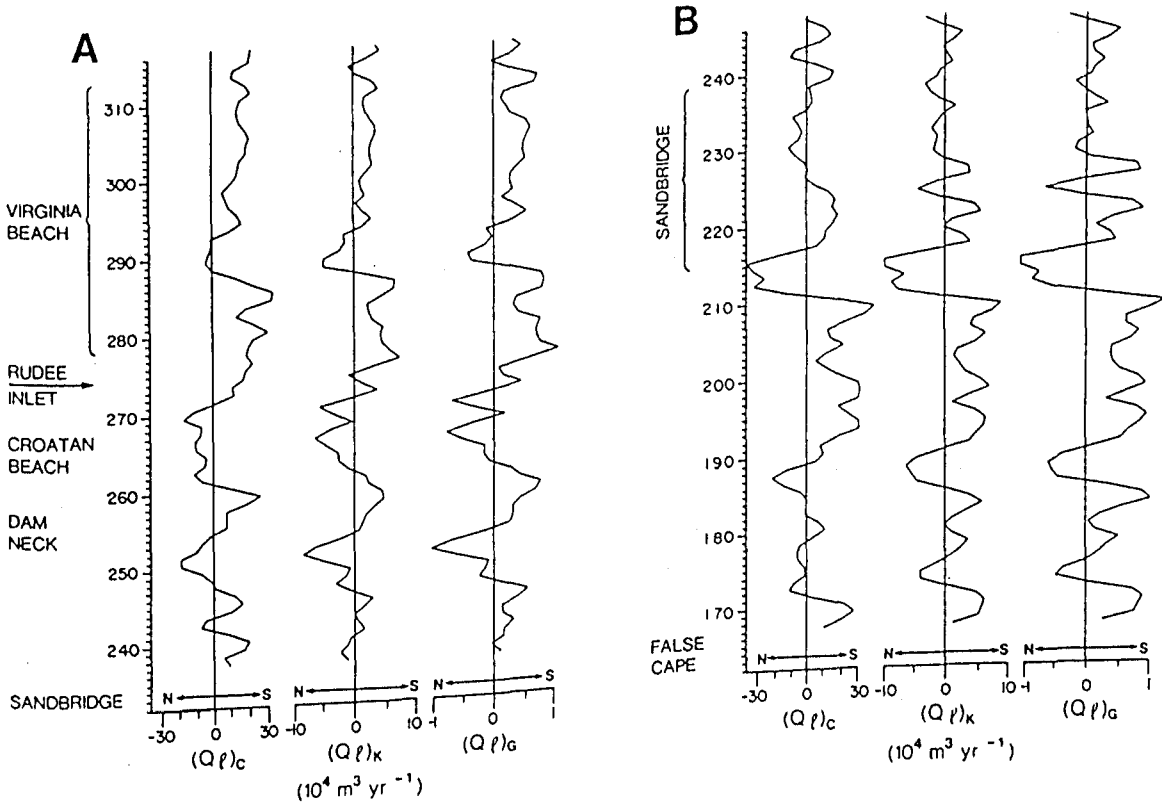


Figure V-7. Predicted alongshore variations in net annual littoral drift volume transport rates  $Q_l$  as estimated from the 55 wave cases for 1982. The subscripts C, K, and G have the same meaning as before.

the most part, qualitatively consistent with predictions reported elsewhere (The Traverse Group, Inc., 1980). However, since our predicted absolute volume transport rates are integrated over the entire surfzone width, they are typically larger than volumes estimated from subaerial beach changes. In general, southerly transport is predicted by all three littoral drift equations for the entire reach of Virginia Beach north of Rudee Inlet (sectors 275-310). A similar result was obtained by The Traverse Group, Inc. who applied a version of the CERC Formula. However, as pointed out by The Traverse Group, Inc. (1980), it is widely known that there is a net northerly sediment flux off Virginia Beach. The discrepancy probably reflects the fact that northerly transport is due to non-wave-generated northerly currents related to circulation associated with the Chesapeake Bay entrance.

South of Rudee Inlet, along Croatan Beach and south of Dam Neck (sectors 245-270) northerly-directed littoral drift prevails overall, although local reversals are also predicted. Along the Sandbridge reach, transport directions alternate but there is a weak tendency for southerly transport to prevail when littoral drift is averaged over the whole reach. South of Sandbridge, in the vicinity of sector 210, a highly pronounced node of littoral drift divergence is predicted by all three methods. The existence of a transport node in this vicinity has been widely reported as a cause of pronounced coastal retreat locally (Everts et al., 1983).

### 3. Alongshore gradients in littoral drift

The absolute rates ( $q_\ell$  or  $Q_\ell$ ) of littoral drift are not direct causes of either erosion or accretion. Erosional or accretionary changes in the volume of sand stored in a beach are determined by the gradients in alongshore sediment flux  $\delta q_\ell$  and  $\delta Q_\ell$ . Specifically, when the

rate of littoral drift entering a given coastal sector exceeds the rate exiting the sector, accretion results. Erosion results when output exceeds input; there is no change when input and output are equal. The gradients were approximated from

$$\delta q_{\ell} = (q_{\ell})_u - (q_{\ell})_d / \Delta y$$

and

$$\delta Q_{\ell} = (Q_{\ell})_u - (Q_{\ell})_d / \Delta y \tag{91}$$

where the subscripts u and d respectively designate the littoral drift rates at the updrift and downdrift ends of a sector and  $\Delta y$  is the alongshore length of a sector which is 250 m. Negative values imply that erosion should occur and positive values imply that accretion should occur if all sediment fluxes were in the form of littoral drift. Onshore-offshore sediment fluxes which are also very important are not taken into account in the  $\delta q_{\ell}$  and  $\delta Q_{\ell}$  estimates. The function of the  $\delta q_{\ell}$  and  $\delta Q_{\ell}$  estimates is thus simply to indicate the likely contribution that littoral drift makes to beach change.

Alongshore variations in  $\delta q_{\ell}$  estimated on the basis of the three littoral drift equations discussed earlier and as predicted for the modal, northeaster, and hurricane wave cases are illustrated in Figures V-8 - V-10. By all three methods and for all three wave cases, we see alongshore alternations between erosion and accretion; minimal changes, either negative or positive, are predicted for the resort strip of Virginia Beach even during northeaster and hurricane conditions. Along the Sandbridge reach, volume fluctuations are larger in amplitude, but, averaged over the reach, there is as much local accretion as there is local erosion. We know, of course, that northeasters and hurricanes cause large scale erosion along

'MODAL WAVE'

$\theta_{\infty} = \text{EAST}$

$H_{\infty} = 1.0 \text{ m}$

$T = 9.0 \text{ s}$

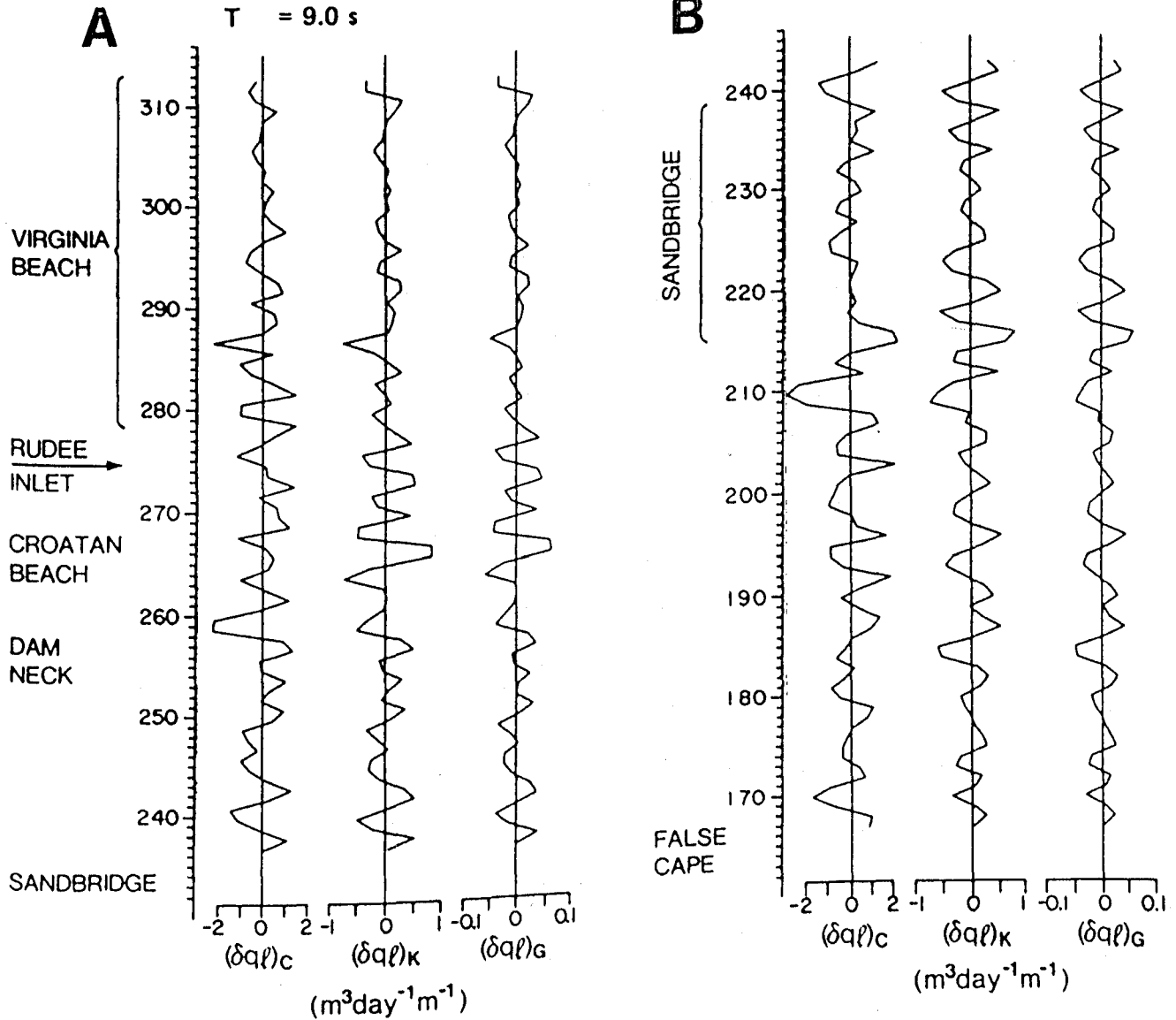


Figure V-8. Predicted alongshore variations in littoral drift gradients,  $\delta q_l$ , associated with the modal waves. Positive values imply an accretionary effect. As before, the subscripts C, K, and G indicate how  $q_l$  was estimated.

'NORTHEASTERLY WAVE'

$\theta_{\infty} = \text{NORTHEAST}$

$H_{\infty} = 2.1 \text{ m}$

$T = 8.0 \text{ s}$

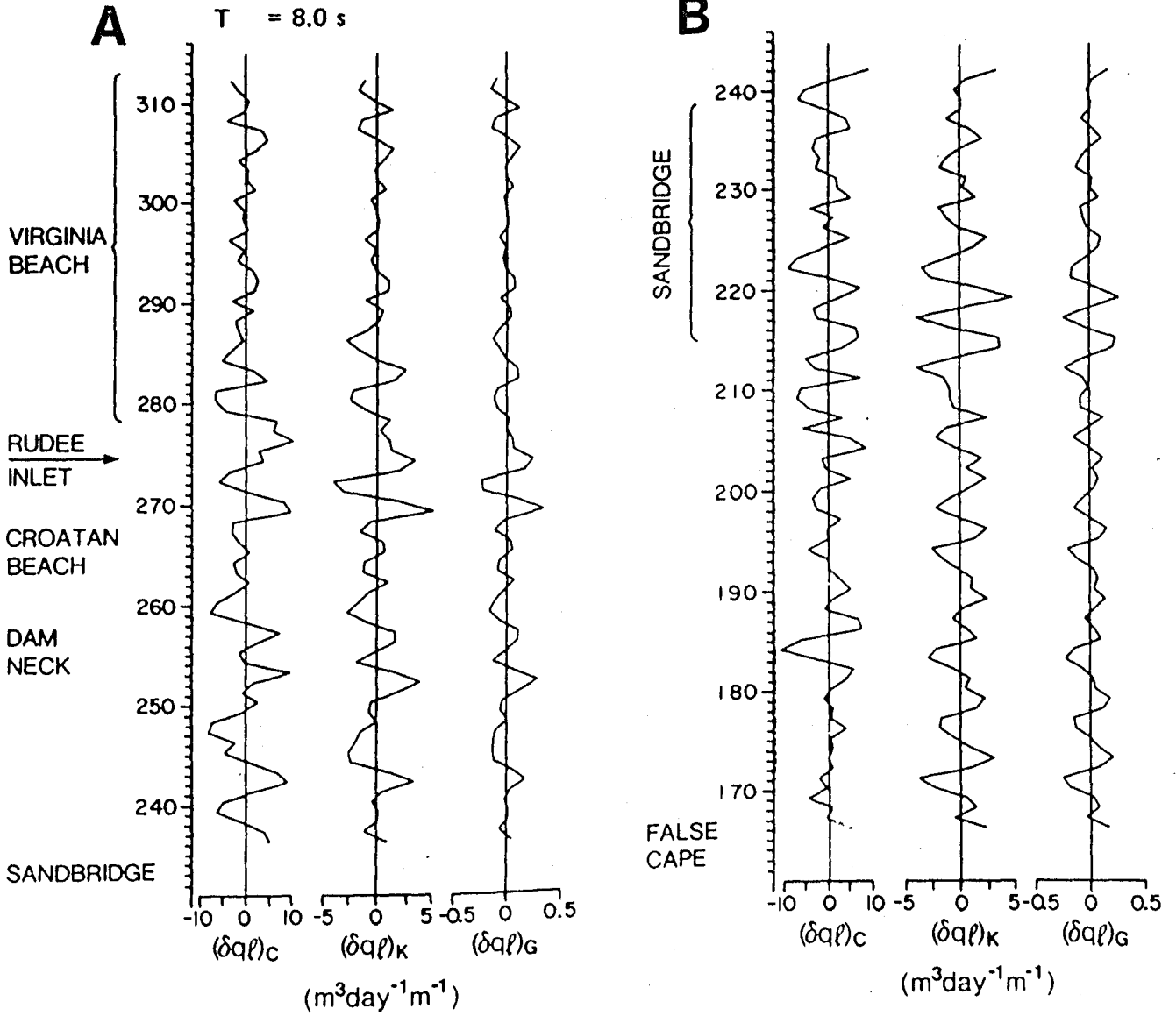


Figure V-9. Predicted alongshore variations in littoral drift gradients,  $\delta q_l$ , associated with the "northeasterly" waves.

'HURRICANE WAVE'

$\theta_{\infty} = \text{EAST}$

$H_{\infty} = 6.0 \text{ m}$

$T = 15.0 \text{ s}$

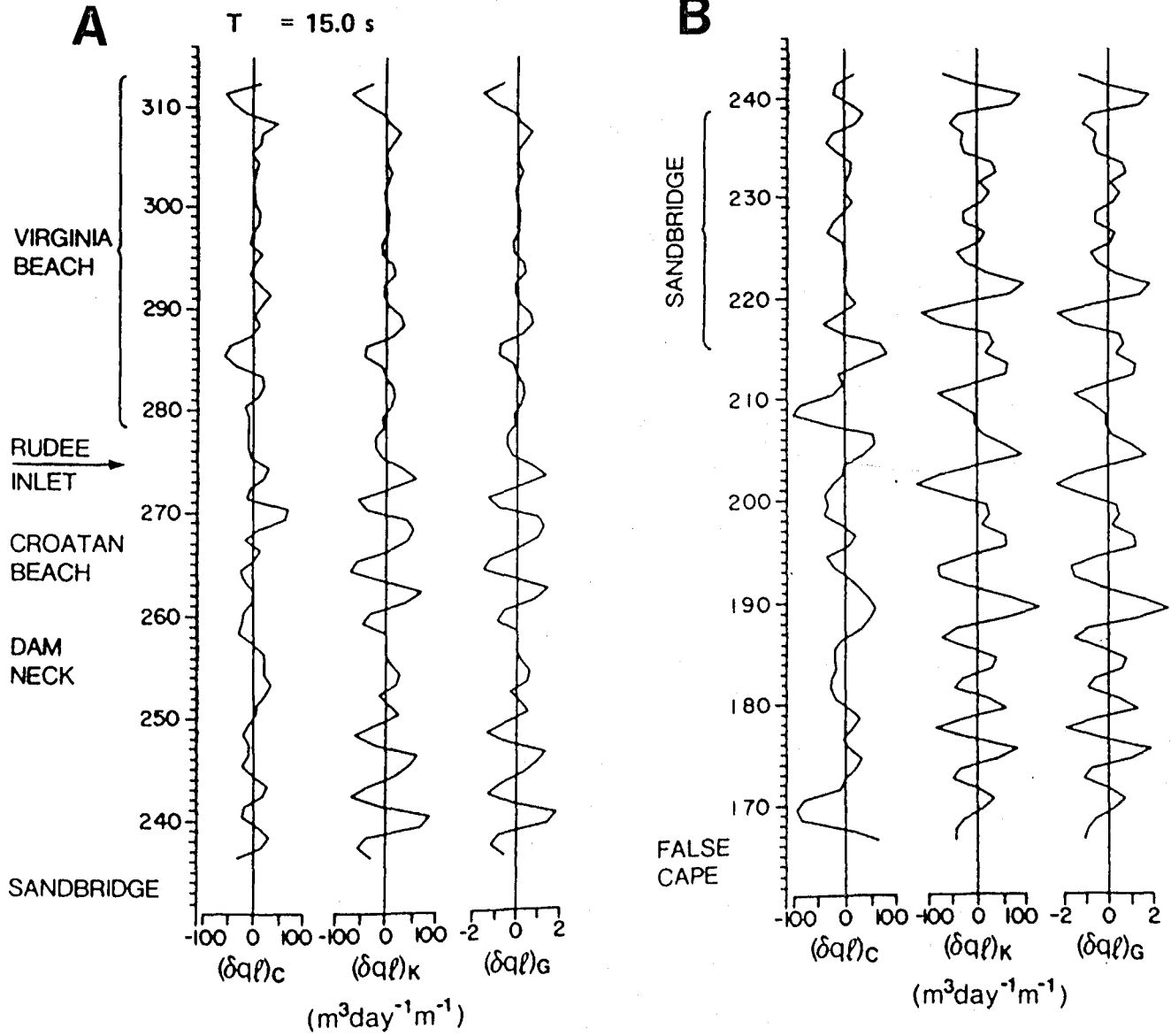


Figure V-10. Predicted alongshore variations in littoral drift gradient,  $\delta q_l$  associated with the "hurricane" waves.

virtually all sectors. We must infer from Figures V-8 - V-10 that littoral drift is not the main culprit responsible for this erosion. Significant quantities of sand must be transported offshore during storms.

Figure V-11 shows the net annual beach sand volume changes,  $\delta Q_\ell$ , due to littoral drift alone as predicted for the specific example of the 1982 wave data used in these analyses. Again, appreciable alongshore alternations between net erosion and accretion are apparent. The least important net changes are predicted to occur along Virginia Beach between sectors 294 and 308. The most prominent change is the erosional response to littoral drift divergence at sector 210 south of Sandbridge. Moderate accretion of Croatan Beach and Dam Neck is predicted due to sediment influx from the south.

The  $\delta Q_\ell$  values are much less impressive when averaged over several kilometers. Table V-1 lists the averages of  $(\delta Q_\ell)_C$ ,  $(\delta Q_\ell)_K$ , and  $(\delta Q_\ell)_G$  for the northern region (Sandbridge to Cape Henry; sectors 240-315) and southern region (False Cape to Sandbridge; sectors 165-240). Overall, the northern region is predicted to accrete as a consequence of littoral drift gradients whereas the southern region is expected to experience some erosion.

Table V-1

Predicted Net Changes in Regional Beach Volume  
 Due to Littoral Drift Gradients  
 (based on 55 sets of wave conditions observed in 1982)  
 Cubic meters per year per meter of alongshore beach width

	Northern Region (sectors 240-315)	Southern Region (sectors 165-240)
$\overline{(\delta Q_\ell)_C}$	+ 18.86	- 13.94
$\overline{(\delta Q_\ell)_K}$	+ 3.35	- 2.71
$\overline{(\delta Q_\ell)_G}$	+ 0.002	- 0.22

NET FOR 1982

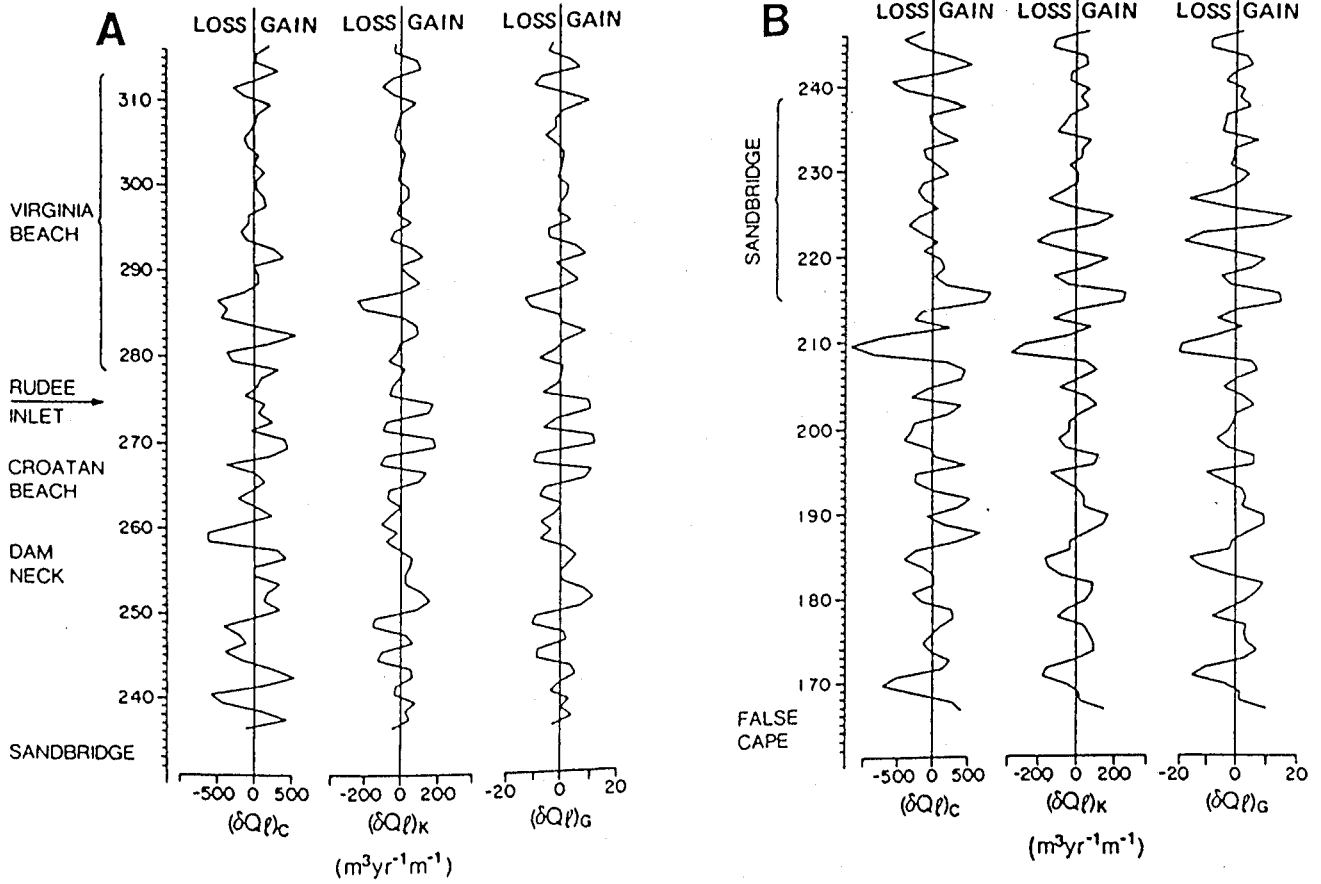


Figure V-11. Predicted alongshore variations in net annual littoral drift gradients,  $\delta Q_l$ , based on the 55 wave cases for 1982.

From the results reported above, the only observed beach behaviors that can be wholly or partially explained by littoral drift with any degree of confidence are the pronounced erosion in the vicinity of sector 210 and the accretion south of Rudee Inlet. Neither the chronic and often severe erosion of most of the Sandbridge reach nor the need for annual renourishment of the resort sectors of Virginia Beach can be explained in terms of littoral drift and its alongshore gradients. This means that, for the most part, the erosion involves offshore transport from the intertidal beach, through the surfzone, and onto the shoreface. Once outside the surfzone, the sand must be subject to redistribution by tidal and wind driven currents interacting with shoaling waves.

## VI BEACH STABILITY AND CROSS-SHORE SEDIMENT FLUX

In the foregoing discussion it was noted that, with perhaps two exceptions, the behavior of the beaches between Cape Henry and False Cape cannot be explained in terms of shore-parallel sediment transport. Sand fluxes in the shore-normal dimension appear to be more important, at least insofar as erosional tendencies along the Virginia Beach and Sandbridge reaches are concerned. We need to examine some reasons why these beaches are unstable with respect to offshore sand transport.

### A. Background

In reality, beach cut can take place in response to a number of processes including accentuated runup, high setup, and scarping by rip currents (Wright, 1981). Subsequent seaward transport of the sand across the surfzone is driven by a combination of near-bottom return flows, rip currents, and long-period (infragravity) oscillations (Komar, 1976; Wright and Short, 1984).

We possess insufficient data to attempt explicit modelling of cross-shore transport in terms of the actual transport mechanisms. However, we can address the question of the relative likelihood of a beach remaining stable, experiencing erosion, or experiencing accretion in a more implicit way. For purposes of a first order estimate, it has been widely demonstrated that whether or not a beach erodes, accretes, or exists in equilibrium depends on three primary factors: (1) the ratio  $H_b/T$ ; (2) the size of the beach sand or, more exactly, the median settling velocity,  $w_s$ , of the sand particles; and (3) the configuration of the surfzone topography.

Dean (1973) and Dalrymple and Thompson (1977) proposed a dimensionless parameter

$$\Omega = H_b / (w_s T) \quad (92)$$

as an index of beach stability that incorporates information concerning breaker characteristics as well as sediment properties. Dalrymple and Thompson (1977) conducted laboratory experiments which showed  $\Omega \sim 1$  to be the highest value at which a steep, accreted (reflective) beach could remain stable. At higher values the steep beach was replaced by a barred surfzone profile. Wright et al. (1985) analyzed a 6½ year data set consisting of daily observations from a high energy beach and found that the critical  $\Omega$  value above which erosion occurs depends on the beach and surfzone slope and configuration. Consistent with the results of Dalrymple and Thompson (1977), Wright et al. (1985) found that steep, unbarred "reflective" beaches are only stable so long as  $\Omega < 1$ . When  $\Omega > 6$  only low gradient "dissipative" beaches with very wide surfzones can exist in equilibrium and not undergo erosion. However, for such highly stable dissipative conditions to occur, there must be an abundant reserve of nearshore or beach sand. Between the two extremes are intermediate beach states and intermediate critical  $\Omega$  values. The intermediate beach states are: the low-tide terrace/ridge and runnel state; the transverse bar and rip state; the rhythmic bar and beach state; and the longshore bar and trough state (Wright et al., 1985). Respectively, the associated critical  $\Omega$  values are roughly 2.4, 3.2, 3.5, and 4.7 (Wright et al., 1985). Unfortunately, reliable data concerning the prevailing beach states of the reaches between Cape Henry and False Cape are lacking. However, from the limited available profiles and aerial photographs, it appears that these beaches most commonly are in the

low tide terrace to longshore bar-trough states. Hence, the critical  $\Omega$  values above which these beaches will experience erosion probably lie somewhere between 2.5 and 4.0. Rarely are the beaches either fully reflective or fully dissipative.

#### B. Model Predictions of Beach Stability

From the breaking wave "climate" results presented in Section IV and the existing data concerning the alongshore variation in grain size and  $w_s$ , it is possible to estimate the frequencies of occurrence and exceedence of various  $\Omega$  values. Figure VI-1 summarizes these results for sectors 300, 290, and 220. Because the intertidal and subtidal beach of sector 300 are composed primarily of relatively fine native sand with a median grain size of only 0.16 mm ( $w_s = 0.016 \text{ m s}^{-1}$ ), the corresponding  $\Omega$  values are high; reflective conditions would be unstable for 96% of the time and for at least 34% of the time only a fully dissipative beach could be expected to remain stable. In fact, beaches at this northern end of the region are probably sustained by the fact that northerly transport of sand outside the surfzone nourishes the surfzone and beach.

Artificial nourishment of the tourist beaches just to the south with coarser sand ( $D_{50} = 0.27 \text{ mm}$ ;  $w_s = 0.032 \text{ m s}^{-1}$ ) significantly lowers the  $\Omega$  values. The beach at this sector is probably unstable for 19% to 38% of the time (Fig. VI-1B). In contrast to sector 300 (or in contrast to the native sand conditions), dissipative conditions would be required to maintain stability in sector 290 during only the highest 2% of wave conditions. A very similar situation characterizes the Sandbridge reach (Fig. VI-1C). However, owing to the deep, sediment deficient shoreface fronting

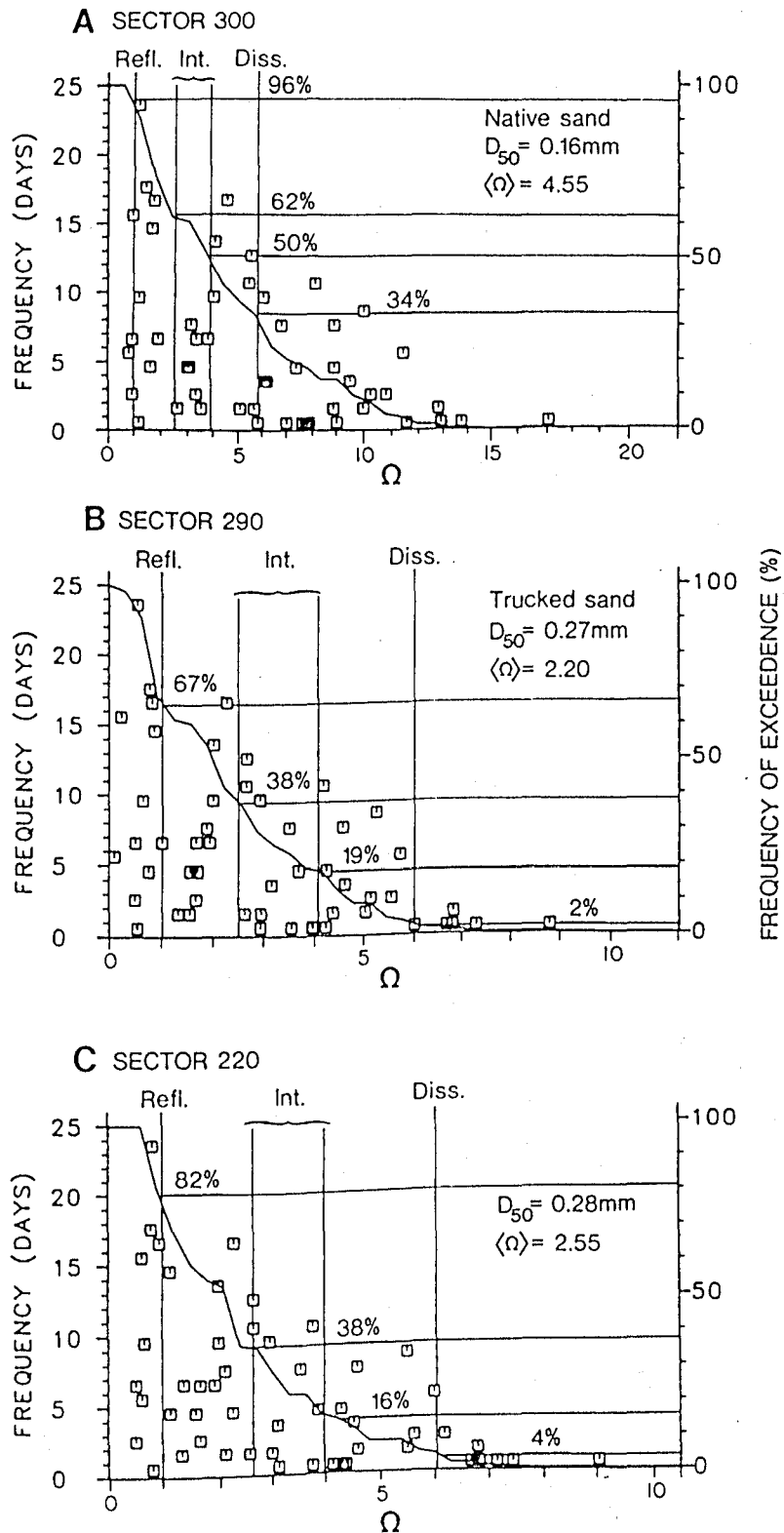


Figure VI-1. Frequency and frequency of exceedence of the parameter  $\Omega$  (eq. 92) as estimated from the predicted breaker conditions for the 55 wave cases representative of 1982. (A) sector 300; (B) sector 290; (C) sector 220.

Sandbridge, the potential for shoreward return of sand along that reach is less than elsewhere.

### C. Sea Level Rise and Chronic Beach Instability

The modelling results presented herein have been focused on the short term, day-to-day dynamic variability of the beaches and have not been intended to address the question of long-term (decades or longer) coastal change. However, it must be noted, before leaving the subject of onshore-offshore sediment exchange, that even though it is waves and wave-generated processes that perform the work whereby sand is moved, these energetic processes operate against a background of slow sea level rise. Data from Hampton Roads indicate that in recent years the local vertical rate of rise has been 43 cm (17 inches) per century (Hicks et al., 1983); there are predictions that the rate of rise will accelerate to as much as 1 meter (39 inches) per century. Vertical sea level increases of several centimeters translate into horizontal shoreline transgressions of several meters. Increasingly, as sea level rises, sand transported offshore during storms becomes locked up in sand sinks on the shelf and, perhaps, in the lower bay, thereby exacerbating the problem of sand-deficient nearshore and shoreface zones.

## VII IMPLICATIONS FOR EROSION CONTROL AND BEACH NOURISHMENT

Decisions concerning future human efforts to control beach erosion along the beaches from Cape Henry to False Cape should be influenced by the following results from the foregoing analyses: (1) During severe storms, the breakers along the Sandbridge reach are higher than elsewhere so that reach is most threatened by storms; (2) Littoral drift probably makes significant contributions to accretion at the northern end of Croatan Beach and to erosion south of Sandbridge; (3) Elsewhere it is inferred that gradients in littoral drift contribute little to shoreline change; (4) Offshore loss of sand is a major cause of erosion along most sectors; (5) Most sectors are unstable with respect to shore-normal sand loss for much of the time; this instability is greatest where the beach is composed of fine sand or where narrow, non-dissipative nearshore profiles prevail.

The need for erosion mitigation along the Sandbridge reach has been discussed at length by others (e.g. Dolan et al., 1985). Whether or not provision of such protection is worthwhile from economic or other considerations is not the subject of our enquiry. It was pointed out in Section III of this report that permission has been granted for residents to bulkhead the entire Sandbridge reach. Following a relatively short-lived period of modest protection, bulkheads alone will ultimately be ineffective in halting erosion. Once the waves impinge directly on the bulkheads, the offshore loss of sand during storms will probably be exacerbated. The only shore protection remedy that is likely to provide even interim term protection for Sandbridge is large scale sand nourishment of the entire

reach. The annual nourishment rate of  $383,000 \text{ m}^3 \text{ yr}^{-1}$  ( $500,000 \text{ yd}^3 \text{ yr}^{-1}$ ) proposed by Dolan et al. (1985) is probably appropriate.

The results of our littoral drift model calculations suggest that the use of groins or groin fields would be inappropriate as a shore protection method along most stretches of this coast. Groins might reduce the divergent littoral transport from the littoral drift node south of Sandbridge. However, such groins would need to span the entire surfzone and groin construction would have to be accompanied by large scale sand nourishment. It is unlikely that the benefits would justify the extreme expense of such a project.

For all eroding sectors of the study region, sand nourishment must be considered the best shore protection measure. However, the estimates of frequencies of exceedance of  $\Omega$  as presented in Section VI provide some insights as to the appropriate size of the fill sand as well as the possible mode of sand introduction. In particular, as a crude estimate, we could expect sand with a median particle diameter less than about 0.25 mm to be unstable and subject to seaward removal from the intertidal beach at least 25 percent of the time. Sand used to nourish the intertidal beach should be at least 0.25 mm in diameter or larger.

It must be recalled that the stability of a beach is increased when the beach is fronted by a wide, low-gradient dissipative surfzone. Material with a median grain size finer than 0.25 mm could be used to flatten and widen the surfzone of a reach if the material were available in sufficiently large quantities. Material used in this manner could probably be as fine as 0.125 mm.

## VIII CONCLUSIONS AND PROGNOSIS

Beaches and their hinterlying dunes and beach ridges are advancing seaward in many parts of the world. In many areas, including the southeastern corner of Australia, the beaches remain relatively stable despite the fact that high waves are the rule, the shelf is narrow, and there is a deficiency of shoreface sand. But along the Virginia portion of the Middle Atlantic Bight, the shore is undergoing a landward transgression generally. Locally, this transgression is slowed or reversed via human intervention; however, erosion mitigation is intrinsically very expensive and ephemeral. An insidious -and accelerating- rise in mean sea level, a deficiency of reworkable shoreface sand, a lack of input of new sand from rivers, and a general unavailability of backshore sand all contribute to the regional transgression. We cannot solve this problem: ultimately the sea will have its way with our shores.

In the short term, however, we can either delay the inevitable or plan our retreat in a reasoned way provided that we understand the processes which confront us. The analyses performed in this study were aimed at identifying the most threatened localities, ascertaining the major local causes of erosion or accretion, and evaluating the suitability of different shore protection methods. The basic questions posed in the introduction to this report were identified on the basis of the applied aims. For reasons already noted, the methodologies by which these questions were addressed were quite imperfect. This fact notwithstanding, we offer, with caution, the following "answers":

The complexity of the shoreface morphology fronting the coastal region from Cape Henry to False Cape causes varying degrees of wave modification by refraction and frictional dissipation. Shoreface profiles are shallower off the Virginia Beach resort strip than they are off Sandbridge. As a result, breaker heights off Sandbridge during severe storms are appreciably larger than elsewhere. Longshore variations in breaker height also provide a significant driving force for longshore currents and littoral drift.

Locally, littoral drift can be quite strong at any given time. Over the year, however, gradients in net littoral drift are apparently only responsible for the accretion of Croatan Beach and the erosion of the nodal sectors south of Sandbridge. Observed erosion and accretion elsewhere cannot be adequately explained by littoral drift gradients. This suggests that, for most sectors, groins would be ineffective and would possibly be detrimental.

A substantial proportion of the sand eroded from the intertidal and subaerial portions of the beach is probably transported seaward to sinks on the shoreface and shelf, and in the lower bay. Owing to the narrowness and steepness of the nearshore profiles, the beaches are highly sensitive to offshore sand transport and are subject to erosion for 15% to 40% of the time. Nourishment with sand larger than 0.25 mm increases stability somewhat. An ideal beach nourishment program would include large-scale injections of sand into the surfzone if sufficient quantities of fill material were available. However, such a replenishment program would probably not be economically feasible.

## IX REFERENCES

- Bagnold, R.A., 1963. Beach and Nearshore Processes; Part I: Mechanics of Marine Sedimentation. In: Hill, M.N. (Ed.), The Sea, Vol. 3, Wiley-Interscience, pp. 507-528.
- Beardsley, R.C. and Boicourt, W.C., 1981. On Estuarine and Continental-Shelf Circulation in the Middle Atlantic Bight. In: Warren, B.A. and Wunsch, C. (Eds.), Evolution of Physical Oceanography, MIT Press, pp. 198-233.
- Beauchamp, R.G., 1974. Marine Environmental Planning Guide for the Hampton Roads/Norfolk Naval Operating Area. U.S. Naval Oceanographic Office Spec. Publ. No. 250, Washington, D.C., 262 pp.
- Belknap, D.F. and Kraft, J.C., 1977. Holocene Relative Sea Level Changes and Coastal Stratigraphic Units on the Northwest Flank of the Baltimore Cannon Trough Geosyncline. J. Sed. Petrol. 47:610-629.
- Birkemeier, W.A., DeWall, A.E., Gorbics, C.S. and Miller, H.C., 1981. A User's Guide to C.E.R.C.'s Field Research Facility. U.S. Army Corps of Engineers, C.E.R.C. MR 81-7.
- Boicourt, W.C. and Hacker, P.W., 1976. Circulation on the Atlantic Continental Shelf of the United States, Cape May to Cape Hatteras. Mem. Soc. Royale Sci. Liege, 16th Series, 10:187-200.
- Boon, J.D., Bohlen, W.F. and Wright, L.D., 1987. Estuarine Versus Inner Shelf Disposal Sites: A Comparison of Benthic Current Regimes. Coastal Sediments '87, Proc. (Conf. of ASCE, May 12-14, 1987, New Orleans, Louisiana), pp. 571-583.
- Bowen, A.J., 1969. Rip Currents, 1. Theoretical Investigations. J. Geophys. Res., 74:5467-5478.
- Bowen, A.J., Inman, D.L. and Simmons, V.P., 1968. Wave "Set-Down" and "Set-Up". J. Geophys. Res., 73:2569-2577.
- Boyd, C.D., 1985. Final Phase I GDM for Beach Erosion Control and Hurricane Protection at Sandbridge Beach, Virginia Beach, Virginia. Report by Norfolk District Corps of Engineers, Dept. of the Army, 10 pp.
- Bretschneider, C.L. and Reid, R.O., 1954. Modification of Wave Height Due to Bottom Friction, Percolation and Refraction, Beach Erosion Board, Tech. Memo. No. 45.
- Bumpus, D.F., 1965. Residual Drift Along the Bottom on the Continental Shelf in the Middle Atlantic Bight Area. Limnol. and Oceanogr., Suppl. 10:R50-R53.

- Butman, B., Noble, M. and Folger, D.W., 1979. Long-Term Observations of Bottom Currents and Bottom Sediment Movement on the Middle Atlantic Continental Shelf. *J. Geophys. Res.*, 84:1187-1205.
- Caldwell, J., 1953. Wave Action and Sand Movement Near Anaheim Bay, California. Tech. Memo. No. 68, Beach Erosion Board.
- CERC, 1984. Shore Protection Manual, 4th Ed. U.S. Army Engineer Waterways Experiment Station, Coastal Engineering Res. Center, Vicksburg, Miss.
- Christoffersen, J.B. and Jonsson, I.G., 1985. Bed-Friction and Dissipation in a Combined Current and Wave Motion. *Ocean Engineering*, 12(5): 387-424.
- Dally, W.R., Dean, R.G. and Dalrymple, R.A., 1984. Modelling Wave Transformation in the Surf Zone. U.S. Army Engineer Waterways Experiment Station, Vicksburg, Miss., Misc. Paper CERC-84-8.
- Dalrymple, R.A. and Thompson, W.W., 1977. Study of Equilibrium Beach Profiles. *Proc. 15th Int. Conf. Coastal Eng.*, pp. 1277-1296.
- Dean, R.G., 1973. Heuristic Models of Sand Transport in the Surf Zone. *Proc. Conf. on Engineering Dynamics in the Surf Zone*, Sydney, pp. 208-214.
- Dean, R.G., 1985. Review of Evert's Report, Yearly Maintenance Requirements for Fill Material at Sandbridge Virginia. Report submitted to R. Dolan by R.G. Dean, 6 pp.
- Dolan, R., Hayden, B. and Wayland, R., 1985. Sandbridge Beach and Back Bay, Virginia, Analysis of Shoreline Erosion, Storm Surge, and Back Bay Flooding. Technical Report prepared for the Sandbridge Beach Restoration Association by Coastal Research Associates, Charlottesville, VA, 70 pp. + 5 appendices.
- Duane, D.B., Field, M.E., Meisburger, E.P., Swift, D.J.P. and Williams, S.J., 1972. Linear Shoals on the Atlantic Inner Continental Shelf, Florida to Long Island. In: Swift, D.J.P., Duane, D.B. and Pilkey, O.H. (Eds.), *Shelf Sediment Transport, Process and Pattern*, Dowden, Hutchinson and Ross, Stroudsburg, PA, pp. 447-498.
- Eaton, R.O., 1950. Littoral Processes on Sandy Coasts. *Proc. 1st Int. Conf. Coastal Eng.*, pp. 140-154.
- Ebersole, B.A., Cialone, M.A. and Prater, M.D., 1986. Regional Coastal Processes Numerical Modelling System. Report 1. RCPWAVE - A Linear Wave Propagation Model for Engineering Use. U.S. Army Corps of Engineers, Tech. Rept. CERC-86-4, 160 pp.
- Everts, C.H. (no date). Yearly Maintenance Requirements for Fill Material at Sandbridge Virginia. Report by Moffatt & Nichol Engineers, 16 pp.

- Everts, C.H., Battley, J.P., Jr. and Gibson, P.N., 1983. Shoreline Movements; Report 1: Cape Henry, Virginia to Cape Hatteras, North Carolina, 1849-1980. U.S. Army Engineer Waterways Experiment Station, Vicksburg, Mississippi, Technical Report CERC-83-1.
- Field, M.E., 1979. Sediments, Shallow Subbottom Structure, and Sand Resources of the Inner Continental Shelf, Central Delmarva Peninsula. U.S. Army Corps of Engineers, Coastal Engineering Research Center Technical Paper No. 79-2, 122 pp.
- Froemer, N.L., 1980. Sea Level Variability in Chesapeake Bay. Mar. Geol., 36:289-305.
- Goldsmith, V., Morris, W.D., Byrne, R.J. and Whitlock, C.H., 1974. Wave Climate Model of the Mid-Atlantic Shelf and Shoreline (Virginian Sea). NASA SP-358, VIMS SRAMSOE No. 38, 148 pp.
- Goldsmith, V., Sturm, S.C. and Thomas, G.R., 1977. Beach Erosion and Accretion at Virginia Beach, Virginia and Vicinity. U.S. Army Corps of Engineers, Coastal Engineering Research Center, Fort Belvoir, Virginia, M.R. 77-12, 185 pp.
- Gourlay, M.R., 1982. Nonuniform Alongshore Currents and Sediment Transport - A One-Dimensional Approach. Civil Eng. Res. Rept. No. CE31, Dept. Civ. Eng., Univ. of Queensland, St. Lucia, Queensland.
- Grant, W.D. and Madsen, O.S., 1979. Combined Wave and Current Interaction with a Rough Bottom, J. Geophys. Res., 84:1797-1808.
- Grant, W.D. and Madsen, O.S., 1982. Movable Bed Roughness in Unsteady Oscillatory Flow, J. Geophys. Res., 87:469-481.
- Green, M.O., personal communication. Virginia Institute of Marine Science, Gloucester Point, Virginia.
- Green, T., 1986. Edge Waves Near a Seawall. Coastal Engineering, 10:119-125.
- Hicks, S.D., Debaugh, H.A., Jr. and Hickman, L.E., 1983. Sea Level Variations for the United States 1855-1980. National Ocean Service, NOAA, Rockville, Maryland.
- Inman, D.L. and Bagnold, R.A., 1963. Beach and Nearshore Processes; Part II: Littoral Processes. In: Hill, M.N. (Ed.), The Sea, Vol. 3, Wiley-Interscience, pp. 529-553.
- Jonsson, I.G., 1966. Wave Boundary Layers and Friction Factors. Proc. 10th Int. Conf. Coastal Eng., pp. 127-148.
- Kamphuis, J.W., 1975. Friction Factor Under Oscillatory Waves. ASCE, J. Wat. and Harb. Div., 102(WW2):135-144.

- Kinsman, B., 1965. *Wind Waves, Their Generation and Propagation on the Ocean Surface*. Dover, New York, 676 pp.
- Komar, P.D., 1975. *Nearshore Currents: Generation by Obliquely Incident Waves and Longshore Variations in Breaker Height*. Proc. Symp. *Nearshore Sediment Dynamics*, Wiley, New York.
- Komar, P.D., 1976. *Beach Processes and Sedimentation*, Prentice-Hall, New Jersey, 429 pp.
- Komar, P.D., 1979. Beach-Slope Dependence of Longshore Currents. *J. Waterw. Port, Coastal and Ocean Div.*, ASCE, 105(WW4):460-464.
- Komar, P.D., 1983. *Nearshore Currents and Sand Transport on Beaches*. In: Johns (Ed.), *Physical Oceanography of Coastal and Shelf Seas*. Elsevier, New York, pp. 67-109.
- Komar, P.D. and Inman, D.L., 1970. Longshore Sand Transport on Beaches. *J. Geophys. Res.*, 73(30):5914-5927.
- Kraus, N.C. and Sasaki, T.O., 1979. Effects of Wave Angle and Lateral Mixing on the Longshore Current. *Coastal Eng. in Japan*, 22:59-74.
- Larras, J., 1957. *Plages et Cotes de Sable - Eyroller*, Paris.
- LeBlond, P.H. and Mysak, L.A., 1978. *Waves in the Ocean*, Elsevier, Amsterdam.
- Le Mehaute, B., 1976. *An Introduction to Hydrodynamic and Water Waves*. Springer-Verlag, New York, 315 pp.
- Le Mehaute, B. and Brebner, A., 1961. *An Introduction to Coastal Morphology and Littoral Processes*. C.E. Research Report No. 14, Dept. of Civil Eng., Queen's Univ., Kingston, Ontario.
- Lighthill, J., 1978. *Waves in Fluids*, Cambridge Univ. Press, Cambridge, 504 pp.
- Longuet-Higgins, M.S., 1970a. Longshore Currents Generated by Obliquely Incident Sea Waves, 1. *J. Geophys. Res.*, 75(33):6778-6789.
- Longuet-Higgins, M.S., 1970b. Longshore Currents Generated by Obliquely Incident Sea Waves, 2. *J. Geophys. Res.*, 75(33):6790-6801.
- Longuet-Higgins, M.S., 1972. Recent Progress in the Study of Longshore Currents. In: Meyer, R.E. (Ed.), *Waves on Beaches and Resulting Sediment Transport*, Academic Press, New York, pp. 203-248.
- Longuet-Higgins, M.S. and Stewart, R.W., 1962. Radiation Stress and Mass Transport in Gravity Waves, with Application to Surf Beats. *J. Fluid Mech.*, 13:481-504.

- Longuet-Higgins, M.S. and Stewart, R.W., 1964. Radiation Stresses in Water Waves; A Physical Discussion, with Applications. Deep-Sea Research, 11:529-562.
- Ludwick, J.C., 1977. Jet-like Coastal Currents and Bottom Sediment Transport off Virginia Beach, Virginia. Trans. Am. Geophys. Union, 58:408.
- Ludwick, J.C., 1978. Coastal Currents and an Associated Sand Stream Off Virginia Beach, Virginia. J. Geophys. Res., 83(C5):2365-2372.
- Lundgren, H., 1972. Turbulent Currents in the Presence of Waves. Proc. 13th Int. Conf. Coastal Eng., pp. 623-634.
- Madsen, O.S., 1976. Wave Climate of the Continental Margin: Elements of its Mathematical Description. In: Stanley, D.J. and Swift, D.J.P. (Eds.), Marine Sediment Transport and Environmental Management, Wiley, New York, pp. 65-90.
- Mooers, C.N.K., 1976. Wind Driven Currents on the Continental Margin. In: Stanley, D.J. and Swift, D.J.P. (Eds.), Marine Sediment Transport and Environmental Management, New York, Wiley, pp. 29-52.
- Munch-Peterson, J., 1938. Littoral Drift Formula. Beach Erosion Board Bull., 4(4):1-31.
- Nielsen, P., 1983. Analytical Determination of Nearshore Wave Height Variation Due to Refraction, Shoaling and Friction. Coastal Eng., 7(3):233-252.
- Nielsen, P., Green, M.O. and Coffey, F.C., 1982. Suspended Sediment Under Waves. Tech. Rept. 82/6, Coastal Studies Unit, Univ. of Sydney, Sydney, Australia, 157 pp.
- Nummedal, D., personal communication. Louisiana State University, Professor of Geology, Baton Rouge, Louisiana.
- Payne, L.H., 1970. Sediments and Morphology of the Continental Shelf Off Southeast Virginia. Thesis, Columbia University, 70 pp.
- Phillips, O.M., 1977. The Dynamics of the Upper Ocean. 2nd Ed. Cambridge Univ. Press, Cambridge, 1977.
- Redfield, A.C., 1958. The Influence of the Continental Shelf on the Tides on the Atlantic Coast of the United States. J. Mar. Res., 17:432-448.
- Resio, D.T. and Hayden, B.P., 1973. An Integrated Model of Storm-Generated Waves. Tech. Rept. 8, Dept. Environmental Science, University of Virginia, 273 pp.

- Saint-Marc, M.G.S. and Vincent, M.G., 1954. Transport Littoral, Formation de Fleches et de Tombolos. Proc. 5th Int. Conf. Coastal Eng., pp. 296-328.
- Savage, R.P., 1962. Laboratory Determination of Littoral Transport Rates. J. Waterw. and Harbours Div., ASCE, 88(WW2):69-92.
- Saville, T., 1954. North Atlantic Coast Wave Statistics Hindcast by Bretschneider - Revised Sverdrup-Munk Method. Tech. Mem. 55, Beach Erosion Board, U.S. Army Corps of Engineers.
- Smith, R. and Sprinks, T., 1975. Scattering of Surface Waves by a Conical Island. J. Fluid Mech., 72(2):373-384.
- Stubblefield, W.L. and Duane, D.B., in press. Processes Producing North America's East Coast Sand and Gravel Resources: A Review. Marine Mining Journal.
- Svendsen, I.A. and Jonsson, I.G., 1976. Hydrodynamics of Coastal Regions. Tech. Univ. of Denmark, 282 pp.
- Swart, D.H., 1974. Offshore Sediment Transport and Equilibrium Beach Profiles. Delft Hydr. Lab. Publ. No. 131.
- Swift, D.J.P., Holliday, B., Avignone, N. and Shideler, G., 1972. Anatomy of a Shoreface Ridge System, False Cape, Virginia. Mar. Geol. 12:59-84.
- The Traverse Group, Inc., 1980. Beach Erosion Control and Hurricane Protection at Virginia Beach, Virginia. Coastal Processes Evaluation. Tech. Rept. obtained under contract to the U.S. Army Coastal Engineering Research Center, 207 pp. plus appendices.
- Thompson, E.F., 1977. Wave Climate at Selected Locations Along U.S. Coast. U.S. Army Corps of Engineers, C.E.R.C. Technical Report 77-1.
- U.S. Army Corps of Engineers, Norfolk District, 1984. Beach Erosion Control and Hurricane Protection. Main Report Phase 1-GDM and Supplemental EIS, 114 pp. plus supplements.
- Vemulakonda, S.R., 1984. Erosion Control of Scour During Construction, Report 7, Current - A Wave-Induced Current Model. Tech. Rept. HL-80-3, U.S. Army Engineers Water. Expt. Station, Vicksburg, Miss.
- Vincent, C.E., Swift, D.J.P. and Hillard, B., 1981. Sediment Transport in the New York Bight, North American Atlantic Shelf, Mar. Geol., 42:369-398.

- Waterway Survey and Engineering Ltd., 1986. Engineering Study for Disposal of Dredged Material from Atlantic Ocean Channel on Sandbridge Beach Between Back Bay and Dam Neck. Report prepared for Norfolk District Corps of Engineers largely by Dr. Cyril Galvin, Coastal Engineer, 79 pp. plus appendices.
- Watts, G.M., 1953. A Study of Sand Movement at South Lake Worth Inlet, Florida. Tech. Memo. No. 42, Beach Erosion Board.
- Weggel, J.R., 1972. Maximum Breaker Height. ASCE, J. Waterw. Harb. and Coastal Eng. Div., 78(WW4):529-548.
- Williams, S.J., in review. Sand Resources Offshore Virginia Cape Henry to Virginia Beach.
- Wright, L.D., 1981. Beach Cut in Relation to Surf Zone Morphodynamics. Proc. 17th Int. Conf. Coastal Eng., Sydney, Australia, pp. 978-996.
- Wright, L.D. and Short, A.D., 1984. Morphodynamic Variability of Surf Zones and Beaches: A Synthesis. Mar. Geol., 56:93-118.
- Wright, L.D., Guza, R.J. and Short, A.D., 1982. Dynamics of a High Energy Dissipative Surfzone. Mar. Geol., 45:41-62.
- Wright, L.D., Short, A.D. and Green, M.O., 1985. Short-Term Changes in the Morphodynamic States of Beaches and Surfzones: An Empirical Predictive Model. Mar. Geol., 62:339-364.
- Wright, L.D., Boon, J.D., Green, M.O. and List, J.H., 1986a. Response of the Mid Shoreface of the Southern Mid-Atlantic Bight to a "Northeaster". Geo-Marine Letters, 6:153-160.
- Wright, L.D., Nielsen, P., Shi, N.C. and List, J.H., 1986b. Morphodynamics of a Bar-Trough Surfzone. Mar. Geol., 70:251-285.